

ZJK-807: A Selective PROTAC Degrader of KRAS^{G12D} Overcoming Resistance in Pancreatic Cancer

Zhaojuan Liu,¹ Heping Zheng,¹ Yanqing Tian, Zhuoyue Li, Sai Zhang, Siqi Zhang, Shumin Ma,*
Xiao Wang,* and Chong Qin*



Cite This: <https://doi.org/10.1021/acs.jmedchem.5c01034>



Read Online

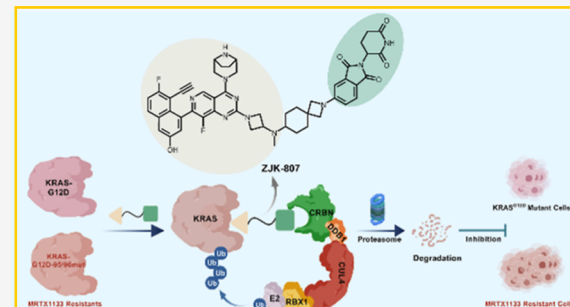
ACCESS |

Metrics & More

Article Recommendations

Supporting Information

ABSTRACT: Pancreatic cancer driven by the KRAS^{G12D} mutation faces therapeutic challenges from KRAS undruggability and acquired resistance to inhibitors like MRTX1133 via secondary mutations (e.g., Q95/Y96). Here, we report ZJK-807, a novel cereblon (CRBN)-based proteolysis targeting chimera (PROTAC), conjugating a KRAS^{G12D} inhibitor to a CRBN ligand. It selectively degrades KRAS^{G12D} ($DC_{50} = 79.5 \pm 5.4$ nM in AsPC-1 cells) with minimal impact on wild-type KRAS or other mutants (G12C/S/V, G13D), inducing mutant-specific cytotoxicity. Critically, ZJK-807 overcomes secondary mutation resistance by degrading mutant KRAS^{G12D} and suppressing resistant cell growth where MRTX1133 fails. Transcriptomic analysis revealed that ZJK-807 suppresses RAS/MAPK signaling and uniquely modulates TNF signaling and eukaryotic ribosome biogenesis, suggesting distinct mechanistic advantages. In vivo, ZJK-807 (30 mg/kg subcutaneous) achieved 47% tumor growth inhibition in AsPC-1 xenografts with favorable pharmacokinetics. This study presents a CRBN-based PROTAC to selectively target and degrade resistant KRAS^{G12D} mutants, establishing a groundbreaking approach for KRAS-driven malignancies.



ZJK-807: A CRBN-based PROTAC Overcoming Secondary Mutations for Selective KRAS^{G12D} Degradation in Pancreatic Cancer

INTRODUCTION

The Kirsten rat sarcoma viral oncogene homologue (KRAS) gene is a major oncogenic driver in human cancers, covering nearly all types of cancers.^{1–3} As a molecular switch in intracellular signaling, KRAS regulates receptor tyrosine kinase (RTK) pathways. In normal cells, endogenous KRAS predominantly exists in an inactive GDP-bound state. However, oncogenic mutations in KRAS impair its GTPase activity, locking KRAS in a constitutively active GTP-bound state.⁴ This leads to persistent activation of downstream pathways, including the Mitogen-Activated Protein Kinase (MAPK) and Phosphatidylinositol-3 Kinase (PI3K) cascades, driving tumor progression.^{5,6} KRAS mutations are primarily single base missense alterations, with 98% occurring in codons 12 (G12), 13 (G13), and 61 (Q61). Notable mutations include G12D, G12C, G12V, G13D, and Q61H.⁷ The KRAS^{G12D} mutation is particularly prevalent in pancreatic ductal adenocarcinoma (PDAC) and colorectal cancer (CRC), representing a significant proportion of KRAS-driven malignancies.^{8,9}

KRAS is a pivotal driver of tumorigenesis but has historically been deemed "undruggable" due to its smooth surface and high GTP affinity.¹⁰ Recent advances, however, have yielded targeted inhibitors against specific KRAS mutations, such as AMG510¹¹ and MRTX849^{12,13} for KRAS^{G12C}, MRTX1133,^{14,15} HRS-4642,¹⁶ RMC-9805¹⁷ and TH-Z series¹⁸ for KRAS^{G12D}, and the pan-KRAS inhibitor BI-2865.¹⁹ MRTX1133 (1), HRS-4642

(2), and RMC-9805 (3) (Figure 1) have demonstrated potent antitumor activity and high selectivity as KRAS^{G12D} inhibitors in pancreatic cancer and nonsmall cell lung cancer.^{14–18} All three compounds have advanced into clinical trials, with MRTX1133 (1) in a phase 1/2 trial (NCT05737706), HRS-4642 (2) in a phase 1b/2 trial (NCT05533463), and RMC-9805 (3) in a phase 1/1b trial (NCT06040541). The development of MRTX1133 (1) has now been terminated by Bristol Myers Squibb due to highly variable pharmacokinetics and failure to meet predefined exposure thresholds.²⁰ Preliminary data from HRS-4642 (2) presented at the 2023 ESMO Congress, revealed a partial response in 1 of 13 with evaluable KRAS^{G12D} mutant solid tumor patients, objective response rate (ORR) = 7.7%.²¹ RMC-9805 (3) against second-line or later pancreatic cancer, has shown more promising activity with an ORR of 30%.²²

Acquired resistance mediated by secondary mutations poses a significant barrier to sustained efficacy. It was observed that the V9W²³ and H95Q/L Y96D²⁴ secondary mutations of KRAS^{G12D} lead to acquired resistance to MRTX1133. Structural

Received: April 12, 2025

Revised: August 25, 2025

Accepted: September 16, 2025



ACS Publications

© XXXX American Chemical Society

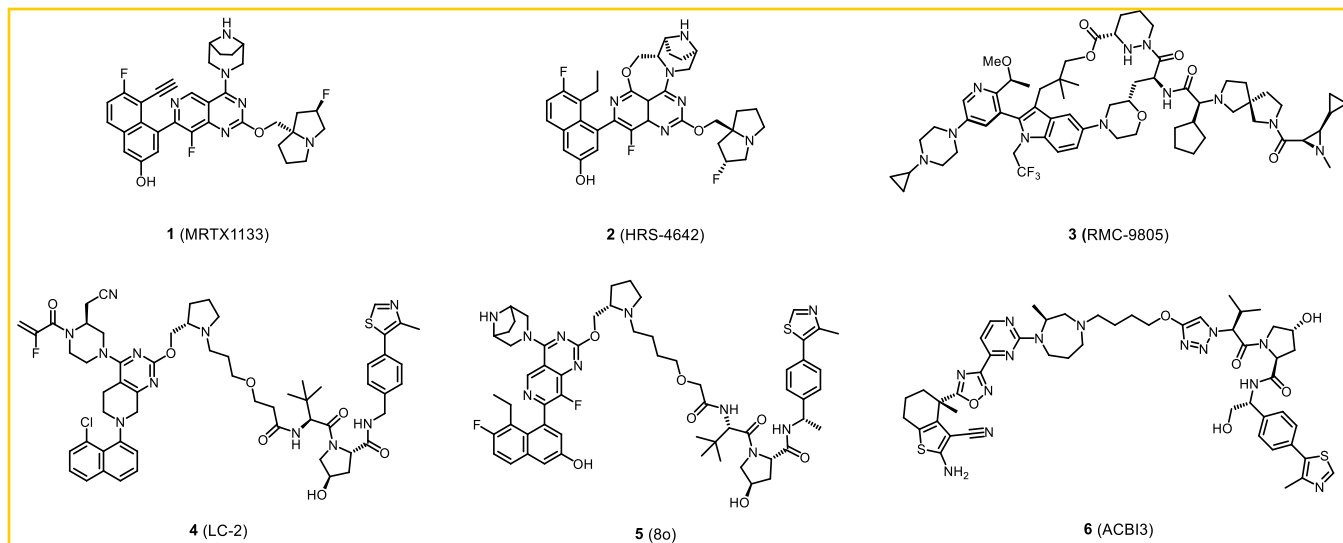


Figure 1. Chemical structures of representative KRAS^{G12D} inhibitors (MRTX1133, HRS-4642, RMC-9805) and KRAS^{G12C} (LC-2), KRAS^{G12D} (8o), Pan-KRAS (ACBI3) degraders.

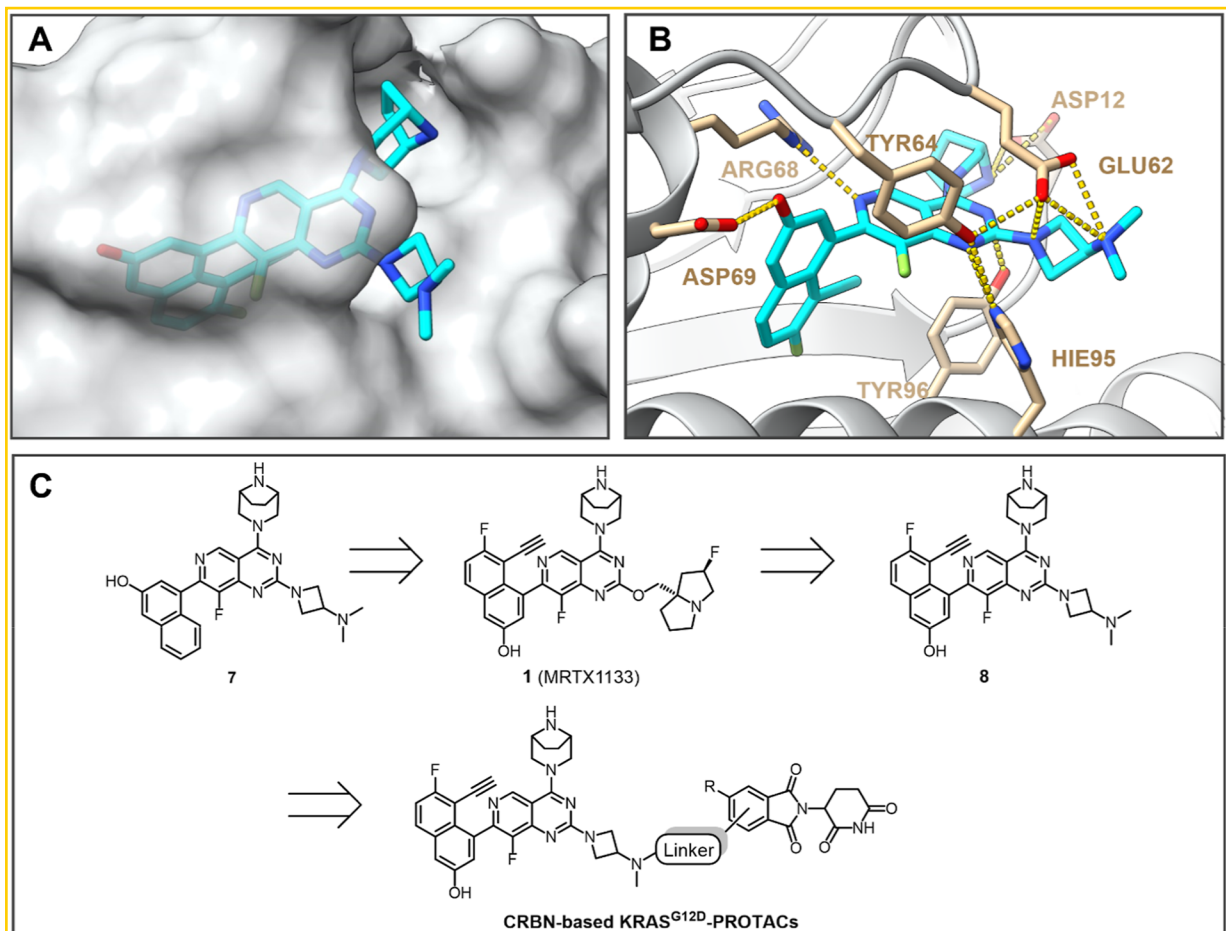
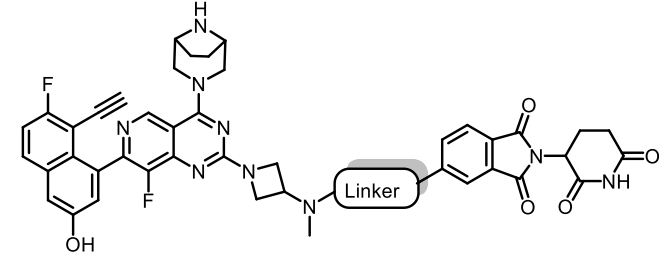
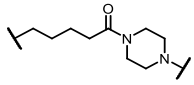
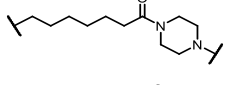
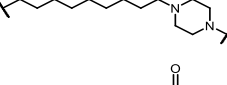
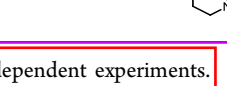


Figure 2. Design of CRBN PROTACs Targeting KRAS^{G12D}. (A) Molecular docking results for compounds 8 and KRAS^{G12D} (PDB: 7RPZ). (B) Predicted binding pose of compound 8 (cyan) with KRAS^{G12D} (white ribbons). Hydrogen bonds and salt bridges are depicted by yellow lines. (C) Design of KRAS^{G12D} PROTACs based on the analogues of thalidomide and compound 8.

analyses revealed that the V9W mutation disrupts the hydrogen-bonding network critical for inhibitor binding to the switch II pocket, replacing valine's isopropyl group with tryptophan's bulkier indole ring, thus reducing affinity.²³ Similarly, secondary mutations in residues R68, H95, and Y96 in the switch-II pocket

of the KRAS^{G12C}, as well as in KRAS^{G12C} alleles such as G12D/W/R/V, have been linked to resistance against inhibitors like sotorasib and adagrasib.²⁵ These findings highlight a common resistance mechanism where secondary mutations alter inhibitor-binding sites without abolishing protein function,

Table 1. Investigation of Linker Length^a


Compound	Linker	%KRAS ^{G12D} protein degradation in AsPC-1 at certain concentration of compound		
		0.1 μM	1 μM	10 μM
A01		0 ± 0	10 ± 4	4 ± 6
A02		0 ± 0	26 ± 2	57 ± 6
A03		67 ± 6	77 ± 4	85 ± 3
A04		39 ± 12	82 ± 0.3	84 ± 5

^aAll the data are the average of two independent experiments.

underscoring the need for alternative therapeutic strategies to address this challenge in KRAS-driven cancers.

Proteolysis-targeting chimeras (PROTACs) consist of a target protein ligand, an E3 ubiquitin ligase ligand, and a linker, forming a ternary complex that induces ubiquitination and subsequent proteasomal degradation of the target protein.^{26,27} Protein degradation via PROTACs represents a promising strategy to overcome drug resistance by fundamentally eliminating target proteins entirely, potentially bypassing resistance conferred by mutations or compensatory pathway activation.²⁸ For instance, AR-targeting PROTACs such as ARV-766 can degrade clinically relevant androgen receptor mutants (L702H, H87SY and T878A) that confer resistance to enzalutamide in prostate cancer.²⁹ Similarly, EGFR PROTACs effectively eliminate osimertinib-resistant mutants (C797S, T790M) in nonsmall cell lung cancer by bypassing kinase domain mutations that prevent inhibitor binding.^{30,31} Moreover, BTK-targeting PROTACs NX-2127 overcome the common C481S resistance mutation in B-cell malignancies.³² These examples demonstrate how PROTACs maintain efficacy against mutated targets through E3 ligase-mediated degradation, offering a robust solution to drug resistance. In sight of this, we developed PROTAC targeted to KRAS^{G12D} with the expectation to improve efficacy by degrading the target and overcoming secondary mutations.

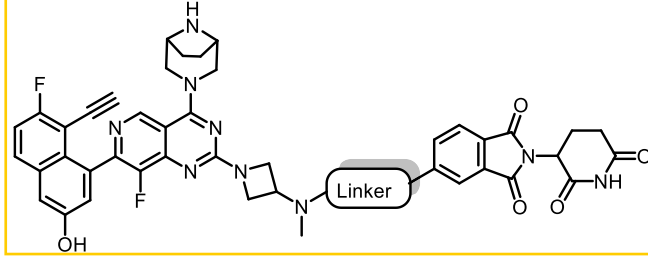
In recent years, various degraders LC-2³³ (4), 8o³⁴ (5) and ACBI3³⁵ (6) (Figure 1) targeting KRAS^{G12C}, KRAS^{G12D}, and pan-KRAS have been developed, offering novel strategies for KRAS-targeted therapy. The KRAS^{G12D} PROTAC 8o (5), which combines an MRTX1133 analog with a VHL ligand, achieves efficient KRAS^{G12D} degradation.³⁴ Astellas Pharma has advanced ASP-3082 (NCT05382559) into clinical trials as the first and currently only VHL-recruiting KRAS^{G12D} targeted

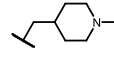
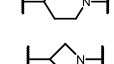
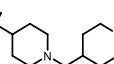
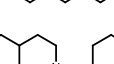
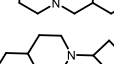
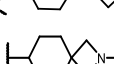
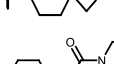
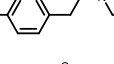
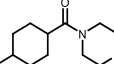
degrader in development.³⁶ Moreover, companies such as Huadong Medicine (WO2025061079A1),³⁷ Haisco Pharmaceutical (CN119219669A)³⁸ and Shanghai Blueray Biopharma (WO2024050742A1)³⁹ have both revealed patents describing potent degraders of KRAS^{G12D}. Notably, Kunjia Pharmaceuticals's CRBN-based PROTAC RP03707 has shown particularly robust degradation efficiency coupled with significant *in vivo* antitumor efficacy, highlighting the expanding arsenal of approaches against this challenging oncogenic target.⁴⁰

In this study, we developed a series of CRBN-based proteolysis targeting chimeras (PROTACs) designed to target KRAS^{G12D}, culminating in the discovery of ZJK-807, a CRBN-based PROTAC with notable therapeutic promise for pancreatic cancer. Through *in vitro* and *in vivo* studies, ZJK-807 demonstrated potent and selective degradation of KRAS^{G12D}, along with antiresistance effects and a well-defined mechanism. ZJK-807 exhibits superior pharmacokinetic properties compared to the previously reported VHL-based KRAS G12D PROTAC compound 8o. These findings highlight ZJK-807 as a promising therapeutic agent for KRAS^{G12D}-driven pancreatic cancer.

RESULTS AND DISCUSSION

Design and Optimization of PROTACs Targeting KRAS^{G12D}. MRTX1133 is derived from a comprehensive structure–activity relationship (SAR) exploration of various site substituents, utilizing pyrido[4,3-*d*]pyrimidine as the scaffold.¹⁵ Among these, compound 7 exhibited significant affinity for KRAS^{G12D} when the substituent at the C2 position was 3-dimethylamino-1-azetidine substituent. Consequently, we replaced the C2 substituent of MRTX1133 with this substituent to synthesize Compound 8. To assess the feasibility of Compound 8 as a warhead targeting KRAS^{G12D}, we predicted

Table 2. Investigation of Rigid Linkers^a


Compound	Linker	%KRAS ^{G12D} protein degradation in AsPC-1 at certain concentration of compound		
		0.1 μM	1 μM	10 μM
A05		0 ± 0	11 ± 0.4	0 ± 0
A06		0 ± 0	35 ± 1	33 ± 3
A07		0 ± 0	0 ± 0	6 ± 8
A08		26 ± 0.1	36 ± 5	25 ± 0.4
A09		44 ± 5	31 ± 5	32 ± 2
A10		45 ± 0.01	61 ± 3	31 ± 2
A11 (ZJK-807)		76 ± 2	85 ± 2	83 ± 2
A12		35 ± 6	16 ± 3	3 ± 4
A13		53 ± 9	8 ± 4	0 ± 0

^aAll the data are the average of two independent experiments.

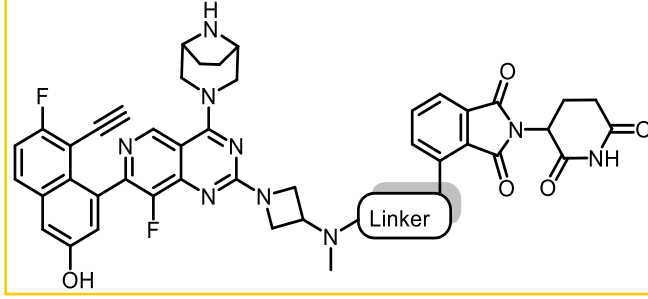
its binding model of compound 8 in complex with KRAS^{G12D}. The analysis revealed that the C2 position is solvent-exposed (Figure 2A), suggesting that this site is highly suitable for conjugation with an E3 ligase ligand via various linker chemistries. Furthermore, most key interactions between MRTX1133 and KRAS^{G12D} have been conservatively preserved (Figure 2B), including the salt bridge and hydrogen-bonding interactions between the nitrogen of the C4 substituent and ASP12, as well as the hydrogen-bonding interactions of the hydroxyl group of the C7 substituent with ASP69. Notably, despite the change in the substituent at the C2 position, the protonated N in this substituent remains capable of forming hydrogen bond and salt bridge interaction networks with GLU62, TYR64, HIE95 and TYR96.

CRBN ligands are well-established for their favorable drug-like characteristics, particularly their ability to enhance oral bioavailability—a critical attribute for therapeutic development. Notably, all orally administered PROTACs currently progressing through clinical trials employ CRBN ligands, reflecting their superior pharmacokinetic profiles and translational potential. Comparative analysis of E3 ligase ligands in PROTACs reveals distinct oral absorption profiles.⁴¹ MDM2- and IAP-based PROTACs exhibit unfavorable physicochemical properties,

including high molecular weight (MW), excessive lipophilicity (cLogP, cLogD), and rotatable bonds. VHL-targeting PROTACs show improved drug-like space alignment but remain constrained by rotatable bonds and hydrogen bond donors (HBDs). In contrast, CRBN-directed PROTACs display enhanced oral absorption potential, with lower MW, reduced cLogP, and HBD counts closer to conventional drug-like thresholds.⁴¹

In contrast, prior KRAS-targeted PROTACs have predominantly utilized VHL ligands. While these efforts have provided valuable proof-of-concept, compounds such as 8o exhibited suboptimal in vivo pharmacokinetic performance, limiting their clinical utility. Therefore, thalidomide analogues were chosen to hijack CRBN, compound 8 was selected as the KRAS^{G12D} warhead for the design of KRAS^{G12D} PROTAC (Figure 2C).

Compounds A01~A04 which contain semirigid linkers incorporating a piperazine group and 4 to 10 methylene groups, were first synthesized and their ability to degrade KRAS^{G12D} was assessed in the KRAS^{G12D} mutant cell line AsPC-1. The degradation efficiency was evaluated by Western blotting at concentrations of 0.1, 1, and 10 μM following 24 h of incubation (Table 1 and Figure S1). Our data indicated that with the extension of linker length, the degradation level of KRAS^{G12D}

Table 3. Investigation of Different Linking Positions of the Cereblon Ligand^a


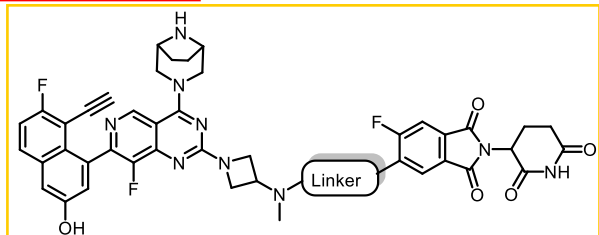
Compound	Linker	%KRAS ^{G12D} protein degradation in AsPC-1 at certain concentration of compound		
		0.1 μM	1 μM	10 μM
B01		25 ± 1	38 ± 0.5	28 ± 2
B02		31 ± 3	25 ± 3	20 ± 2
B03		0 ± 0	0 ± 0	6 ± 3
B04		64 ± 0.1	80 ± 1	40 ± 6
B05		10.6 ± 15.0	45 ± 4	4 ± 6
B06		6 ± 8	5 ± 6	0 ± 0
B07		7 ± 10	22 ± 3	12 ± 6
B08		22 ± 9	25 ± 4	38 ± 1

^aAll the data are the average of two independent experiments.

increased. Compound A03, which contains eight methylene units, achieved effective KRAS^{G12D} degradation of 77 ± 4% and 85 ± 3% at 1 μM and 10 μM respectively. Compound A04, which contains two additional methylene groups compared to the linker in compound A03, significantly reduced KRAS^{G12D} levels by 82 ± 0.3% and 84 ± 5% at 1 μM and 10 μM respectively. We further evaluated the antiproliferative activity of these compounds in the KRAS^{G12D} mutant cell line AsPC-1. Compound A03 significantly inhibited cell growth, exhibiting an IC₅₀ value of 0.67 ± 0.22 μM while compound A04 demonstrated greater efficacy with an IC₅₀ value of 0.29 ± 0.18 μM (Table S1).

The use of rigid linkers has been reported to enhance the solubility and stability of ternary complex, thereby effectively improving the degradation activity of the compounds.⁴² Accordingly, we synthesized compounds A05~A13 with rigid linkers and evaluated the KRAS^{G12D} degradation efficacy of these compounds in AsPC-1 cell line using Western blotting after 24 h of incubation at concentrations of 0.1, 1, and 10 μM (Table 2 and Figure S1). Compound A05, which features a piperidine group, and compound A06, which contains one fewer methylene group, slightly reduced KRAS^{G12D} levels by 11 ± 0.4% and 35 ± 1% at 1 μM respectively. Both compounds exhibited a hook effect at a high concentration of 10 μM and

were less effective than compound A04. Compound A07, which includes an azetidine group, nearly lost its ability to degrade the KRAS^{G12D} protein. We subsequently synthesized compounds A08~A13, which have two cycles in the linker. Compound A08, featuring with two piperidine group, achieved a KRAS^{G12D} reduction of 36 ± 5% at 1 μM. And compound A09, obtained by reducing the linker in compound A08 by one methylene group, modestly decreased KRAS^{G12D} level of 44 ± 5% at 0.1 μM and displayed a hook effect at high concentration. Compound A10, which includes a piperidine group and an azetidine group, induced KRAS^{G12D} degradation by 61 ± 3% and 31 ± 2% at 1 μM and 10 μM, respectively, and also showed a hook effect at 10 μM. Introducing a 2-azaspiro[3.5]nonane ring into the linker resulted in compound A11 (ZJK-807), which was significantly more potent. Compound ZJK-807 effectively reduced KRAS^{G12D} levels by 85 ± 2% at 1 μM and achieved an IC₅₀ value of 0.22 ± 0.06 μM (Table S1), demonstrating comparable efficacy to compound A04. Compound A12 and compound A13, which feature two cycles and an amide group, were less potent than compound ZJK-807, with the ability to reduce KRAS^{G12D} level of 35 ± 6% and 53 ± 9% at 0.1 μM respectively. A hook effect was observed at high concentrations for both compounds.

Table 4. Investigation of Different Cereblon Ligand^a


Compound	Linker	%KRAS ^{G12D} protein degradation in AsPC-1 at certain concentration of compound		
		0.1 μM	1 μM	10 μM
C01		0 ± 0	0 ± 0	0 ± 0
C02		12 ± 3	28 ± 8	18 ± 2
C03		7 ± 10	0 ± 0	0 ± 0
C04		0 ± 0	0 ± 0	0 ± 0
C05		0 ± 0	0 ± 0	0 ± 0
C06		0 ± 0	11 ± 4	54 ± 7
C07		0 ± 0	0.5 ± 0.7	0 ± 0
C08		0 ± 0	0.8 ± 1	4 ± 6

^aAll the data are the average of two independent experiments.

Table 5. PKs of Compounds in Mice^a

compound	route	dose (mg/kg)	T _{1/2} (h)	T _{max} (h)	C _{max} (ng/mL)	AUC _{last} (h·ng/mL)	MRT _{inf_obs} (h)
A04	IP	30	1.85 ± 0.417	0.417 ± 0.144	722 ± 92	3883 ± 147	7.91 ± 1.34
ZJK-807	IP	30	1.67 ± 0.500	0.5 ± 0.0	7086 ± 883	26103 ± 3691	4.92 ± 0.93
ZJK-807	SC	30	7.43 ± 0.69	0.33 ± 0.14	9869 ± 2649	26346 ± 3999	6.08 ± 0.57

^aData are shown as the mean ± standard deviation (SD).

Next, we synthesized compounds B01~B08 by changing the linking position from the *meta*- to the *ortho*-position of the phenyl ring of the thalidomide in compounds A05~A10, A12, and A13. The ability of these compounds to degrade KRAS^{G12D} was assessed in AsPC-1 cell through Western blotting after 24 h of incubation at concentrations of 0.1, 1, and 10 μM (Table 3 and Figure S1). Most of the compounds exhibited similar degradation activity of KRAS^{G12D} protein as the corresponding *meta*-substituted compounds. Additionally, a hook effect was observed in most of the compounds. Compound B04, which showed the best degradation ability among these compounds, reduced KRAS^{G12D} level of 64 ± 0.1% and 80 ± 1% at 0.1 μM and 1 μM, respectively, and a hook effect was also observed. (Table 4).

It is well recognized that installation of a fluorine atom at the C6 position of pomalidomide-based PROTACs can reduce hydrogen bond and enhance the reasonable distribution of druglike properties.⁴³ Therefore, we synthesized compounds

C01~C08 by introducing a fluorine atom at position 6 of the phenyl ring of thalidomide in compounds A05~A10, A12, and A13. Western blotting results revealed that most of these compounds completely lost the degradation activity of KRAS^{G12D} compared to the corresponding compounds without fluorine. Compound C06 was the most potent degrader of these compounds, modestly reducing KRAS^{G12D} level by 54 ± 7% at 10 μM (Table 4 and Figure S1).

Pharmacokinetic Studies of Potent KRAS^{G12D} PROTACs. Subsequently, we evaluated the pharmacokinetic properties (PK) of A04 and A11 (ZJK-807) in mice. After intraperitoneal (IP) administration at a dose of 30 mg/kg, the half-lives (T_{1/2} = 1.85 and 1.67 h) of both compounds were similar. However, the maximum plasma concentration of ZJK-807 (C_{max} = 7086 ± 883 ng/mL) was approximately 10 times higher than that of A04 (C_{max} = 722 ± 92 ng/mL), and furthermore, the plasma exposure level of ZJK-807 (AUC_{last} = 26103 ± 3691 h·ng/mL) was approximately 7 times higher than

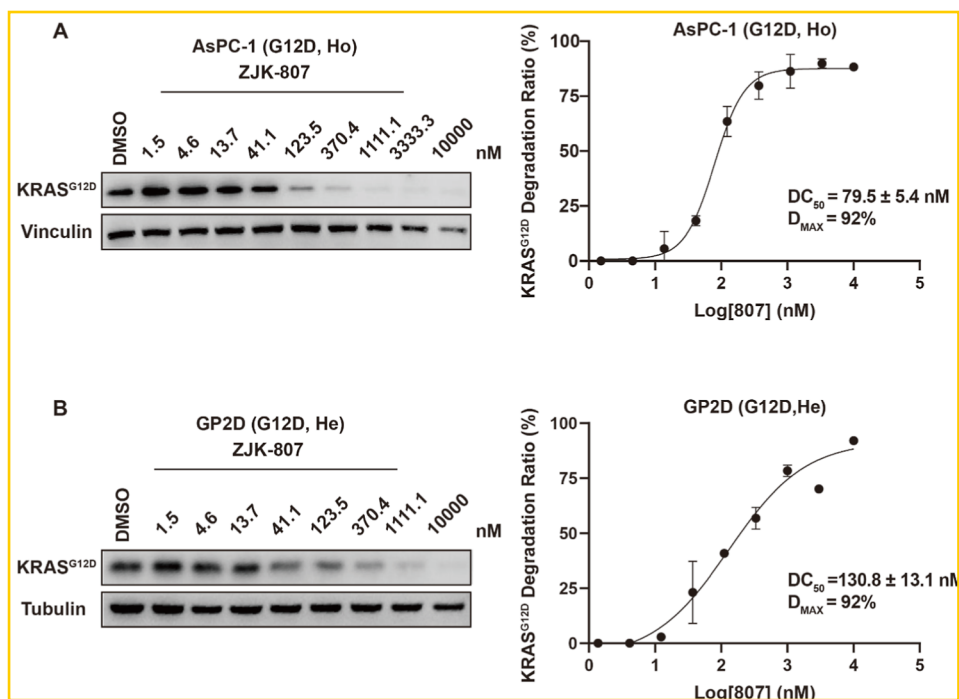


Figure 3. Degradation of KRAS^{G12D} by ZJK-807 in different cell lines. Western blot analysis of KRAS^{G12D} in AsPC-1 (A), GP2D (B) cells treated with ZJK-807 at specified concentrations for 24 h. Vinculin or Tubulin was used as a loading control. The right panel shows the dose–response curve for KRAS^{G12D} degradation. Data are representative of two independent experiments. Error bars represent standard deviation.

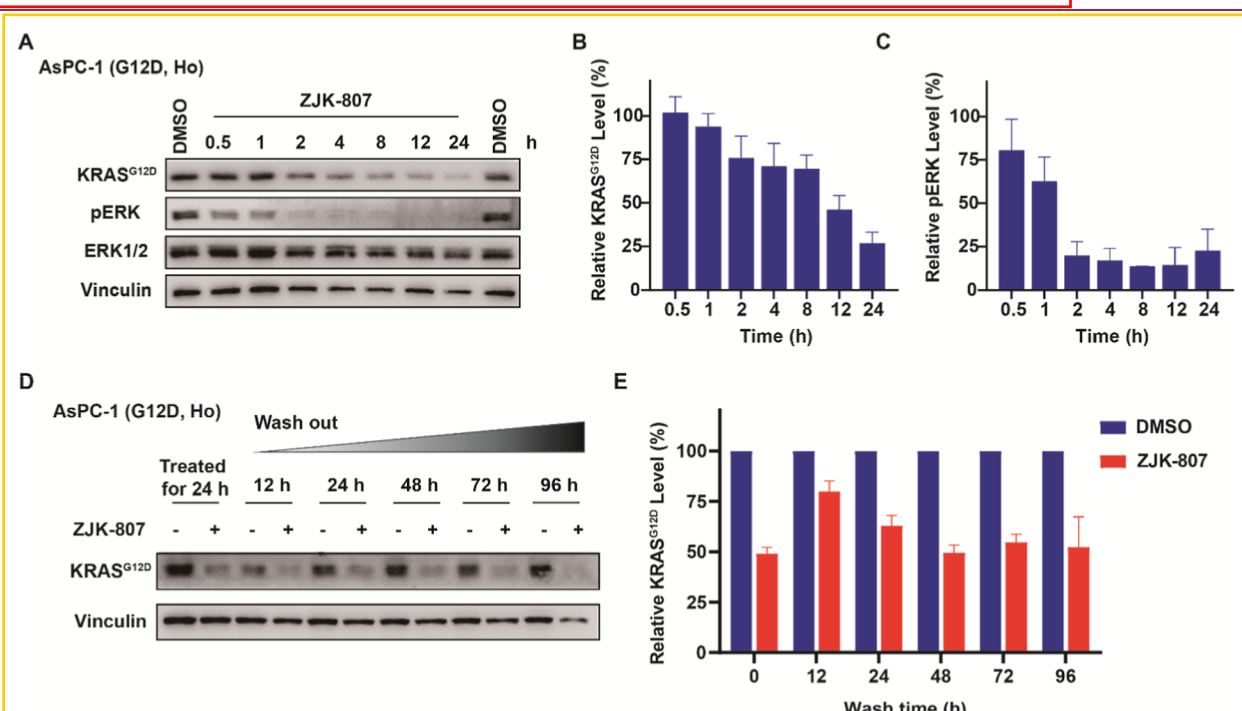


Figure 4. Degradation dynamics analysis of KRAS^{G12D} and pERK signaling in AsPC-1 cells treated with ZJK-807. (A) Western blot of KRAS^{G12D}, pERK, ERK1/2, and Vinculin levels at indicated time points (0.5–24 h) after 10 μ M ZJK-807 or DMSO treatment. Quantitative analysis relative KRAS^{G12D} (B) and pERK (C) levels over 0.5–24 h. (D) Western blot analysis of KRAS^{G12D} levels at specific time points post wash-out after 24 h treatment of AsPC-1 cells with 10 μ M ZJK-807. (E) Quantitative analysis relative KRAS^{G12D} levels post wash-out compared to DMSO control. Data are representative of two independent experiments. Error bars represent standard deviation.

that of A04 ($AUC_{last} = 3883 \pm 147 \text{ h}\cdot\text{ng/mL}$) (Table 5). The above data suggest that compounds with rigid linkers have superior PK properties compared to flexible linkers. To address the short half-life of ZJK-807 following IP administration, we explored alternative administration routes to prolong its

retention in mice. Following subcutaneous (SC) administration at 30 mg/kg, ZJK-807 exhibited favorable PK properties, including $T_{1/2} = 7.43 \pm 0.69 \text{ h}$, $C_{max} = 9869 \pm 2649 \text{ ng/mL}$, $AUC_{last} = 26346 \pm 3999 \text{ h}\cdot\text{ng/mL}$, $MRT_{INE,obs} = 6.08 \pm 0.57 \text{ h}$ (Table 5). Our data suggest that the half-life of ZJK-807 by SC

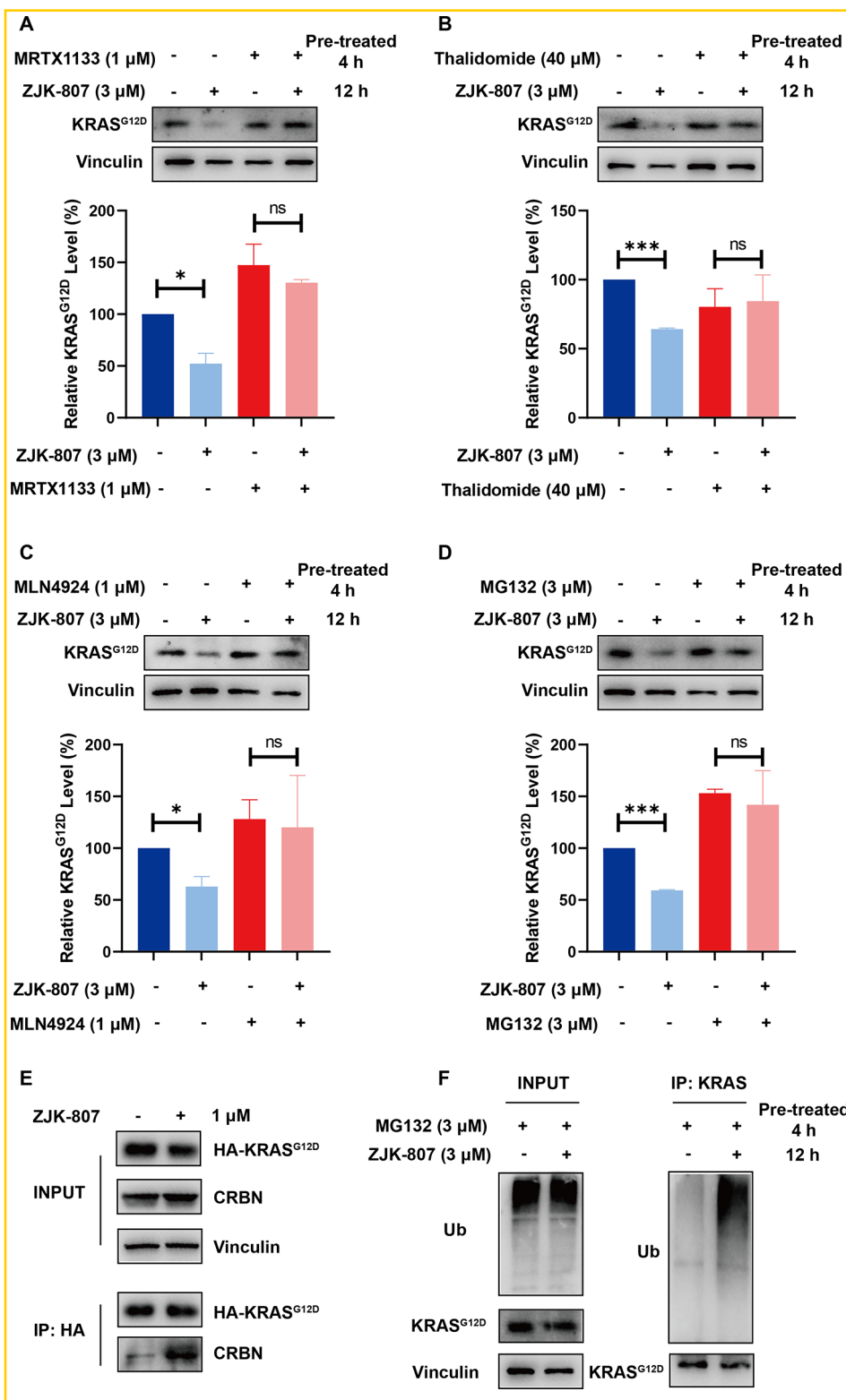


Figure 5. Mechanistic validation of ZJK-807 mediated KRAS^{G12D} degradation. AsPC-1 cells were pretreated with 1 μ M MRTX1133 (A), 40 μ M Thalidomide (B), 1 μ M MLN4924 (C) and 3 μ M MG132 (D) for 4 h followed by a 12 h cotreatment with 3 μ M ZJK-807. The indicated protein levels were determined by Western blot analysis, with Vinculin serving as the loading control. Quantification for KRAS^{G12D} is plotted at the bottom. Quantified data represents mean \pm SD from two independent replicates. Differences in means between groups were analyzed by two-tailed unpaired *t*-test using GraphPad Prism 9.4.1 software. **P* < 0.05, ***P* < 0.001, ns, not significant. Immunoprecipitation analysis of ternary complex formation and polyubiquitination of KRAS^{G12D}. (E) AsPC-1 cells were transfected with HA-KRAS^{G12D} into 48 h and then lysates were treated with 1 μ M of ZJK-807 for 16 h. Immunoprecipitation (IP) with anti-HA antibody followed by IB with anti-KRAS and anti-CRBN. (F) AsPC-1 cells were pretreated with 3 μ M MG132 (proteasome inhibitor) for 4 h followed by a 12 h cotreatment with 3 μ M ZJK-807. Cell lysates were immunoprecipitated with anti-KRAS antibody and probed with anti-Ubiquitin antibody.

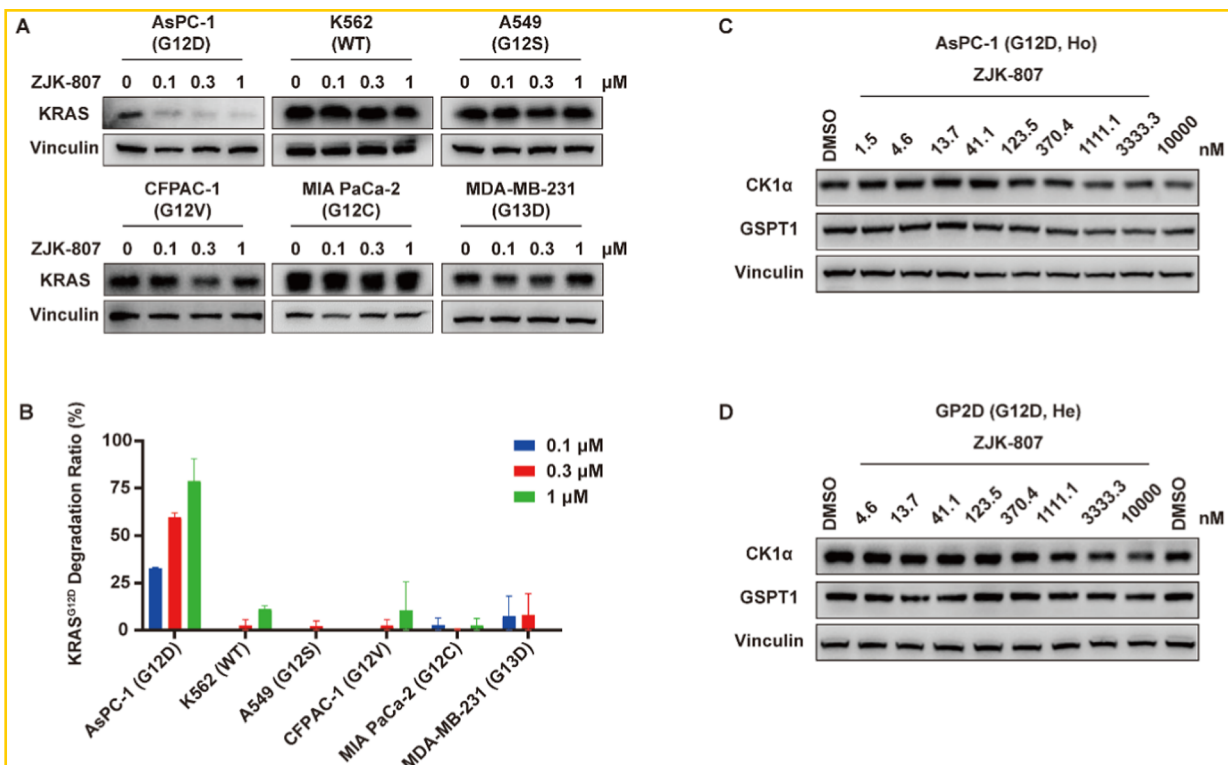


Figure 6. Degradation selectivity of PROTAC ZJK-807 without CCRN off-target effects. (A) Western blot analysis of AsPC-1 (KRAS^{G12D}), MIA PaCa-2 (KRAS^{G12C}), A549 (KRAS^{G12S}), CFPAC-1 (KRAS^{G12V}), MDA-MB-231 (KRAS^{G13D}) and K562 (KRAS^{WT}) cells after 24 h treatment with 0.1, 0.3, 1 μ M ZJK-807, with Vinculin serving as the loading control. (B) Quantification for KRAS^{G12D} is plotted at the bottom. Quantified data represents mean \pm SD from two independent replicates. Western blot analysis of CK1 α , GSPT1, and Vinculin serving as the loading control on AsPC-1 (C) and GP2D (D) cells after 24 h treated with ZJK-807 at specified concentrations.

administration at 30 mg/kg is approximately 4-fold longer than that by IP administration. We expected to optimize the PK parameters of CCRN-PROTAC while maintaining a high degradation efficacy. To evaluate this, we administered ZJK-807 and 8o subcutaneously at 10 mg/kg and assessed its PK parameters. Comparative analysis revealed that ZJK-807 exhibited approximately 2.2-fold higher plasma exposure than 8o when both compounds were administered subcutaneously at the same dose (Table S2). The improvement in PK properties of ZJK-807 compared to 8o is similar to the difference in PK properties between compound A04 and ZJK-807. We speculate that this improvement is due to the introduction of a rigid linker, which enhances the solubility and stability of the compound.⁴²

Further Evaluation of the Degradation Induced by ZJK-807 in KRAS^{G12D} Cell Lines. To further evaluate the effect of ZJK-807 on KRAS^{G12D} protein degradation in three KRAS^{G12D} mutant cell lines, cells were treated with ZJK-807 for 24 h. A dose-dependent reduction in KRAS^{G12D} protein levels was observed. ZJK-807 exhibited a DC₅₀ of 79.5 \pm 5.4 nM and D_{MAX} of 92% in AsPC-1 cells (Figure 3A), a DC₅₀ of 130.8 \pm 13.1 nM and D_{MAX} of 92% in GP2D cells (Figure 3B), and a DC₅₀ of 313.8 \pm 99.9 nM and D_{MAX} of 70% in AGS cells (Figure S2). These results indicate that ZJK-807 is more effective in degrading KRAS^{G12D} in pancreatic cancer cells AsPC-1 compared to colorectal GP2D and gastric cancer cells AGS.

Based on these findings, we further investigated the dynamic effects of ZJK-807 on KRAS^{G12D} protein levels and ERK signaling in AsPC-1 cells. Treatment with ZJK-807 resulted in a time-dependent reduction in KRAS^{G12D} levels and a significant decrease in pERK levels, observed as early as 2 h post-treatment,

indicating sustained downregulation of the ERK pathway for up to 24 h (Figure 4A–C). To assess the durability of KRAS^{G12D} degradation, cells were treated with 10 μ M ZJK-807 for 24 h, washed with PBS, and replenished with fresh complete medium. KRAS^{G12D} protein levels remained consistently low at 12, 24, 48, 72, and 96 h postelution, suggesting prolonged degradation even after drug removal (Figure 4D, E). These results demonstrate that ZJK-807 effectively degrades KRAS^{G12D}, modulates ERK signaling, and maintains its effects post-treatment.

Degradation Mechanism of KRAS^{G12D} Induced by Compound ZJK-807. Next, we investigated whether ZJK-807-induced target protein degradation is dependent on the ubiquitin-proteasome system (UPS). To further validate the mechanism, AsPC-1 cells were pretreated with the KRAS^{G12D} inhibitor MRTX1133 (1 μ M) and the CCRN ligand thalidomide (40 μ M) for 4 h prior to the addition of 3 μ M ZJK-807 for 12 h of cotreatment (Figure 5A, B). As expected, ZJK-807-induced KRAS^{G12D} degradation was significantly alleviated by the competitive binding of these two ligands. To further assess target engagement competition, AsPC-1 cells were pretreated with MRTX1133 (0.01–1 μ M) for 4 h followed by cotreatment with ZJK-807 (3 μ M) for 12 h. The results showed that MRTX1133 had a concentration-dependent inhibitory effect on ZJK-807-mediated degradation (Figure S3). As shown in the results, pretreatment with the NEDD8-activating E1 enzyme inhibitor MLN4924 (1 μ M) or the proteasome inhibitor MG132 (3 μ M) for 4 h followed by cotreatment with 3 μ M ZJK-807 for 12 h effectively attenuated the degradation of KRAS^{G12D} protein in AsPC-1 cells (Figure 5C, D). Collectively, these findings strongly demonstrate that

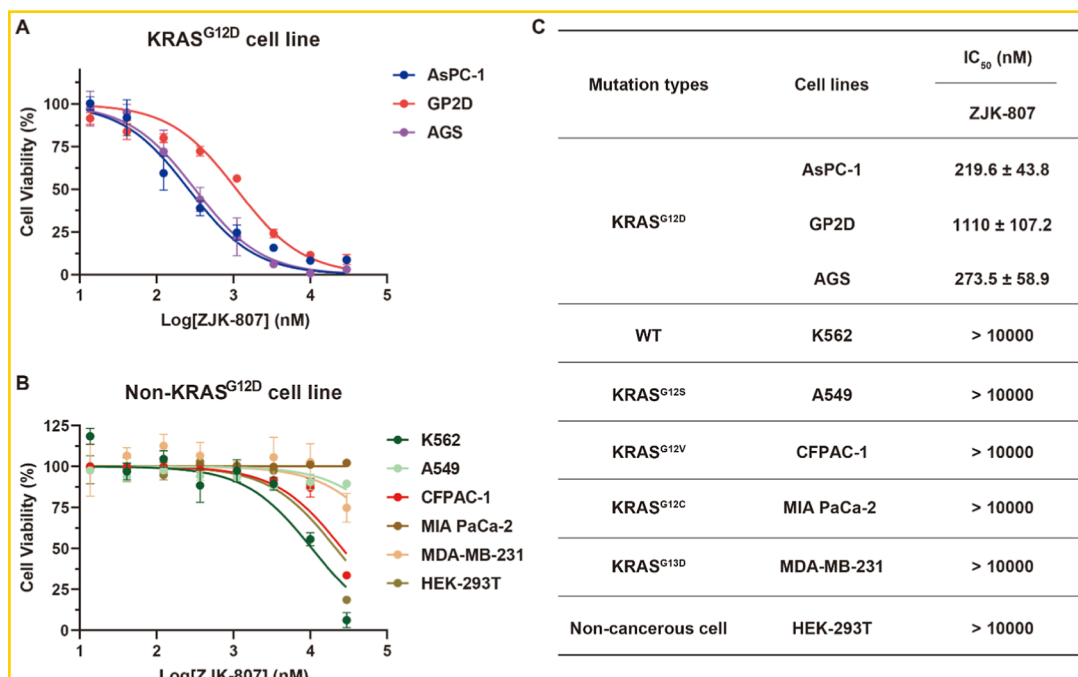


Figure 7. Growth inhibition of ZJK-807 in various cell lines. KRAS^{G12D} mutant cells (A) and other KRAS mutant (KRAS^{WT}, KRAS^{G12S}, KRAS^{G12V}, KRAS^{G12C}, KRAS^{G13D}) cells and noncancerous cell (B) were treated with ZJK-807 at indicated concentration for 3 or 5 days. Cell viability was determined with CCK-8 assay. Quantified data represents mean ± SD from three independent replicates. (C) IC₅₀ values are shown as mean of three independent experiments ($n = 3$).

ZJK-807-induced degradation of KRAS^{G12D} is mediated by the ubiquitin-proteasome system and is dependent on the engagement of both KRAS^{G12D} and the CRBN E3 ligase complex.

Then we performed immunoprecipitation analysis in AsPC-1 cells for mechanistic analysis. For ternary complex analysis, HA-KRAS^{G12D} plasmid was transfected into AsPC-1 cells, and we demonstrated that ZJK-807 promoted the strong recruitment of HA-KRAS^{G12D} to CRBN E3 ligase, proving the formation of ternary complexes (Figure 5E). Furthermore, we detected the ubiquitination formation and showed that ZJK-807 significantly enhanced the polyubiquitination of KRAS^{G12D} compared to the control (Figure 5F). In conclusion, mechanistic analyses performed by immunoprecipitation analysis suggest that ZJK-807 promoted the formation of a complex between the E3 ligase CRBN and KRAS^{G12D}, and facilitated the ubiquitination and degradation of KRAS^{G12D}.

ZJK-807 Potently and Selectively Degrades Oncogenic KRAS^{G12D}. To evaluate the selective degradation activity of ZJK-807 against KRAS mutant proteins, we systematically assessed its degradation activity in a variety of KRAS mutant cell lines. ZJK-807 was treated in AsPC-1 (KRAS^{G12D}), MIA PaCa-2 (KRAS^{G12C}), A549 (KRAS^{G12S}), CFPAC-1 (KRAS^{G12V}), MDA-MB-231 (KRAS^{G13D}) mutant cell lines and K562 (KRAS^{WT}) cell lines with concentrations of 0.1, 0.3, and 1 μM for 24 h. The results demonstrated that ZJK-807 induced significant, concentration-dependent degradation of KRAS protein in AsPC-1 (KRAS^{G12D}) cells (Figure 6A,B). In contrast, no appreciable degradation of KRAS protein was observed in other KRAS mutant cell lines (Figure 6A,B). To assess potential CRBN-mediated off-target effects, AsPC-1 and GP2D cells were treated with specific concentrations of ZJK-807 for 24 h to assess the effects of typical CRBN substrate proteins CK1α and GSPT1. Our data indicate that in both cell lines, ZJK-807 treatment does not induce concentration-dependent degrada-

tion of CK1α or GSPT1 (Figure 6C,D). These findings indicate that ZJK-807 exhibits highly selective degradation activity against KRAS^{G12D} mutant protein, with minimal effects on other KRAS mutations or wild-type KRAS and does not cause CRBN-mediated off-target toxicity. This selective degradation profile provides strong evidence supporting the further development of ZJK-807 as a KRAS^{G12D}-selective degrader.

Selective Anti-Proliferative Activity of ZJK-807 Against KRAS^{G12D} Mutant Cancer Cells. To evaluate the antiproliferative activity of the degrader ZJK-807 against KRAS mutant cell lines, we systematically assessed its effects on cancer cell lines harboring KRAS^{G12D}, KRAS^{G12C}, KRAS^{G12S}, KRAS^{G12V}, and KRAS^{G13D} mutations, as well as those with wild-type KRAS. HEK-293T was included as controls. Consistent with its degrading activity, ZJK-807 exhibited antiproliferative effects on KRAS^{G12D} mutant cell lines, with IC₅₀ values of 219.6 ± 43.8 nM in AsPC-1, 273.5 ± 58.9 nM in AGS, and 1110 ± 107.2 nM in GP2D cells (Figure 7A,C). In contrast, no substantial antiproliferative activity was observed in cell lines with wild-type or other KRAS mutations (Figure 7B,C). Notably, ZJK-807 demonstrated no inhibitory effects on the normal cell line HEK-293T, indicating its low cytotoxicity. Collectively, these findings suggest that ZJK-807 possesses high selectivity for the proliferation against KRAS^{G12D} mutant cells, with minimal off-target effects on other KRAS mutants or normal cells, highlighting its potential as a selective KRAS^{G12D} degrader for cancer therapy.

Evaluation of the Biological Activity and Potential Resistance Mechanism of ZJK-807 against Secondary Mutant Resistance. H95 and Y96 serve as the key to MRTX1133 binding to KRAS, and mutation of these residues abrogate sensitivity to MRTX1133. To address the challenge of overcoming drug resistance, we constructed KRAS^{G12D/Y95mut} and KRAS^{G12D/Y96mut} secondary mutants and assessed the degra-

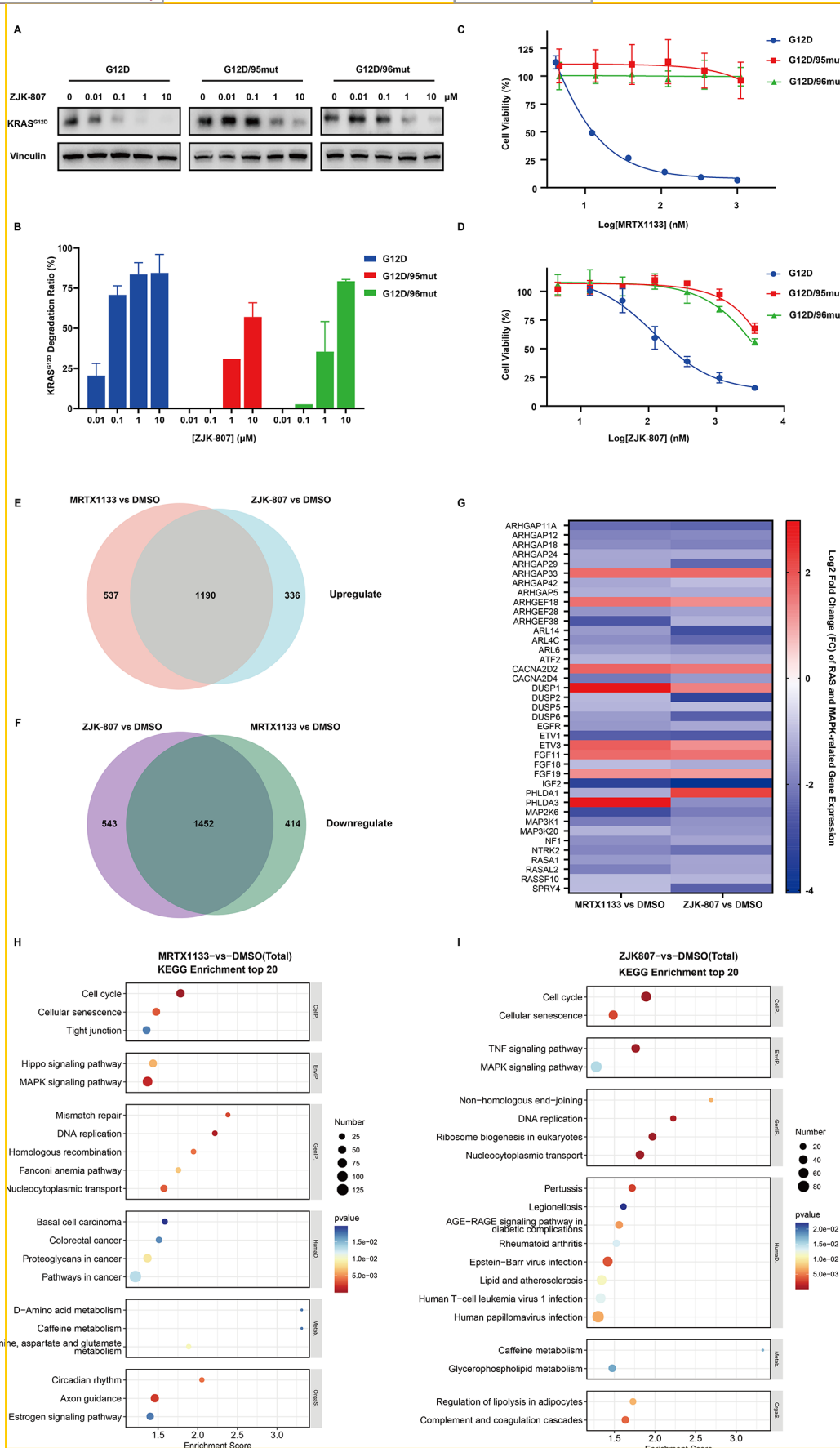


Figure 8. Activity of ZJK-807 against MRTX1133-resistant mutants and transcriptional regulation analysis. (A,B) AGS cells were transfected with KRAS^{G12D/95mut} or KRAS^{G12D/96mut} for 48 h. The secondary mutants cells were treated with specific concentrations ZJK-807 (0.01–10 μ M) for 24 h. Western blot analysis of KRAS^{G12D} levels, Vinculin served as a loading control; Quantitative analysis of the degradation rate of KRAS^{G12D} at the bottom,

Figure 8. continued

quantified histograms were analyzed using GraphPad Prism. (C,D) Growth inhibition of KRAS^{G12D/95mut} or KRAS^{G12D/96mut} cells treated with MRTX1133 or ZJK-807 for 3 days. Cell viability was determined with CellTiter-Glo assay. (E,F) Venn diagrams comparing significantly upregulated and downregulated genes (DEGs) (\log_2 fold change ≥ 2 , $p < 0.05$) after treatment with MRTX1133 (300 nM, 48 h) or ZJK-807 (10 μ M, 48 h) in AsPC-1 cells. (G) Heatmap showing differential expression of RAS- and MAPK-related gene sets in ZJK-807-treated versus MRTX1133-treated AsPC-1 cell (\log_2 fold change ≥ 2 , $p < 0.05$). (H, I) KEGG pathway analysis of the top 20 significantly enriched biological pathways following treatment with MRTX1133 or ZJK-807.

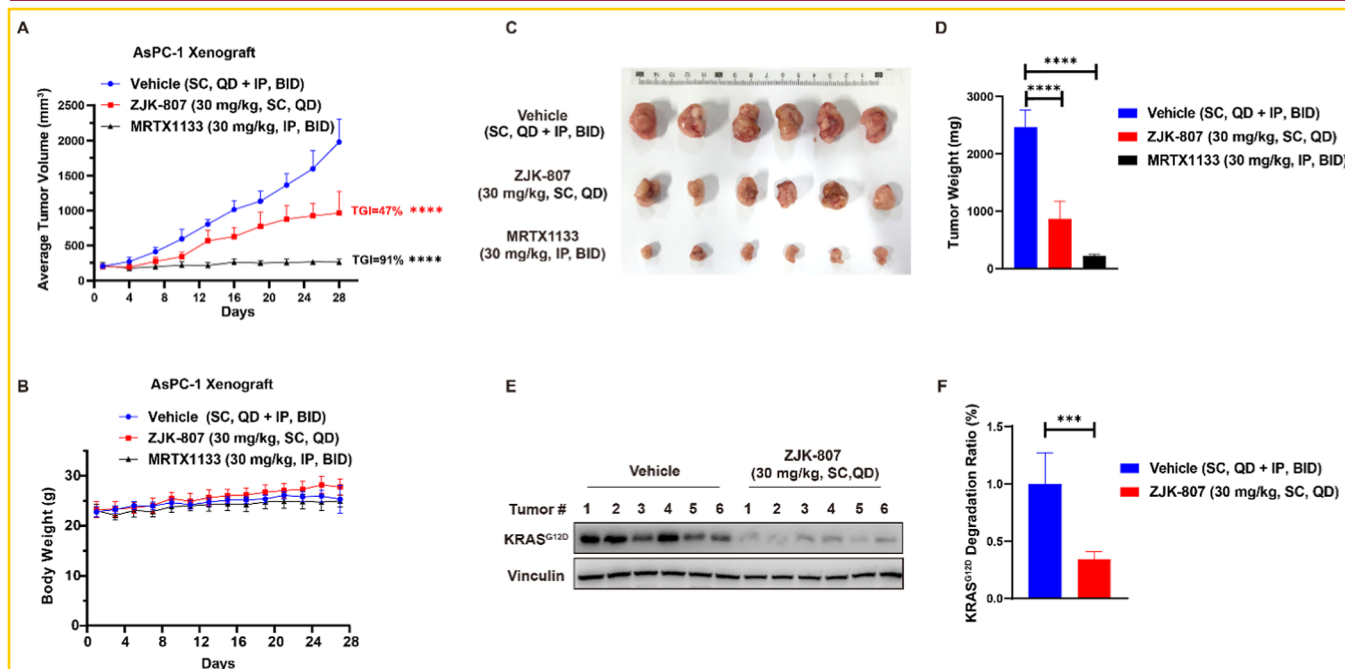


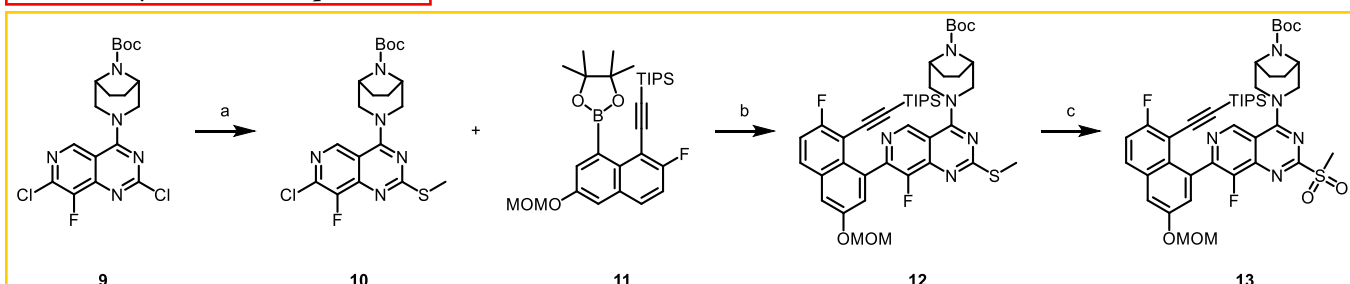
Figure 9. In vivo antitumor efficiency of ZJK-807 in the AsPC-1 xenograft mice. (A) Tumor volumes curves in BALB/c nude mice treated with ZJK-807 (30 mg/kg once daily, SC) or MRTX1133 (30 mg/kg twice daily, IP) for 28 days. Tumor volumes were measured every 3 days. (B) The body weight of BALB/c nude mice (measured every 2 days for 28 days). (C) Macroscopic images of dissected tumors. (D) Quantitative analysis of tumor weights across the control and treatment groups. Differences in means between groups were analyzed by Ordinary one-way ANOVA. Western blot analysis (E) and quantification (F) of KRAS^{G12D} expression in tumor tissues. Differences in means between groups were analyzed by two-tailed unpaired t-test. Data are presented as mean \pm SD. *** $p < 0.001$ and **** $p < 0.0001$.

tion efficacy of ZJK-807. Our data indicate that ZJK-807 retains the ability to reduce KRAS^{G12D} protein levels in a concentration-dependent manner, even in the presence of secondary mutations (Figure 8A,B). These findings suggest that ZJK-807 has the potential to overcome acquired resistance to MRTX1133. To further validate this, we used Ba/F3 cell models expressing KRAS^{G12D}, KRAS^{G12D/95mut} and KRAS^{G12D/96mut} secondary mutants to evaluate the antitumor activity of ZJK-807. We confirmed that Ba/F3 cells harboring KRAS^{G12D/95mut} or KRAS^{G12D/96mut} exhibited acquired resistance to MRTX1133 (Figure 8C). In contrast to MRTX1133, although ZJK-807 exhibited a partial loss of inhibitory potency, it remained capable of suppressing the proliferation of these mutant cells (Figure 8D). Our results collectively indicate that ZJK-807 efficiently degrades secondary mutant KRAS^{G12D} proteins and, to a certain extent, inhibits the growth of resistant cells, highlighting its potential to address MRTX1133 resistance driven by secondary mutations.

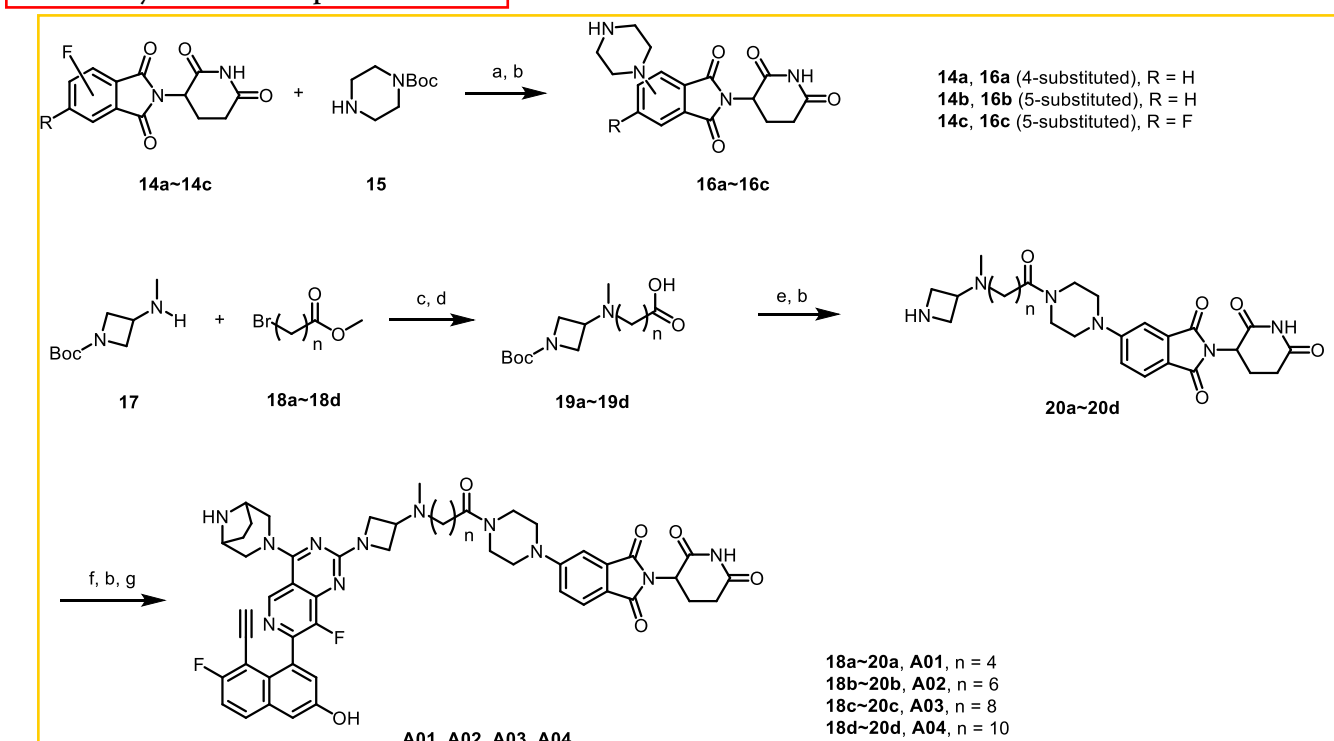
To comprehensively evaluate the genome-wide impact of ZJK-807 and explore its mechanisms, we conducted RNA-seq analysis on AsPC-1 cells treated with either MRTX1133 or ZJK-807. Cluster analysis of differentially expressed genes (DEGs) identified 1526 significantly up-regulated genes following ZJK-807 treatment, with 1190 overlapping those up-regulated by

MRTX1133 (Figure 8E). Additionally, 1995 genes were significantly down-regulated by ZJK-807, of which 1452 overlapped with those down-regulated by MRTX1133 (Figure 8F). Gene Set Enrichment Analysis (GSEA) further revealed that ZJK-807 significantly down-regulated a cluster of genes associated with the RAS and MAPK signaling pathways, a pattern similar to that observed with MRTX1133 (Figure 8G). Pathway analysis using the KEGG database identified the top 20 significantly enriched biological pathways, showing that DEGs were notably enriched in pathways such as the cell cycle and MAPK signaling following ZJK-807 treatment (Figure 8I), consistent with the results from MRTX1133 treatment (Figure 8H). Notably, ZJK-807 also enriched pathways related to the TNF signaling pathway, and Ribosome biogenesis in eukaryotes. These findings suggest distinct downstream effects between KRAS^{G12D} protein degradation and inhibition, and ZJK-807 may additionally exert its anticancer effects in a different way compared with MRTX1133.

Antitumor Activity of ZJK-807 in AsPC-1 Xenograft Tumor Model. Based on its favorable PK profile characterized by prolonged half-life, extended retention time, and high plasma exposure, ZJK-807 was selected for SC administration. The antitumor efficacy of ZJK-807 was evaluated in BALB/c nude mice model bearing AsPC-1 xenograft tumors. When the

Scheme 1. Synthesis of Compound 13^a

^aReagents and conditions: (a) MeSNa, Bn₃NBr, MeOH, 45 °C, 3 h, 85%; (b) cataCXium A Pd G3, K₃PO₄, 1,4-dioxane, H₂O, 110 °C, 16 h, 90%; (c) m-CBPA, DCM, 0 °C, 2 h, 52%. Boc = *tert*-butoxycarbonyl, MOM = methoxymethyl, TIPS = triisopropylsilyl, DIPEA = N,N-diisopropylethylamine.

Scheme 2. Synthesis of Compounds A01-A04^a

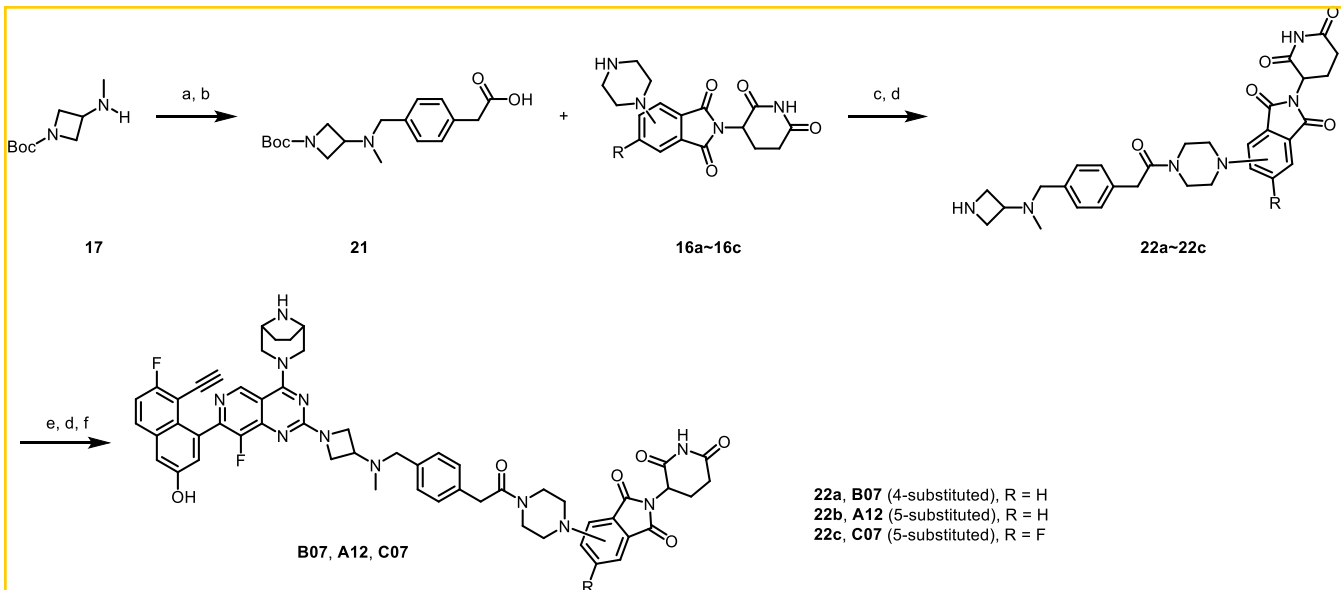
^aReagents and conditions: (a) DIPEA, DMF, 110 °C, 2 h, 75–86%; (b) 4 M HCl in 1,4-dioxane, 0 °C, 45 min; (c) K₃CO₃, MeCN, 60 °C, 6 h; (d) LiOH·H₂O, THF/H₂O, 40 °C, 12 h; (e) 16b, HATU, DIPEA, DMF, rt, 5 h, 43–60% in total; (f) DIPEA, DMF, 45 °C, 5 h; (g) CsF, DMF, rt, 12 h, 32–68% in total. Boc = *tert*-butoxycarbonyl, MOM = methoxymethyl, TIPS = triisopropylsilyl, DIPEA = N,N-diisopropylethylamine.

average tumor volume reached approximately 200 mm³, the mice were randomized into groups (*n* = 6) and administered vehicle, MRTX1133 (30 mg/kg, BID, IP), or ZJK-807 (30 mg/kg, QD, SC) for 28 days. The results depicted that SC administration of ZJK-807 at 30 mg/kg significantly inhibited tumor growth by 47% compared to the vehicle group (Figure 9A). While ZJK-807 demonstrates considerable *in vivo* activity, its efficacy is notably inferior to that of the inhibitor MRTX1133. This disparity in *in vivo* performance aligns closely with the trends observed in vitro, where ZJK-807 likely displays reduced potency relative to MRTX1133. Notably, no body weight loss was observed throughout the treatment period, indicating favorable *in vivo* tolerability (Figure 9B). Tumor tissues were collected and weighed, revealing a significant reduction in tumor weight following ZJK-807 treatment (Figure 9C,D). Furthermore, Western blot analysis was performed to assess KRAS^{G12D} protein expression in the tumor tissues (Figure 9E,F).

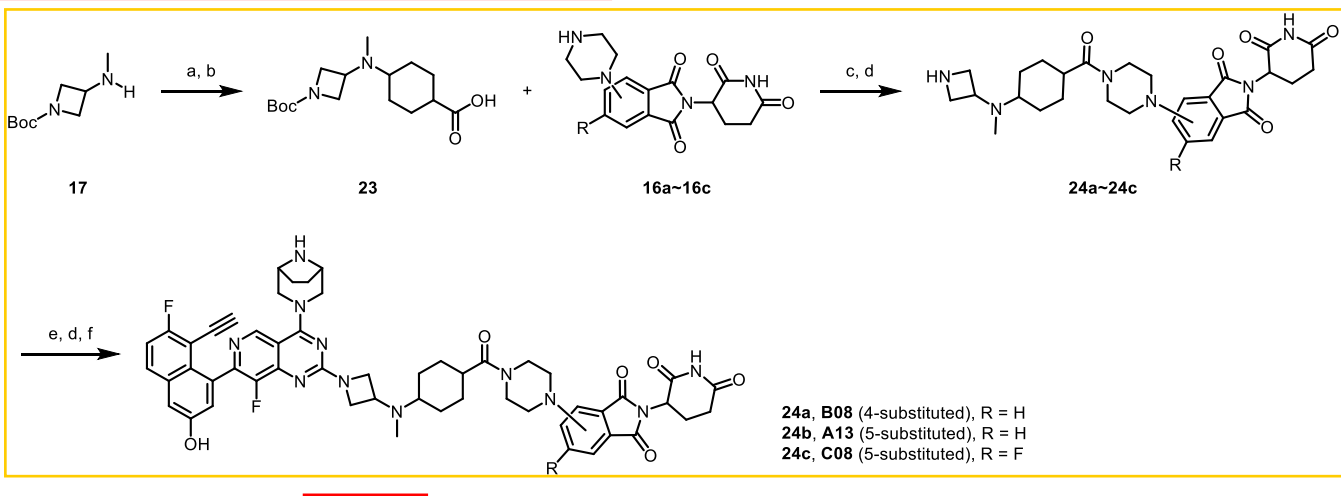
While ZJK-807 exhibited promising antitumor activity, its efficacy was notably less pronounced than that of the inhibitor MRTX1133. This disparity may be attributed to several factors. First, as a PROTAC, ZJK-807 has a larger molecular weight, which could lead to reduced membrane permeability compared to the smaller inhibitor MRTX1133. Second, despite its favorable PK profile, ZJK-807 may result in lower drug exposure at the tumor tissue relative to MRTX1133. These factors could collectively contribute to the observed difference in *in vivo* potency.

CHEMISTRY

The intermediate 9 was prepared as previously reported.¹⁵ The synthesis of compound 13 is shown in Scheme 1. Compound 10 was obtained by a substitution reaction of compound 9 and MeSNa. A Suzuki coupling of compounds 10 and 11 in the

Scheme 3. Synthesis of Compounds B7, A12, and C07^a

^aReagents and conditions: (a) methyl 2-(4-(bromomethyl)phenyl)acetate, K_2CO_3 , MeCN, $60\text{ }^\circ C$, 6 h; (b) $LiOH \cdot H_2O$, THF, H_2O , $40\text{ }^\circ C$, 12 h; (c) HATU, DIPEA, DMF, rt, 5 h [48–63% in total]; (d) 4 M HCl in 1,4-dioxane, MeOH, rt, 1 h; (e) DIPEA, DMF, $45\text{ }^\circ C$, 5 h; (f) CsF, DMF, rt, 12 h, 35–49% in total. Boc = *tert*-butoxycarbonyl, MOM = methoxymethyl, TIPS = triisopropylsilyl, DIPEA = *N,N*-diisopropylethylamine.

Scheme 4. Synthesis of Compounds B08, A13, and C08^a

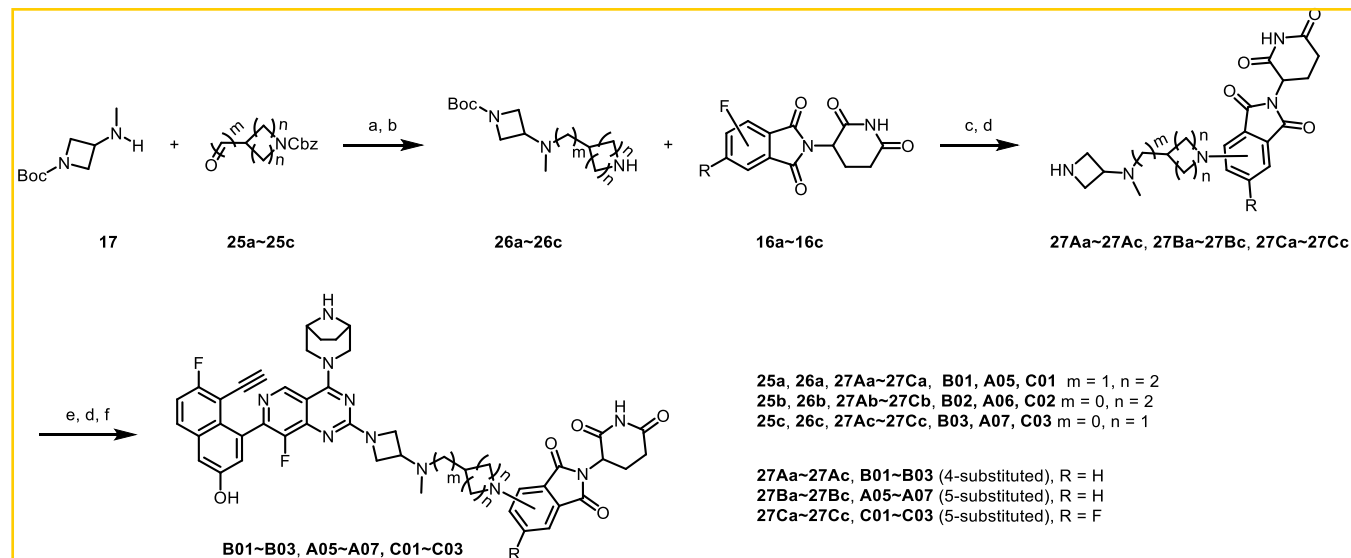
^aReagents and conditions: (a) methyl 4-oxocyclohexane-1-carboxylate, $NaBH(OAc)_3$, DCM, rt, 8 h; (b) $LiOH \cdot H_2O$, THF, H_2O , $40\text{ }^\circ C$, 12 h; (c) HATU, DIPEA, DMF, rt, 5 h [30–42% in total]; (d) 4 M HCl in 1,4-dioxane, MeOH, rt, 1 h; (e) DIPEA, DMF, $45\text{ }^\circ C$, 5 h; (f) CsF, DMF, rt, 12 h, 28–36% in total. Boc = *tert*-butoxycarbonyl, MOM = methoxymethyl, TIPS = triisopropylsilyl, DIPEA = *N,N*-diisopropylethylamine.

presence of cataCXium A Pd G3 and K_3PO_4 in 1,4-dioxane and H_2O gave intermediate 12. Compound 13 was obtained by an oxidation reaction of compound 12 under *m*-CBPA.

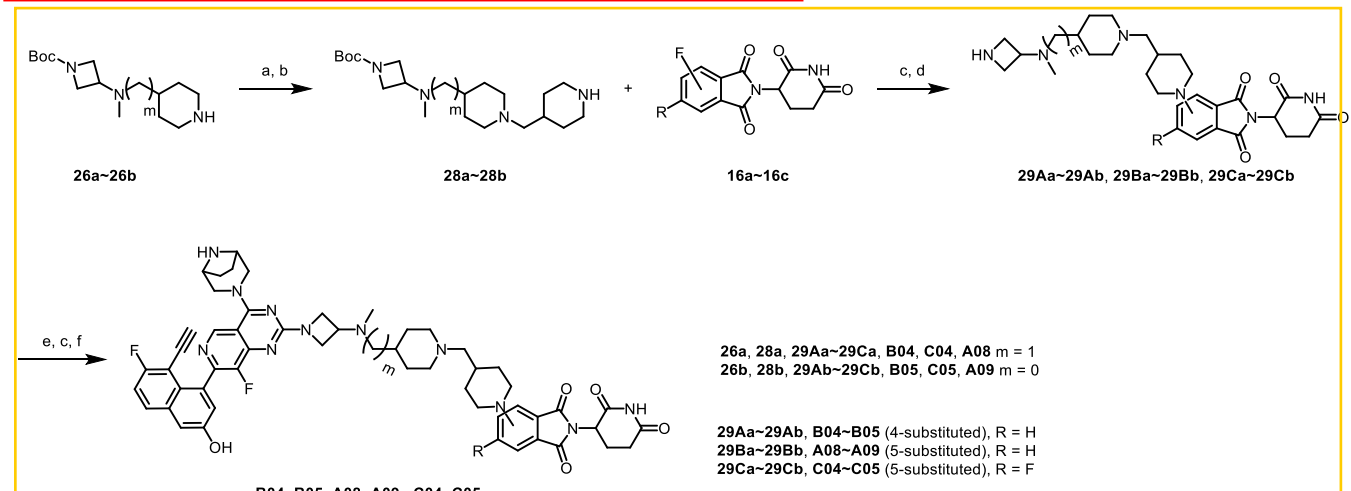
The synthesis of compounds A01 ~ A04 is shown in Scheme 2. The intermediates 16a~16c were obtained from a substitution reaction of compound 15 with the CRBN ligands 14a~14c followed by a deprotection reaction under HCl. After the reaction of compounds with different numbers of methylene groups (18a~18d) and compound 17, a demethylation reaction under $LiOH \cdot H_2O$ was conducted to produce compounds 19a~19d. Compounds 20a~20d were obtained by a condensation reaction of compounds 19a~19d and compound 16b, followed by deprotection under HCl. Compounds A01~A04

were produced from a substitution reaction of 20a~20d with 13 followed by removing the Boc and MOM protecting groups under HCl, and removing the triisopropylsilyl group under CsF.

The synthesis of compounds B07, A12, and C07 is shown in Scheme 3. The intermediates 21 was obtained from a substitution reaction of compound 17 with methyl 2-(4-(bromomethyl)phenyl)acetate followed by a demethylation reaction. Compounds 22a~22c were produced from intermediates 21 and 16a~16c according to the method in Scheme 2. Compounds B07, A12, and C07 were produced from intermediates 13 and 22a~22c according to the method in Scheme 2.

Scheme 5. Synthesis of Compounds B01–B03, A05–A7, and C01–C03^a

^aReagents and conditions: (a) NaBH(OAc), DCM, rt, 8 h; (b) H₂, Pd/C, MeOH, 40 °C, 12 h; (c) DIPEA, DMF, 110 °C, 2 h, 21–52%; (d) 4 M HCl in 1,4-dioxane, MeOH, rt, 1 h; (e) DIPEA, DMF, 45 °C, 5 h; (f) CsF, DMF, rt, 12 h, 32–66% in total. Boc = *tert*-butoxycarbonyl, MOM = methoxymethyl, TIPS = triisopropylsilyl, DIPEA = N,N-diisopropylethylamine.

Scheme 6. Synthesis of Compounds B04–B05, A08–A09, and C04–C05^a

^aReagents and conditions: (a) 25a, NaBH(OAc), DCM, rt, 8 h; (b) H₂, Pd/C, MeOH, 40 °C, 12 h; (c) DIPEA, DMF, 110 °C, 2 h, 34–66%; (d) 4 M HCl in 1,4-dioxane, MeOH, rt, 1 h; (e) DIPEA, DMF, 45 °C, 5 h; (f) CsF, DMF, rt, 12 h, 30–53% in total. Boc = *tert*-butoxycarbonyl, MOM = methoxymethyl, TIPS = triisopropylsilyl, DIPEA = N,N-diisopropylethylamine.

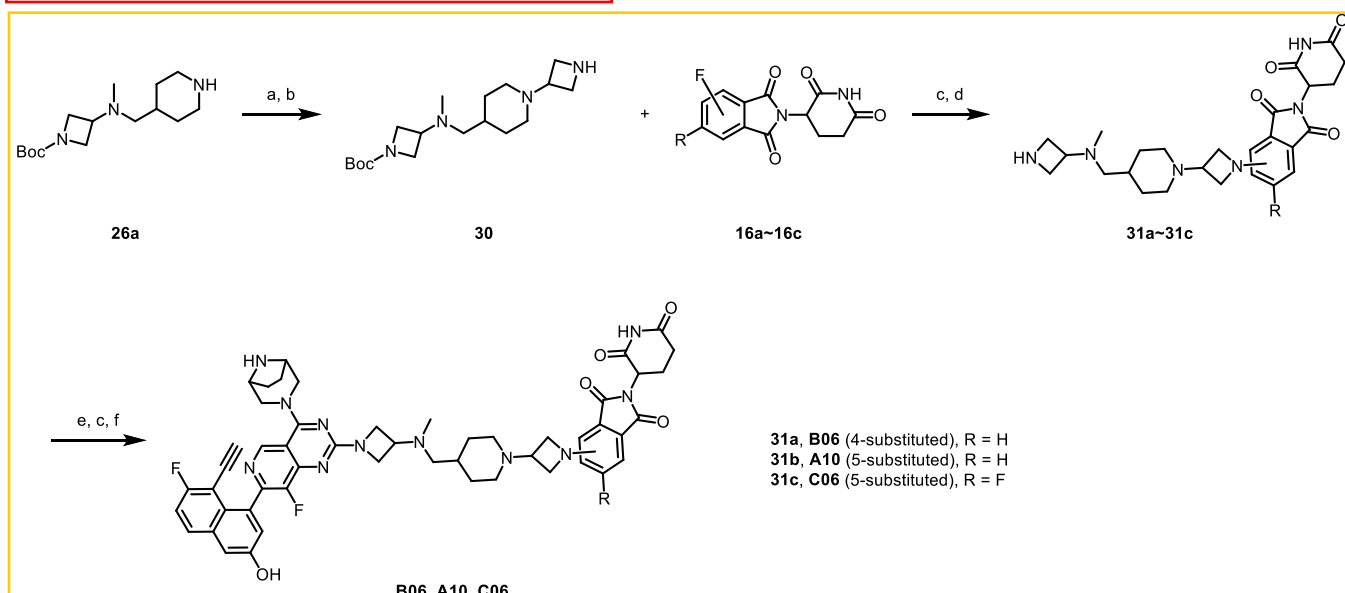
The synthesis of compounds B08, A13, and C08 is shown in Scheme 4. The intermediate 23 was obtained from a reduction amination reaction of compound 17 with methyl 4-oxocyclohexane-1-carboxylate followed by a demethylation reaction. Compounds 24a–24c were produced from intermediates 23 and 16a–16c according to the method in Scheme 2. Compounds B08, A13, and C08 were produced from intermediates 13 and 24a–24c according to the method in Scheme 2.

The synthesis of compounds B01 ~ B03, A05 ~ A07, and C01 ~ C03 is shown in Scheme 5. The intermediates 26a ~ 26c were obtained from a reduction amination reaction of compound 17 with 25a ~ 25c followed by deprotection of the NHCbz group. Compounds 27Aa ~ 27Ad, 27Ba ~ 27Bc, and 27Ca ~ 27Cc were produced from a substitution reaction of

intermediates 26a ~ 26c and 16a ~ 16c. Compounds B01 ~ B03, A05 ~ A07, and C01 ~ C03 were produced from intermediates 13 and compounds 27Aa ~ 27Ad, 27Ba ~ 27Bc, and 27Ca ~ 27Cc according to the method in Scheme 2.

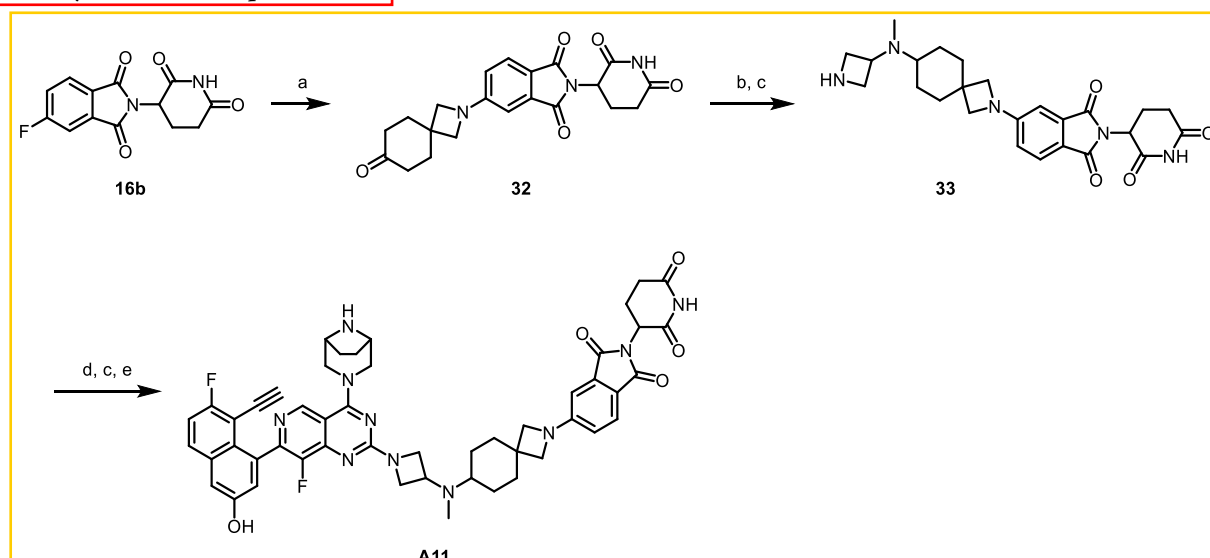
The synthesis of compounds B04 ~ B05, A08 ~ A09, and C04 ~ C05 is shown in Scheme 6. The intermediates 28a ~ 28b were obtained from a reduction amination reaction of compound 26a ~ 26b and benzyl 4-formylpiperidine-1-carboxylate followed by deprotection of the NHCbz group. Compounds 29Aa ~ 29Ab, 29Ba ~ 29Bb, and 29Ca ~ 29Cb were produced from intermediates 28a ~ 28b and 16a ~ 16c according to the method in Scheme 5. Compounds B04 ~ B05, A08 ~ A09, and C04 ~ C05 were produced from intermediates 13 and compounds 29Aa ~ 29Ab, 29Ba ~ 29Bb, and 29Ca ~ 29Cb according to the method in Scheme 2.

Scheme 7. Synthesis of Compounds A10, B06 and C06^a



^aReagents and conditions: (a) 25c, NaBH(OAc), DCM, rt, 8 h; (b) H₂, Pd/C, MeOH, 40 °C, 12 h; (c) DIPEA, DMF, 110 °C, 2 h, 42–55%; (d) 4 M HCl in 1,4-dioxane, MeOH, rt, 1 h; (e) DIPEA, DMF, 45 °C, 5 h; (f) CsF, DMF, rt, 12 h, 39–61% in total. Boc = *tert*-butoxycarbonyl, MOM = methoxymethyl, TIPS = triisopropylsilyl, DIPEA = N,N-diisopropylethylamine.

Scheme 8. Synthesis of Compounds A11^a



^aReagents and conditions: (a) 2-azaspiro[3.5]nonan-7-one, DIPEA, DME, 110 °C, 2 h, 82%; (b) 17, NaBH(OAc)₃, DCM, rt, 8 h, 43%; (c) 4 M HCl in 1,4-dioxane, MeOH, rt, 1 h; (d) DIPEA, DMF, 45 °C, 5 h; (e) CsF, DMF, rt, 12 h, 36% in total. Boc = *tert*-butoxycarbonyl, MOM = methoxymethyl, TIPS = triisopropylsilyl. DIPEA = N,N-diisopropylethylamine.

The synthesis of compounds B06, A10, and C06 is shown in Scheme 7. The intermediate 30 was obtained from a reduction amination reaction of compound 26a and benzyl 3-oxoazetidine-1-carboxylate followed by deprotection of the NHCbz group. Compounds 31a~31c were produced from intermediates 30 and 16a~16c according to the method in Scheme 5. Compounds B06, A10, and C06 were produced from intermediates 13 and compounds 31a~31c according to the method in Scheme 2.

The synthesis of compounds **A11** is shown in Scheme 8. The intermediates **32** was obtained from a substitution reaction of compound **16b** and 2,2-aspiro[3.5]nonan-7-one. Compound

33 was obtained from a reduction amination reaction of compounds **17** and **32** followed by a deprotection reaction under HCl. Compounds **A11** was produced from intermediates **13** and **33** according to the method in Scheme 2.

■ CONCLUSIONS

Pancreatic cancer remains one of the most aggressive and lethal malignancies, with KRAS^{G12D} mutation serving as a central driver of tumorigenesis and progression. Despite decades of research, directly targeting KRAS^{G12D} has proven to be a formidable challenge due to its complex structure and lack of traditional druggable pockets.

Currently, KRAS^{G12D} targeting degraders include both mutant-selective degraders and pan-KRAS degraders. Selective KRAS degraders (e.g., ASP3082, RP03707⁴⁰ for KRAS^{G12D} mutant) exhibit high antitumor activity in specific cancer types through precise degradation of specific mutation types (KRAS^{G12D} is highly prevalent in pancreatic and colorectal cancers), but their efficacy is limited by the singularity of the mutant subtype. Selective degraders are indicated for patients with well-defined driver mutations and easier to optimize for clinical safety due to their target specificity. In contrast, pan-KRAS degraders (e.g., ACBI3³¹) can simultaneously degrade 13 common KRAS mutants (including KRAS^{G12D}, KRAS^{G12V}, etc.), yet the broad spectrum of pan-degraders can also degrade WT-KRAS may be associated with potential off-target risks.

In this study, we addressed this unmet need to degrade KRAS^{G12D} by designing and synthesizing a novel series of PROTACs, which combine KRAS^{G12D} inhibitors with CCRN E3 ligase ligands to achieve targeted degradation of the oncprotein. Among these, ZJK-807 emerged as a standout candidate, demonstrating exceptional selectivity and potency in degrading KRAS^{G12D}, with a IC_{50} value of 79.5 ± 5.4 nM in the AsPC-1 pancreatic cancer cell line. Mechanistically, ZJK-807 effectively recruited CCRN E3 ligase to KRAS^{G12D}, leading to its ubiquitination and subsequent proteasomal degradation, thereby suppressing downstream oncogenic signaling pathways. In addition to its potent degradation activity, ZJK-807 exhibited remarkable antiproliferative effects *in vitro*, significantly inhibiting the growth of KRAS^{G12D}-driven cancer cells. *In vivo*, SC administration of ZJK-807 (30 mg/kg) in an AsPC-1 xenograft model resulted in substantial tumor growth inhibition (TGI = 47%), accompanied by favorable PK properties and minimal systemic toxicity. ZJK-807 also demonstrated anti-resistance properties against KRAS^{G12D} secondary mutation. These findings highlight the therapeutic potential of ZJK-807 as a targeted degrader of KRAS^{G12D}, offering a promising strategy to overcome the limitations of traditional KRAS inhibitors.

EXPERIMENTAL SECTION

Chemistry. Unless otherwise noted, all purchased reagents were used as received without further purification. ^1H NMR and ^{13}C NMR spectra were recorded on a JEOL INM-EPC 400 or Agilent Pro Pulse 500 MHz spectrometer. ^1H NMR spectra were reported in parts per million (ppm) downfield from tetramethylsilane (TMS). Chemical shifts for all compounds are reported in parts per million (ppm, δ). The format of chemical shift was reported as follows: chemical shift, multiplicity (s = singlet, d = doublet, t = triplet, q = quartet, m = multiplet), coupling constant (J values in Hz), and integration. Mass spectral (MS) measurements were carried out using a Waters UPLC mass spectrometer. The high-resolution mass spectrum (HRMS) was acquired using an ESI (electrospray ionization) method on a Bruker Apex IV FTMS mass spectrometer. The final compounds were all purified by a C18 reversed-phase preparative HPLC column with solvent A (0.1% TFA in H_2O) and solvent B (CH_3CN) as eluents. The purity of all the final compounds was confirmed to be >95% by UPLC-MS {10 to 100% MeCN (0.1% TFA)/ H_2O (0.1% TFA) in 15 min}.

General Procedure for the Synthesis of Compounds A01–A04. A mixture of 9 (100 mg, 0.23 mmol, 1.0 equiv), MeSNa (0.06 mL, 0.25 mmol, 1.1 equiv), Bu_3NBr (3 mg, 0.01 mmol, 0.05 equiv), in MeOH was stirred at 45 °C for 3 h. The mixture was diluted with water and extracted with DCM. The organic layers were separated, washed with brine, dried, and concentrated in vacuo. The compound 10 (86 mg, 85%) was obtained by prep-TLC (DCM/MeOH) = 30/1.

A mixture of 10 (86 mg, 0.19 mmol, 1.0 equiv), 11 (118 mg, 0.23 mmol, 1.2 equiv), cataCXium A Pd G3 (14 mg, 0.019 mmol, 0.01 equiv), and K_3PO_4 (121 mg, 0.57 mmol, 3.0 equiv) in 3.2 mL/0.64 mL

(v/v) 1,4-dioxane/ H_2O was stirred under argon at 110 °C for 16 h. After being cooled to rt, the mixture was diluted with water and extracted with DCM. The organic layers were separated, washed with brine, dried, and concentrated in vacuo. The compound 12 (135 mg, 90%) was obtained by prep-TLC (DCM/MeOH) = 30/1. ^1H NMR (400 MHz, $\text{DMSO}-d_6$) δ : 9.16 (s, 1H), 8.13–8.04 (m, 1H), 7.73 (d, J = 2.6 Hz, 1H), 7.53 (t, J = 8.9 Hz, 1H), 7.33 (d, J = 2.6 Hz, 1H), 5.35 (s, 2H), 4.83–4.75 (m, 1H), 4.30–4.16 (m, 2H), 3.83–3.74 (m, 1H), 3.42 (s, 3H), 3.38–3.33 (m, 2H), 2.53 (s, 3H), 1.92–1.78 (m, 3H), 1.68–1.55 (m, 2H), 1.44 (s, 9H), 0.81–0.77 (m, 18H), 0.48–0.38 (m, 3H). m-CBPA (59 mg, 0.34 mmol, 2.0 equiv) was added to a solution of compound 12 (135 mg, 0.17 mmol, 1.0 equiv) in DCM (1.5 mL). The mixture was stirred at 0 °C. After 2 h the mixture was diluted with water and extracted with DCM. The organic layers were separated, washed with brine, dried, and concentrated in vacuo. The compound 13 (72 mg, 52%) was obtained by prep-TLC (DCM/MeOH = 20/1). ^1H NMR (400 MHz, Methanol- d_4) δ : 9.32 (s, 1H), 7.97–7.93 (m, 1H), 7.65 (d, J = 2.5 Hz, 1H), 7.39 (t, J = 8.9 Hz, 1H), 7.28 (d, J = 2.6 Hz, 1H), 5.32 (s, 2H), 5.07–4.99 (m, 1H), 4.52–4.45 (m, 2H), 4.42–4.35 (m, 1H), 4.04–3.96 (m, 1H), 3.64–3.56 (m, 1H), 3.48 (s, 3H), 3.40 (s, 3H), 2.04–1.86 (m, 3H), 1.71–1.64 (m, 1H), 1.52 (s, 9H), 0.87–0.82 (m, 18H), 0.55–0.40 (m, 3H).

A mixture of compounds 15 (100 mg, 0.54 mmol, 1.0 equiv), 14b (149 mg, 0.54 mmol, 1.0 equiv) and DIPEA (0.38 mL, 2.16 mmol, 4.0 equiv) in dry DMF (5 mL) was stirred under argon at 110 °C for 2 h. After being cooled to rt, the mixture was diluted with water and extracted with DCM. The organic layers were separated, washed with brine, dried, and concentrated in vacuo. The intermediate (195 mg, 82%) was obtained by prep-TLC (DCM/MeOH) = 30/1. The intermediate was dissolved in MeOH (5 mL), HCl (4 M in 1,4-dioxane, 2 mL, 16 equiv) was added. The mixture was stirred at 0 °C. After 45 min, the volatiles were removed under reduced pressure to afford compound 16b. The crude compound 16b was used directly for the next step without further purification.

A mixture of Compounds 17 (200 mg, 1.07 mmol, 1.0 equiv), 18a (310 mg, 1.60 mmol, 1.5 equiv) and K_2CO_3 (444 mg, 3.21 mmol, 3.0 equiv) in MeCN (7 mL) was stirred at 60 °C for 6 h. After being cooled to rt, the mixture was diluted with water and extracted with DCM. The organic layer was separated, dried, and concentrated in vacuo. The residue obtained above was dissolved in 20 mL/10 mL (v/v) THF/ H_2O and LiOH· H_2O (224 mg, 5.35 mmol, 5.0 equiv) was added. The mixture was stirred at 45 °C for 12 h. The residue was diluted with water and the pH was adjusted to 2–3 with 3N HCl. The organic layers were separated, washed with brine, dried, and concentrated in vacuo. The crude compound 19a was used directly for the next step without further purification.

To a stirred solution of compounds 19a (306 mg, 1.07 mmol, 1.0 equiv), 16b (296 mg, 1.07 mmol, 1.0 equiv) and DIPEA (0.74 mL, 4.28 mmol, 4.0 equiv) in dry DMF (2 mL) was added HATU (1.2 g mg, 3.21 mmol, 3.0 equiv) at 0 °C. The reaction was allowed to stir at rt for 5 h. The mixture was diluted with water and extracted with DCM. The organic layers were separated, washed with brine, dried, and concentrated in vacuo. The intermediate (340 mg, 52% in total) was obtained by prep-TLC (DCM/MeOH) = 30/1. The intermediate obtained above was dissolved in MeOH (5 mL) and HCl (4 M in 1,4-dioxane, 2 mL, 16 equiv) was added. The mixture was stirred at rt for 1 h. After removing the solvent, the crude compound 20a was obtained and was used directly for the next step without further purification.

A mixture of compounds 20a (100 mg, 0.20 mmol, 1.0 equiv), 13 (164 mg, 0.20 mmol, 1.0 equiv) and DIPEA (0.14 mL, 0.80 mmol, 4.0 equiv) in dry DMF (2 mL) was stirred under argon at 45 °C for 5 h. After being cooled to rt, the mixture was diluted with water and extracted with DCM. The organic layers were separated, washed with brine, dried, and concentrated in vacuo. The residues were dissolved in MeOH (1 mL) and HCl (4 M in 1,4-dioxane, 0.8 mL, 16 equiv) was added. The mixture was stirred at 0 °C. After 45 min, the volatiles were removed under reduced pressure. The residues were dissolved in DMF (0.5 mL) and CsF (304 mg, 2.00 mmol, 10 equiv) was added. The mixture was stirred at rt for 12 h and then was filtered. The organic layers were concentrated in vacuo. Compound A01 (87 mg, 46% in

total) was obtained by preparative HPLC. Following the procedures used to prepare compound A01, compounds A02–A04 were obtained by the same methods.

5-(4-(5-((1-(4-((1R,5S)-3,8-diazabicyclo[3.2.1]octan-3-yl)-7-(8-ethynyl-7-fluoro-3-hydroxynaphthalen-1-yl)-8-fluoropyrido[4,3-d]pyrimidin-2-yl)azetidin-3-yl)(methyl)amino)pentanoyl)piperazin-1-yl)-2-(2,6-dioxopiperidin-3-yl)isoindoline-1,3-dione (A01). ^1H NMR (400 MHz, Methanol- d_4) δ : 8.92 (s, 1H), 7.87 (dd, J = 9.2, 5.7 Hz, 1H), 7.58 (d, J = 41.7 Hz, 1H), 7.38 (d, J = 2.5 Hz, 1H), 7.35–7.26 (m, 2H), 7.23 (d, J = 2.6 Hz, 1H), 7.16 (d, 1H), 5.07 (dd, J = 12.5, 5.5 Hz, 1H), 4.79–4.68 (m, 2H), 4.64–4.49 (m, 4H), 4.36–4.29 (m, 1H), 4.25 (d, J = 9.1 Hz, 2H), 3.95 (d, J = 13.9 Hz, 1H), 3.87 (d, J = 14.1 Hz, 1H), 3.81–3.69 (m, 4H), 3.53 (s, 1H), 3.50–3.43 (m, 4H), 2.94 (s, 3H), 2.88–2.82 (m, 1H), 2.80–2.64 (m, 2H), 2.58 (t, 2H), 2.20–2.08 (m, 6H), 1.91–1.81 (m, 2H), 1.80–1.72 (m, 2H), 1.30–1.28 (m, 2H). ^{13}C NMR (125 MHz, Methanol- d_4) δ : 174.6, 171.7, 169.2, 168.9, 165.5, 165.3, 163.3, 161.6, 156.6, 155.6, 143.9, 135.5, 134.2, 131.7, 131.7, 130.8, 127.0, 126.0, 124.3, 121.0, 119.3, 113.4, 110.9, 109.3, 90.2, 76.2, 56.4, 56.4, 53.7, 52.8, 52.2, 50.4, 48.0, 45.9, 42.3, 33.1, 32.8, 32.2, 28.1, 26.9, 25.8, 25.7, 24.8, 23.8. HRMS (ESI-Q-TOF): m/z calcd for $C_{25}H_{30}F_2N_4O_6$ [M + H] $^+$: 952.4065; found, 952.4088. UPLC–MS: m/z calcd for $C_{25}H_{30}F_2N_4O_6$ [M + H] $^+$: 952.41; found, 952.36. UPLC-retention time: 3.05 min, purity >95%.

5-(4-(7-((1-(4-((1R,5S)-3,8-diazabicyclo[3.2.1]octan-3-yl)-7-(8-ethynyl-7-fluoro-3-hydroxynaphthalen-1-yl)-8-fluoropyrido[4,3-d]pyrimidin-2-yl)azetidin-3-yl)(methyl)amino)heptanoyl)piperazin-1-yl)-2-(2,6-dioxopiperidin-3-yl)isoindoline-1,3-dione (A02). ^1H NMR (400 MHz, Methanol- d_4) δ : 8.97 (s, 1H), 7.89 (dd, 1H), 7.65 (d, J = 8.4 Hz, 1H), 7.42 (d, J = 2.5 Hz, 1H), 7.36 (t, J = 8.8 Hz, 1H), 7.32 (d, J = 8.4 Hz, 1H), 7.28 (d, J = 2.8 Hz, 1H), 7.18 (d, J = 8.3 Hz, 1H), 5.07 (dd, J = 12.4, 5.4 Hz, 1H), 4.84–4.67 (m, 2H), 4.67–4.54 (m, 4H), 4.38–4.30 (m, 1H), 4.25 (d, J = 12.9 Hz, 2H), 4.01 (d, J = 14.5 Hz, 1H), 3.89 (d, J = 14.1 Hz, 1H), 3.77–3.71 (m, 4H), 3.58–3.54 (m, 1H), 3.53–3.44 (m, 4H), 2.93 (s, 3H), 2.88–2.81 (m, 1H), 2.79–2.66 (m, 2H), 2.47 (t, J = 7.3 Hz, 2H), 2.22–2.06 (m, 6H), 1.86–1.76 (m, 2H), 1.71–1.62 (m, 2H), 1.51–1.43 (m, 4H), 1.33–1.28 (m, 2H). ^{13}C NMR (125 MHz, Methanol- d_4) δ : 174.6, 174.1, 171.7, 169.3, 168.9, 165.3, 163.3, 161.4, 156.7, 155.6, 143.5, 135.5, 134.2, 131.8, 131.7, 126.9, 126.0, 124.5, 121.0, 119.3, 117.4, 117.2, 113.7, 110.8, 109.3, 105.2, 105.1, 90.3, 76.1, 62.2, 56.4, 56.4, 53.8, 52.7, 52.2, 50.4, 48.0, 46.0, 42.3, 38.0, 33.6, 32.2, 30.8, 30.7, 30.5, 30.3, 29.5, 25.8, 25.8, 25.7, 24.8, 23.8. HRMS (ESI-Q-TOF): m/z calcd for $C_{31}H_{36}F_2N_4O_6$ [M + H] $^+$: 980.4378; found, 980.4378. UPLC–MS: m/z calcd for $C_{31}H_{36}F_2N_4O_6$ [M + H] $^+$: 980.44; found, 980.44. UPLC-retention time: 3.40 min, purity >95%.

5-(4-((1-(4-((1R,5S)-3,8-diazabicyclo[3.2.1]octan-3-yl)-7-(8-ethynyl-7-fluoro-3-hydroxynaphthalen-1-yl)-8-fluoropyrido[4,3-d]pyrimidin-2-yl)azetidin-3-yl)(methyl)amino)nonanoyl)piperazin-1-yl)-2-(2,6-dioxopiperidin-3-yl)isoindoline-1,3-dione (A03). ^1H NMR (400 MHz, Methanol- d_4) δ : 8.90 (s, 1H), 7.85 (dd, J = 9.2, 5.7 Hz, 1H), 7.64 (d, J = 8.4 Hz, 1H), 7.36 (d, J = 2.5 Hz, 1H), 7.32 (t, J = 9.0 Hz, 1H), 7.29 (d, J = 2.2 Hz, 1H), 7.22 (d, J = 2.6 Hz, 1H), 7.17 (d, J = 8.5 Hz, 1H), 5.05 (dd, J = 12.5, 5.4 Hz, 1H), 4.75–4.67 (m, 2H), 4.61–4.46 (m, 4H), 4.33–4.27 (m, 1H), 4.22 (d, J = 9.0 Hz, 2H), 3.91 (d, J = 14.0 Hz, 1H), 3.86 (d, J = 14.0 Hz, 1H), 3.75–3.68 (m, 4H), 3.49–3.42 (m, SH), 2.90 (s, 3H), 2.86–2.79 (m, 1H), 2.76–2.62 (m, 2H), 2.42 (t, J = 7.5 Hz, 2H), 2.20–2.03 (m, 6H), 1.78–1.69 (m, 2H), 1.65–1.56 (m, 2H), 1.41–1.35 (m, 8H), 1.28–1.25 (m, 2H). ^{13}C NMR (125 MHz, Methanol- d_4) δ : 174.6, 174.1, 171.7, 169.3, 168.9, 163.3, 161.5, 156.7, 155.6, 155.6, 135.5, 134.2, 131.7, 131.6, 127.0, 126.0, 124.3, 121.0, 119.3, 117.3, 117.1, 113.4, 110.9, 109.4, 105.3, 105.2, 90.1, 76.1, 56.4, 56.3, 55.6, 53.7, 52.7, 52.3, 50.4, 48.1, 46.1, 42.3, 38.0, 33.9, 32.2, 30.1, 29.9, 27.4, 26.3, 25.8, 25.7, 25.1, 23.8. HRMS (ESI-Q-TOF): m/z calcd for $C_{37}H_{42}F_2N_4O_6$ [M + H] $^+$: 1008.4691; found, 1008.4699. UPLC–MS: m/z calcd for $C_{37}H_{42}F_2N_4O_6$ [M + H] $^+$: 1008.47; found, 1008.44. UPLC-retention time: 3.91 min, purity >95%.

5-(4-(11-((1-(4-((1R,5S)-3,8-diazabicyclo[3.2.1]octan-3-yl)-7-(8-ethynyl-7-fluoro-3-hydroxynaphthalen-1-yl)-8-fluoropyrido[4,3-d]pyrimidin-2-yl)azetidin-3-yl)(methyl)amino)undecanoyl)piperazin-1-yl)-2-(2,6-dioxopiperidin-3-yl)isoindoline-1,3-dione (A04). ^1H NMR (400 MHz, Methanol- d_4) δ : 8.98 (s, 1H), 7.89 (dd, J = 9.2, 5.6

Hz, 1H), 7.65 (d, J = 8.5 Hz, 1H), 7.41 (d, J = 2.5 Hz, 1H), 7.35 (t, J = 8.9 Hz, 1H), 7.30 (d, J = 2.7 Hz, 2H), 7.17 (d, J = 8.2 Hz, 1H), 5.07 (dd, J = 12.5, 5.4 Hz, 1H), 4.82–4.70 (m, 2H), 4.65–4.53 (m, 4H), 4.36–4.30 (m, 1H), 4.25 (d, J = 11.5 Hz, 2H), 4.00 (d, J = 13.9 Hz, 1H), 3.91 (d, J = 14.0 Hz, 1H), 3.76–3.68 (m, 4H), 3.58–3.54 (m, 1H), 3.50–3.40 (m, 4H), 2.92 (s, 3H), 2.88–2.80 (m, 1H), 2.79–2.64 (m, 2H), 2.42 (t, J = 7.5 Hz, 2H), 2.22–2.04 (m, 6H), 1.82–1.71 (m, 2H), 1.64–1.55 (m, 2H), 1.39–1.28 (m, 14H). ^{13}C NMR (125 MHz, Methanol- d_4) δ : 174.6, 174.4, 171.7, 169.3, 168.9, 165.4, 165.3, 163.3, 161.5, 156.7, 155.6, 155.6, 135.5, 134.2, 131.7, 127.0, 126.0, 124.4, 121.0, 119.3, 117.3, 117.1, 113.5, 110.9, 109.4, 105.3, 105.2, 76.1, 56.4, 56.3, 55.6, 53.7, 52.7, 52.3, 50.4, 48.1, 46.1, 42.3, 38.0, 33.9, 32.2, 30.7, 30.4, 30.4, 30.3, 30.1, 27.5, 26.4, 25.8, 25.7, 25.1, 23.8, 23.7. HRMS (ESI-Q-TOF): m/z calcd for $C_{45}H_{56}F_2N_4O_6$ [M + H] $^+$: 1036.5004; found, 1036.5054. UPLC–MS: m/z calcd for $C_{45}H_{56}F_2N_4O_6$ [M + H] $^+$: 1036.50; found, 1036.51. UPLC-retention time: 4.06 min, purity >95%.

General Procedure for the Synthesis of Compounds B07, A12, and C07. A mixture of Compounds 17 (200 mg, 1.07 mmol, 1.0 equiv), methyl 2-(4-(bromomethyl)phenyl)acetate (389 mg, 1.60 mmol, 1.5 equiv) and K_2CO_3 (444 mg, 3.21 mmol, 3.0 equiv) in MeCN (7 mL) was stirred at 60 °C for 6 h. After being cooled to rt, the mixture was diluted with water and extracted with DCM. The organic layer was separated, dried, and concentrated in vacuo. The residue obtained above was dissolved in 20 mL/10 mL (v/v) THF/H₂O and LiOH·H₂O (224 mg, 5.35 mmol, 5.0 equiv) was added. The mixture was stirred at 45 °C for 12 h. The residue was diluted with water and the pH was adjusted to 2–3 with 3N HCl. The organic layers were separated, washed with brine, dried, and concentrated in vacuo. The crude compound 21 was used directly for the next step without further purification.

To a stirred solution of compounds 21 (357 mg, 1.07 mmol, 1.0 equiv), 16a (366 mg, 1.07 mmol, 1.0 equiv) and DIPEA (0.74 mL, 4.28 mmol, 4.0 equiv) in dry DMF (4 mL) was added HATU (1.22 g, 3.21 mmol, 3.0 equiv) at 0 °C. The reaction was allowed to stir at rt for 5 h. The mixture was diluted with water and extracted with DCM. The organic layers were separated, washed with brine, dried, and concentrated in vacuo. The intermediate (337 mg, 48% in total) was obtained by prep-TLC (DCM/MeOH) = 20/1. The intermediate obtained above was dissolved in MeOH (5 mL) and HCl (4 M in 1,4-dioxane, 2 mL, 16 equiv) was added. The mixture was stirred at rt for 1 h. After removing the solvent, the crude compound 22a was obtained and was used directly for the next step without further purification.

A mixture of compounds 22a (100 mg, 0.18 mmol, 1.0 equiv), 13 (148 mg, 0.18 mmol, 1.0 equiv) and DIPEA (0.12 mL, 0.72 mmol, 4.0 equiv) in dry DMF (2 mL) was stirred under argon at 45 °C for 5 h. After being cooled to rt, the mixture was diluted with water and extracted with DCM. The organic layers were separated, washed with brine, dried, and concentrated in vacuo. The residues were dissolved in MeOH (0.5 mL) and HCl (4 M in 1,4-dioxane, 0.8 mL, 16 equiv) was added. The mixture was stirred at 0 °C. After 45 min, the volatiles were removed under reduced pressure. The residues were dissolved in DMF (0.5 mL) and CsF (273 mg, 1.80 mmol, 10 equiv) was added. The mixture was stirred at rt for 12 h and then was filtered. The organic layers were concentrated in vacuo. Compound B07 (63 mg, 35% in total) was obtained by preparative HPLC. Following the procedures used to prepare compound B07, compounds A12, C07 were obtained by the same methods.

4-(4-(2-(4-((1-(4-((1R,5S)-3,8-diazabicyclo[3.2.1]octan-3-yl)-7-(8-ethynyl-7-fluoro-3-hydroxynaphthalen-1-yl)-8-fluoropyrido[4,3-d]pyrimidin-2-yl)azetidin-3-yl)(methyl)amino)methyl)phenyl)acetyl)piperazin-1-yl)-2-(2,6-dioxopiperidin-3-yl)isoindoline-1,3-dione (B07). ^1H NMR (400 MHz, Methanol- d_4) δ : 8.96 (s, 1H), 7.89 (dd, 1H), 7.63 (t, J = 7.7 Hz, 1H), 7.58–7.49 (m, 2H), 7.44–7.35 (m, 5H), 7.29–7.21 (m, 2H), 5.09 (dd, 1H), 4.80–4.72 (m, 2H), 4.59–4.47 (m, 4H), 4.42–4.37 (m, 2H), 4.25 (d, 2H), 3.91 (s, 3H), 3.81–3.76 (m, 3H), 3.50–3.49 (m, 1H), 3.29–3.22 (m, 4H), 2.85 (s, 3H), 2.78–2.66 (m, 2H), 2.52–2.41 (m, 1H), 2.37–2.31 (m, 1H), 2.22–2.04 (m, 6H), 1.31–1.28 (m, 2H). ^{13}C NMR (125 MHz, Methanol- d_4) δ : 174.7, 174.6, 171.6, 169.3, 168.8, 168.5, 168.0, 165.4, 163.2, 161.4, 155.6, 151.0, 151.0, 139.2, 136.9, 136.8, 135.5, 135.4, 134.2, 132.7, 131.2,

127.0, 124.8, 124.6, 124.3, 119.2, 117.2, 117.0, 116.8, 113.3, 90.2, 76.1, 56.4, 55.9, 53.9, 52.3, 52.1, 51.6, 50.4, 43.2, 40.8, 37.9, 32.1, 31.7, 30.7, 25.8, 25.7, 25.0, 23.7, 23.6. HRMS (ESI-Q-TOF): m/z calcd for $C_{55}H_{50}F_2N_1O_6^+ [M + H]^+$: 1000.4065; found, 1000.4093. UPLC-MS: m/z calcd for $C_{55}H_{50}F_2N_1O_6^+ [M + H]^+$: 1000.41; found, 1000.28. UPLC-retention time: 3.38 min, purity >95%.

5-(4-(2-((1-(4-((1R,5S)-3,8-diazabicyclo[3.2.1]octan-3-yl)-7-(8-ethynyl-7-fluoro-3-hydroxynaphthalen-1-yl)-8-fluoropyrido[4,3-d]-pyrimidin-2-yl)azetidin-3-yl)(methyl)amino)methyl)phenyl)acetyl)piperazin-1-yl)-2-(2,6-dioxopiperidin-3-yl)isoindoline-1,3-dione (A12). 1H NMR (400 MHz, Methanol- d_4) δ : 8.91–8.88 (m, 1H), 7.85 (dd, $J = 9.1, 5.6$ Hz, 1H), 7.59 (d, $J = 8.4$ Hz, 1H), 7.57–7.52 (m, 2H), 7.41 (d, $J = 7.7$ Hz, 2H), 7.36–7.29 (m, 2H), 7.21–7.17 (m, 1H), 7.12 (dd, $J = 9.8, 5.7$ Hz, 2H), 5.05 (dd, $J = 12.7, 5.4$ Hz, 1H), 4.75–4.66 (m, 2H), 4.59–4.41 (m, 4H), 4.38–4.33 (m, 2H), 4.24 (d, $J = 10.5$ Hz, 2H), 3.90 (s, 3H), 3.75–3.68 (m, 3H), 3.45–3.43 (m, 1H), 2.91–2.87 (m, 4H), 2.86–2.84 (m, 1H), 2.83–2.80 (m, 1H), 2.77–2.73 (m, 1H), 2.73–2.69 (m, 1H), 2.66 (s, 3H), 2.18–2.07 (m, 6H), 1.29–1.28 (m, 2H). ^{13}C NMR (125 MHz, Methanol- d_4) δ : 174.6, 171.7, 171.7, 169.2, 169.2, 168.8, 168.8, 165.4, 165.2, 163.2, 161.4, 161.4, 156.6, 139.2, 134.2, 132.8, 131.1, 131.1, 126.0, 121.0, 120.9, 119.3, 117.3, 117.1, 113.4, 109.4, 90.2, 76.1, 56.4, 55.9, 54.0, 52.7, 52.3, 50.4, 50.4, 47.9, 46.4, 42.6, 40.4, 33.1, 32.2, 30.7, 30.5, 25.8, 25.7, 23.8. HRMS (ESI-Q-TOF): m/z calcd for $C_{55}H_{50}F_2N_1O_6^+ [M + H]^+$: 1000.4065; found, 1000.4082. UPLC-MS: m/z calcd for $C_{55}H_{50}F_2N_1O_6^+ [M + H]^+$: 1000.41; found, 1000.44. UPLC-retention time: 3.62 min, purity >95%.

5-(4-(2-((1-(4-((1R,5S)-3,8-diazabicyclo[3.2.1]octan-3-yl)-7-(8-ethynyl-7-fluoro-3-hydroxynaphthalen-1-yl)-8-fluoropyrido[4,3-d]-pyrimidin-2-yl)azetidin-3-yl)(methyl)amino)methyl)phenyl)acetyl)piperazin-1-yl)-2-(2,6-dioxopiperidin-3-yl)-6-fluoroisoindoline-1,3-dione (C07). 1H NMR (400 MHz, Methanol- d_4) δ : 8.90 (s, 1H), 7.86 (dd, $J = 9.2, 5.6$ Hz, 1H), 7.64–7.59 (m, 1H), 7.57–7.53 (m, 2H), 7.48 (d, $J = 11.1, 2.3$ Hz, 1H), 7.44–7.39 (m, 2H), 7.35–7.31 (m, 2H), 7.14 (dd, 1H), 5.07 (dd, $J = 12.8, 5.5, 2.9$ Hz, 1H), 4.77–4.65 (m, 2H), 4.63–4.42 (m, 4H), 4.41–4.36 (m, 2H), 4.24 (d, $J = 11.3$ Hz, 2H), 3.90 (s, 3H), 3.76–3.67 (m, 3H), 3.49–3.44 (m, 1H), 3.24–3.07 (m, 4H), 2.90 (s, 3H), 2.87–2.80 (m, 1H), 2.78–2.74 (m, 1H), 2.73–2.68 (m, 1H), 2.68–2.62 (m, 1H), 2.21–2.07 (m, 6H), 1.29–1.28 (m, 2H). ^{13}C NMR (125 MHz, DMSO- d_6) δ : 172.8, 169.9, 168.8, 166.6, 166.1, 163.6, 161.1, 159.8, 158.5, 158.4, 158.3, 156.4, 154.2, 154.2, 145.0, 145.0, 132.5, 131.6, 129.7, 129.7, 128.7, 125.1, 122.8, 116.1, 115.9, 114.0, 111.5, 109.5, 65.1, 54.2, 54.1, 51.1, 49.1, 45.1, 41.0, 31.0, 30.0, 29.1, 29.1, 28.9, 28.7, 28.6, 26.6, 24.6, 24.5, 22.1, 18.7. HRMS (ESI-Q-TOF): m/z calcd for $C_{55}H_{50}F_2N_1O_6^+ [M + H]^+$: 1018.3970; found, 1018.9836. UPLC-MS: m/z calcd for $C_{55}H_{50}F_2N_1O_6^+ [M + H]^+$: 1018.40; found, 1018.46. UPLC-retention time: 3.29 min, purity >95%.

General Procedure for the Synthesis of Compounds B08, A13, and C08. A mixture of Compounds 17 (200 mg, 1.07 mmol, 1.0 equiv) and methyl 4-oxocyclohexane-1-carboxylate (250 mg, 1.60 mmol, 1.5 equiv) in DCM (5 mL) was stirred at rt for 30 min. NaBH(OAc)₄ (680 mg, 3.21 mmol, 3.0 equiv) was added and the mixture was stirred at rt for another 8 h. The mixture was diluted with water and extracted with DCM. The organic layer was separated, dried, and concentrated in vacuo. The residue obtained above was dissolved in 20 mL/10 mL (v/v) THF/H₂O and LiOH-H₂O (224 mg, 5.35 mmol, 5.0 equiv) was added. The mixture was stirred at 45 °C for 12 h. The residue was diluted with water and the pH was adjusted to 2–3 with 3N HCl. The organic layers were separated, washed with brine, dried, and concentrated in vacuo. The crude compound 23 was used directly for the next step without further purification.

To a stirred solution of compounds 23 (334 mg, 1.07 mmol, 1.0 equiv), 16a (366 mg, 1.07 mmol, 1.0 equiv) and DIPEA (0.74 mL, 4.28 mmol, 4.0 equiv) in dry DMF (4 mL) was added HATU (1.22 g, 3.21 mmol, 3.0 equiv) at 0 °C. The reaction was allowed to stir at rt for 5 h. The mixture was diluted with water and extracted with DCM. The organic layers were separated, washed with brine, dried, and concentrated in vacuo. The intermediate (204 mg, 30% in total) was obtained by prep-TLC (DCM/MeOH) = 20/1. The intermediate obtained above was dissolved in MeOH (1 mL) and HCl (4 M in 1,4-dioxane, 1.2 mL, 16 equiv) was added. The mixture was stirred at rt for 1

h. After removing the solvent, the crude compound 24a was obtained and was used directly for the next step without further purification.

A mixture of compounds 24a (100 mg, 0.18 mmol, 1.0 equiv), 13 (148 mg, 0.18 mmol, 1.0 equiv) and DIPEA (0.12 mL, 0.72 mmol, 4.0 equiv) in dry DMF (2 mL) was stirred under argon at 45 °C for 5 h. After being cooled to rt, the mixture was diluted with water and extracted with DCM. The organic layers were separated, washed with brine, dried, and concentrated in vacuo. The residues were dissolved in MeOH (0.5 mL) and HCl (4 M in 1,4-dioxane, 0.8 mL, 16 equiv) was added. The mixture was stirred at 0 °C. After 45 min, the volatiles were removed under reduced pressure. The residues were dissolved in DMF (0.5 mL) and CsF (273 mg, 1.80 mmol, 10 equiv) was added. The mixture was stirred at rt for 12 h and then was filtered. The organic layers were concentrated in vacuo. Compound B08 (41 mg, 28% in total) was obtained by preparative HPLC. Following the procedures used to prepare compound B08, compounds A13, C08 were obtained by the same methods.

4-(4-(4-((1-(4-((1R,5S)-3,8-diazabicyclo[3.2.1]octan-3-yl)-7-(8-ethynyl-7-fluoro-3-hydroxynaphthalen-1-yl)-8-fluoropyrido[4,3-d]-pyrimidin-2-yl)azetidin-3-yl)(methyl)amino)cyclohexane-1-carbonyl)piperazin-1-yl)-2-(2,6-dioxopiperidin-3-yl)isoindoline-1,3-dione (B08). 1H NMR (400 MHz, Methanol- d_4) δ : 8.93 (s, 1H), 7.89 (dd, $J = 9.2, 5.6$ Hz, 1H), 7.69 (t, $J = 7.8$ Hz, 1H), 7.42 (d, $J = 7.2$ Hz, 1H), 7.39 (d, 1H), 7.36–7.30 (m, 2H), 7.28–7.22 (m, 1H), 5.11 (dd, $J = 12.5, 5.4$ Hz, 1H), 4.76–4.70 (m, 2H), 4.63–4.50 (m, 6H), 4.25 (d, $J = 9.6$ Hz, 2H), 3.95 (d, $J = 14.3$ Hz, 1H), 3.88 (d, $J = 13.8$ Hz, 1H), 3.81–3.75 (m, 4H), 3.49–3.44 (m, 2H), 2.89 (s, 1H), 2.85 (s, 3H), 2.79–2.76 (m, 1H), 2.75–2.71 (m, 1H), 2.18–2.05 (m, 12H), 1.93–1.87 (m, 2H), 1.83–1.75 (m, 2H), 1.29–1.28 (m, 2H). ^{13}C NMR (126 MHz, Methanol- d_4) δ : 175.7, 174.6, 171.6, 168.8, 168.1, 165.5, 165.2, 163.3, 161.6, 155.6, 151.2, 137.0, 135.5, 134.2, 131.7, 131.6, 127.0, 124.8, 124.2, 119.3, 116.9, 113.2, 105.4, 90.1, 76.2, 64.0, 56.4, 53.4, 52.7, 52.5, 52.3, 51.9, 50.5, 47.2, 45.4, 42.9, 34.1, 33.7, 33.1, 32.2, 30.8, 27.3, 25.8, 25.7, 23.7, 23.7. HRMS (ESI-Q-TOF): m/z calcd for $C_{55}H_{50}F_2N_1O_6^+ [M + H]^+$: 978.4221; found, 978.4241. UPLC-MS: m/z calcd for $C_{55}H_{50}F_2N_1O_6^+ [M + H]^+$: 978.42; found, 978.53. UPLC-retention time: 3.34 min, purity >95%.

5-(4-(4-((1-(4-((1R,5S)-3,8-diazabicyclo[3.2.1]octan-3-yl)-7-(8-ethynyl-7-fluoro-3-hydroxynaphthalen-1-yl)-8-fluoropyrido[4,3-d]-pyrimidin-2-yl)azetidin-3-yl)(methyl)amino)cyclohexane-1-carbonyl)piperazin-1-yl)-2-(2,6-dioxopiperidin-3-yl)isoindoline-1,3-dione (A13). 1H NMR (400 MHz, Methanol- d_4) δ : 8.94 (s, 1H), 7.90 (dd, $J = 9.2, 5.6$ Hz, 1H), 7.71 (d, $J = 8.5$ Hz, 1H), 7.41 (d, $J = 2.5$ Hz, 1H), 7.38 (d, $J = 2.7$ Hz, 1H), 7.35 (d, $J = 8.9$ Hz, 1H), 7.26 (d, $J = 2.5$ Hz, 1H), 7.24 (d, $J = 2.3$ Hz, 1H), 5.08 (dd, $J = 12.5, 5.5$ Hz, 1H), 4.81–4.71 (m, 2H), 4.66–4.51 (m, 6H), 4.25 (d, $J = 11.0$ Hz, 2H), 3.97 (d, $J = 13.9$ Hz, 1H), 3.88 (d, $J = 14.0$ Hz, 1H), 3.79–3.74 (m, 4H), 3.55–3.52 (m, 2H), 2.90 (s, 1H), 2.86 (s, 3H), 2.79–2.75 (m, 1H), 2.74–2.71 (m, 1H), 2.19–2.03 (m, 12H), 1.97–1.87 (m, 2H), 1.85–1.74 (m, 2H), 1.30–1.29 (m, 2H). ^{13}C NMR (125 MHz, Methanol- d_4) δ : 175.8, 174.6, 171.7, 169.3, 168.9, 165.3, 163.3, 161.5, 156.8, 155.6, 143.9, 135.6, 134.3, 131.7, 131.6, 130.8, 126.0, 124.3, 121.2, 119.4, 117.3, 117.1, 113.3, 109.5, 76.2, 64.1, 56.4, 53.5, 52.7, 52.3, 34.1, 33.7, 33.1, 32.2, 30.8, 30.7, 30.5, 30.3, 28.1, 27.2, 25.8, 25.7, 23.8. HRMS (ESI-Q-TOF): m/z calcd for $C_{55}H_{50}F_2N_1O_6^+ [M + H]^+$: 978.4221; found, 978.4205. UPLC-MS: m/z calcd for $C_{55}H_{50}F_2N_1O_6^+ [M + H]^+$: 978.42; found, 978.60. UPLC-retention time: 3.38 min, purity >95%.

5-(4-(4-((1-(4-((1R,5S)-3,8-diazabicyclo[3.2.1]octan-3-yl)-7-(8-ethynyl-7-fluoro-3-hydroxynaphthalen-1-yl)-8-fluoropyrido[4,3-d]-pyrimidin-2-yl)azetidin-3-yl)(methyl)amino)cyclohexane-1-carbonyl)piperazin-1-yl)-2-(2,6-dioxopiperidin-3-yl)-6-fluoroisoindoline-1,3-dione (C08). 1H NMR (400 MHz, DMSO- d_6) δ : 11.13 (s, 1H), 10.71 (s, 1H), 9.65–9.54 (m, 1H), 9.46–9.32 (m, 1H), 8.94 (s, 1H), 7.97 (t, $J = 7.6$ Hz, 1H), 7.76 (d, $J = 11.1$ Hz, 1H), 7.52–7.43 (m, 2H), 7.40 (s, 1H), 7.18 (s, 1H), 5.11 (dd, $J = 12.7, 5.5$ Hz, 1H), 4.66–4.51 (m, 2H), 4.47–4.38 (m, 6H), 4.23–4.19 (m, 2H), 3.88–3.80 (m, 2H), 3.66–3.63 (m, 2H), 3.29–3.17 (m, 4H), 2.77 (s, 1H), 2.71 (s, 3H), 2.65–2.60 (m, 1H), 2.59–2.55 (m, 1H), 2.09–1.85 (m, 12H), 1.82–1.76 (m, 2H), 1.71–1.61 (m, 2H), 1.26–1.20 (m, 2H). ^{13}C NMR (125 MHz, DMSO- d_6) δ : 173.0, 172.8, 169.9, 166.6, 166.2, 166.2,

163.6, 161.1, 158.5, 156.4, 154.2, 151.3, 149.2, 148.0, 147.9, 145.1, 145.1, 132.5, 128.7, 125.1, 124.0, 123.9, 122.9, 116.1, 115.9, 114.1, 112.2, 112.0, 111.6, 109.5, 74.9, 54.2, 54.1, 51.5, 49.9, 49.5, 49.1, 45.0, 40.8, 32.6, 32.2, 31.0, 24.6, 24.5, 22.1. HRMS (ESI-Q-TOF): *m/z* calcd for C₂₅H₃₁F₃N₁O₆⁺ [M + H]⁺: 996.4127; found, 996.4138. UPLC-MS: *m/z* calcd for C₂₅H₃₁F₃N₁O₆⁺ [M + H]⁺: 996.41; found, 996.50. UPLC-retention time: 3.39 min; purity >95%.

General Procedure for the Synthesis of Compounds B01~B03 A05~A07 and C01 ~ C03

A mixture of Compounds 17 (200 mg, 1.07 mmol, 1.0 equiv), 25a (396 mg, 1.60 mmol, 1.5 equiv) in DCM (5 mL) was stirred at rt for 30 min. NaBH(OAc)₃ (680 mg, 3.21 mmol, 3.0 equiv) was added and the mixture was stirred at rt for another 8 h. The mixture was diluted with water and extracted with DCM. The organic layer was separated, dried, and concentrated in vacuo. The residue obtained above was dissolved in MeOH (5 mL) and Pd/C (10% Pd/C (55% Water)) (114 mg, 0.2 eq, 20 wt %) was added. The mixture was stirred at 40 °C under H₂ (balloon) after degassing with H₂ for three times. After 12 h, the reaction mixture was filtered, the filtrate was collected and concentrated in vacuo to afford compound 26a, and was used directly for the next step without further purification.

To a stirred solution of compounds 26a (303 mg, 1.07 mmol, 1.0 equiv), 16a (366 mg, 1.07 mmol, 1.0 equiv) and DIPEA (0.74 mL, 4.28 mmol, 4.0 equiv) in dry DMF (4 mL) was stirred under argon at 110 °C for 2 h. After being cooled to rt, the mixture was diluted with water and extracted with DCM. The organic layers were separated, washed with brine, dried, and concentrated in vacuo. The intermediate (121 mg, 21% in total) was obtained by prep-TLC (DCM/MeOH) = 25/1. The intermediate was dissolved in MeOH (0.5 mL), HCl (4 M in 1,4-dioxane, 0.9 mL, 16 equiv) was added. The mixture was stirred at 0 °C. After 45 min, the volatiles were removed under reduced pressure to afford compound 27Aa. The crude compound 27Aa was used directly for the next step without further purification.

A mixture of compounds 27Aa (100 mg, 0.22 mmol, 1.0 equiv), 13 (181 mg, 0.22 mmol, 1.0 equiv) and DIPEA (0.15 mL, 0.88 mmol, 4.0 equiv) in dry DMF (2 mL) was stirred under argon at 45 °C for 5 h. After being cooled to rt, the mixture was diluted with water and extracted with DCM. The organic layers were separated, washed with brine, dried, and concentrated in vacuo. The residues were dissolved in MeOH (0.5 mL) and HCl (4 M in 1,4-dioxane, 0.9 mL, 16 equiv) was added. The mixture was stirred at 0 °C. After 45 min, the volatiles were removed under reduced pressure. The residues were dissolved in DMF (0.5 mL) and CsF (334 mg, 2.20 mmol, 10 equiv) was added. The mixture was stirred at rt for 12 h and then was filtered. The organic layers were concentrated in vacuo. Compound B01 (62 mg, 32% in total) was obtained by preparative HPLC. Following the procedures used to prepare compound B01, compounds B02 ~ B03, A05 ~ A07, and C01 ~ C03 were obtained by the same methods.

4-(4-((1-(4-(3,8-diazabicyclo[3.2.1]octan-3-yl)-7-(8-ethynyl-7-fluoro-3-hydroxynaphthalen-1-yl)-8-fluoropyrido[4,3-d]pyrimidin-2-yl)azetidin-3-yl)(methyl)amino)methyl)piperidin-1-yl)-2-(2,6-dioxopiperidin-3-yl)isoindoline-1,3-dione (B01). ¹H NMR (400 MHz, Methanol-*d*₄) δ: 8.97 (s, 1H), 7.90 (dd, *J* = 9.1, 5.6 Hz, 1H), 7.65 (t, *J* = 7.8 Hz, 1H), 7.42 (d, *J* = 2.5 Hz, 1H), 7.38 (d, *J* = 6.8 Hz, 1H), 7.35 (d, 1H), 7.32 (d, *J* = 8.5 Hz, 1H), 7.29 (d, *J* = 2.5 Hz, 1H), 5.09 (dd, *J* = 12.4, 5.4 Hz, 1H), 4.83–4.70 (m, 2H), 4.67–4.54 (m, 4H), 4.41–4.33 (m, 1H), 4.26 (d, *J* = 11.3 Hz, 2H), 4.00 (d, *J* = 13.6 Hz, 1H), 3.90 (d, *J* = 14.1 Hz, 1H), 3.80 (d, *J* = 11.9 Hz, 2H), 3.59–3.50 (m, 1H), 3.21–3.13 (m, 2H), 3.00 (s, 3H), 2.97–2.93 (m, 1H), 2.88–2.81 (m, 1H), 2.78–2.68 (m, 2H), 2.18–2.09 (m, 6H), 2.00–1.93 (m, 2H), 1.70–1.60 (m, 2H), 1.30–1.26 (m, 2H). ¹³C NMR (125 MHz, Methanol-*d*₄) δ: 174.6, 171.7, 169.0, 168.0, 165.2, 165.1, 163.3, 161.3, 155.6, 151.7, 136.8, 135.3, 134.2, 126.8, 125.0, 124.6, 118.6, 117.4, 117.2, 116.2, 113.9, 110.7, 105.1, 104.9, 90.4, 76.0, 61.0, 57.3, 56.3, 53.7, 51.9, 50.4, 38.4, 33.0, 32.4, 32.2, 30.9, 30.7, 30.4, 25.8, 25.7, 23.7, 23.6. HRMS (ESI-Q-TOF): *m/z* calcd for C₄₈H₄₇F₃N₁₀O₅⁺ [M + H]⁺: 881.3693; found, 881.3715. UPLC-MS: *m/z* calcd for C₄₈H₄₇F₃N₁₀O₅⁺ [M + H]⁺: 881.37; found, 881.49. UPLC-retention time: 3.27 min; purity >95%.

4-(4-((1-(4-(3,8-diazabicyclo[3.2.1]octan-3-yl)-7-(8-ethynyl-7-fluoro-3-hydroxynaphthalen-1-yl)-8-fluoropyrido[4,3-d]-

pyrimidin-2-yl)azetidin-3-yl)(methyl)amino)piperidin-1-yl)-2-(2,6-dioxopiperidin-3-yl)isoindoline-1,3-dione (B02). ¹H NMR (400 MHz, Methanol-*d*₄) δ: 8.97 (s, 1H), 7.90 (dd, *J* = 9.2, 5.6 Hz, 1H), 7.67 (t, *J* = 7.8 Hz, 1H), 7.42 (d, *J* = 2.8 Hz, 1H), 7.39 (d, *J* = 5.4 Hz, 1H), 7.37–7.35 (m, 1H), 7.33 (d, *J* = 2.6 Hz, 1H), 7.31–7.29 (m, 1H), 5.11 (dd, *J* = 12.4, 5.5 Hz, 1H), 4.83–4.71 (m, 2H), 4.68–4.62 (m, 4H), 4.60–4.54 (m, 1H), 4.25 (d, *J* = 11.6 Hz, 2H), 4.02 (d, 1H), 3.98 (d, 1H), 3.90 (d, 2H), 3.70–3.60 (m, 1H), 3.57–3.50 (m, 1H), 3.01 (t, *J* = 10.2 Hz, 2H), 2.93 (s, 3H), 2.88–2.81 (m, 1H), 2.80–2.67 (m, 2H), 2.18–2.13 (m, 6H), 2.11–2.06 (m, 2H), 1.32–1.26 (m, 2H). ¹³C NMR (125 MHz, Methanol-*d*₄) δ: 174.6, 171.6, 168.8, 168.1, 163.2, 161.3, 155.5, 155.5, 151.1, 150.7, 144.5, 144.4, 143.3, 137.0, 135.2, 134.1, 132.0, 131.8, 131.7, 126.8, 125.1, 124.5, 119.0, 117.4, 117.2, 116.8, 113.8, 110.7, 105.1, 104.9, 90.4, 76.0, 62.4, 56.3, 53.8, 53.6, 50.9, 50.4, 33.9, 32.1, 30.7, 25.8, 25.6, 23.6. HRMS (ESI-Q-TOF): *m/z* calcd for C₅₃H₅₆F₃N₁₁O₆⁺ [M + H]⁺: 867.3537; found, 867.3547. UPLC-MS: *m/z* calcd for C₅₃H₅₆F₃N₁₀O₅⁺ [M + H]⁺: 867.35; found, 867.45. UPLC-retention time: 3.26 min; purity >95%.

4-(3-((1-(4-(1(R,S)-3,8-diazabicyclo[3.2.1]octan-3-yl)-7-(8-ethynyl-7-fluoro-3-hydroxynaphthalen-1-yl)-8-fluoropyrido[4,3-d]pyrimidin-2-yl)azetidin-3-yl)(methyl)amino)azetidin-1-yl)-2-(2,6-dioxopiperidin-3-yl)isoindoline-1,3-dione (B03). ¹H NMR (400 MHz, Methanol-*d*₄) δ: 7.89 (dd, *J* = 9.2, 5.6 Hz, 1H), 7.59 (dd, *J* = 8.4, 7.1 Hz, 1H), 7.44–7.39 (m, 1H), 7.35 (t, *J* = 8.9 Hz, 1H), 7.31–7.27 (m, 1H), 7.24 (d, *J* = 7.1 Hz, 1H), 6.85 (d, *J* = 8.4 Hz, 1H), 5.05 (dd, *J* = 12.4, 5.5 Hz, 1H), 4.80–4.68 (m, 2H), 4.58–4.48 (m, 6H), 4.44–4.34 (m, 2H), 4.26 (d, 2H), 3.96 (d, *J* = 13.8 Hz, 1H), 3.89 (d, *J* = 14.0 Hz, 1H), 3.55–3.49 (m, 1H), 2.86 (s, 3H), 2.83–2.76 (m, 1H), 2.75–2.66 (m, 2H), 2.21–2.04 (m, 6H), 1.29–1.27 (m, 2H). ¹³C NMR (125 MHz, Methanol-*d*₄) δ: 174.6, 171.8, 169.0, 168.1, 164.0, 161.6, 161.6, 157.0, 156.0, 150.2, 149.0, 149.0, 141.1, 136.1, 134.9, 132.4, 123.3, 123.1, 121.9, 121.1, 119.6, 119.4, 116.1, 114.0, 112.8, 109.2, 56.3, 54.4, 54.1, 53.8, 52.0, 50.3, 34.0, 33.1, 32.2, 30.7, 30.5, 25.5, 23.7, 23.7. HRMS (ESI-Q-TOF): *m/z* calcd for C₄₈H₄₇F₃N₁₀O₅⁺ [M + H]⁺: 839.3224; found, 839.3222. UPLC-MS: *m/z* calcd for C₄₈H₄₇F₃N₁₀O₅⁺ [M + H]⁺: 839.32; found, 839.27. UPLC-retention time: 3.54 min; purity >95%.

5-4-((1-(4-(3,8-diazabicyclo[3.2.1]octan-3-yl)-7-(8-ethynyl-7-fluoro-3-hydroxynaphthalen-1-yl)-8-fluoropyrido[4,3-d]pyrimidin-2-yl)azetidin-3-yl)(methyl)amino)methyl)piperidin-1-yl)-2-(2,6-dioxopiperidin-3-yl)isoindoline-1,3-dione (A05). ¹H NMR (400 MHz, Methanol-*d*₄) δ: 8.94 (s, 1H), 7.90 (dd, *J* = 9.2, 5.7 Hz, 1H), 7.67 (d, *J* = 8.5 Hz, 1H), 7.41 (d, *J* = 2.5 Hz, 1H), 7.37 (t, 1H), 7.35 (t, *J* = 3.4 Hz, 1H), 7.26 (d, *J* = 2.5 Hz, 1H), 7.23 (dd, *J* = 8.7, 2.3 Hz, 1H), 5.07 (dd, *J* = 12.5, 5.4 Hz, 1H), 4.81–4.70 (m, 2H), 4.64–4.52 (m, 4H), 4.39–4.30 (m, 1H), 4.25 (d, *J* = 10.6 Hz, 2H), 4.09 (d, *J* = 13.2 Hz, 2H), 3.97 (d, *J* = 13.9 Hz, 1H), 3.88 (d, *J* = 14.0 Hz, 1H), 3.53–3.47 (m, 1H), 3.14–3.09 (m, 2H), 3.07–3.04 (m, 1H), 3.00 (s, 3H), 2.88–2.80 (m, 1H), 2.79–2.65 (m, 2H), 2.19–2.07 (m, 6H), 2.00–1.92 (m, 2H), 1.51–1.43 (m, 2H), 1.29–1.28 (m, 2H). ¹³C NMR (125 MHz, Methanol-*d*₄) δ: 174.6, 171.7, 169.4, 168.9, 165.3, 163.3, 161.4, 156.7, 155.6, 155.6, 135.6, 134.2, 132.8, 127.0, 126.9, 126.1, 124.5, 120.1, 119.3, 117.4, 117.2, 113.6, 109.4, 105.2, 105.1, 90.3, 76.1, 60.8, 57.3, 56.4, 53.7, 50.4, 48.3, 38.4, 33.1, 32.7, 32.2, 30.7, 30.5, 30.1, 25.8, 25.7, 23.8, 23.7. HRMS (ESI-Q-TOF): *m/z* calcd for C₅₃H₅₆F₃N₁₀O₅⁺ [M + H]⁺: 881.3693; found, 881.3693. UPLC-MS: *m/z* calcd for C₅₃H₅₆F₃N₁₀O₅⁺ [M + H]⁺: 881.37; found, 881.47. UPLC-retention time: 3.35 min; purity >95%.

5-4-((1-(4-(1(R,S)-3,8-diazabicyclo[3.2.1]octan-3-yl)-7-(8-ethynyl-7-fluoro-3-hydroxynaphthalen-1-yl)-8-fluoropyrido[4,3-d]pyrimidin-2-yl)azetidin-3-yl)(methyl)amino)piperidin-1-yl)-2-(2,6-dioxopiperidin-3-yl)isoindoline-1,3-dione (A06). ¹H NMR (400 MHz, Methanol-*d*₄) δ: 8.97 (s, 1H), 7.90 (dd, *J* = 9.2, 5.7 Hz, 1H), 7.67 (d, *J* = 8.5 Hz, 1H), 7.42 (d, *J* = 2.6 Hz, 1H), 7.38 (d, 1H), 7.35 (t, *J* = 8.9 Hz, 1H), 7.29 (d, *J* = 2.6 Hz, 1H), 7.24 (dd, *J* = 8.6, 2.4 Hz, 1H), 5.08 (dd, *J* = 12.5, 5.4 Hz, 1H), 4.82–4.69 (m, 2H), 4.47–4.59 (m, 4H), 4.57–4.50 (m, 1H), 4.30–4.14 (m, 4H), 3.99 (d, *J* = 12.7 Hz, 1H), 3.90 (t, *J* = 14.2 Hz, 1H), 3.77–3.67 (m, 1H), 3.58–3.48 (m, 1H), 3.06 (t, *J* = 12.6 Hz, 2H), 2.87 (s, 3H), 2.84–2.80 (m, 1H), 2.78–2.66 (m, 2H), 2.16–2.10 (m, 6H), 2.00–1.86 (m, 2H), 1.35–1.26 (m, 2H). ¹³C NMR (125 MHz, Methanol-*d*₄) δ: 174.6, 171.7, 169.3, 168.8,

165.2, 165.1, 163.3, 161.4, 156.1, 155.6, 155.5, 144.5, 144.4, 143.3, 135.5, 134.2, 131.9, 131.8, 131.7, 126.8, 126.1, 124.5, 120.8, 119.7, 117.4, 117.2, 113.8, 110.7, 109.7, 105.1, 105.0, 90.5, 76.0, 62.4, 56.3, 53.8, 53.6, 50.4, 47.4, 33.8, 32.2, 30.7, 25.8, 25.7, 23.7. HRMS (ESI-Q-TOF): *m/z* calcd for $C_{17}H_{45}F_2N_{10}O_5^+$ [M + H]⁺: 867.3537; found, 867.3518. UPLC-MS: *m/z* calcd for $C_{17}H_{45}F_2N_{10}O_5^+$ [M + H]⁺: 867.35; found, 867.31. UPLC-retention time: 3.08 min, purity >95%. *5-(3-((1-(4-((1R,5S)-3,8-diazabicyclo[3.2.1]octan-3-yl)-7-(8-ethynyl-7-fluoro-3-hydroxynaphthalen-1-yl)-8-fluoropyrido[4,3-d]-pyrimidin-2-yl)azetidin-3-yl)(methyl)amino)azetidin-1-yl)-2-(2,6-dioxopiperidin-3-yl)isoindoline-1,3-dione (A07).* ¹H NMR (400 MHz, Methanol-*d*₄) δ : 8.96 (s, 1H), 7.90 (dd, *J* = 9.2, 5.6 Hz, 1H), 7.68 (d, *J* = 8.2 Hz, 1H), 7.42 (d, *J* = 2.5 Hz, 1H), 7.37 (t, *J* = 8.9 Hz, 1H), 7.28 (d, *J* = 2.6 Hz, 1H), 6.92 (d, *J* = 2.1 Hz, 1H), 6.76 (dd, *J* = 8.2, 2.1 Hz, 1H), 5.07 (dd, *J* = 12.4, 5.4 Hz, 1H), 4.84–4.69 (m, 2H), 4.57–4.48 (m, 4H), 4.29 (d, *J* = 10.2 Hz, 2H), 4.25–4.20 (m, 4H), 3.99 (d, *J* = 13.9 Hz, 1H), 3.90 (d, *J* = 14.1 Hz, 1H), 3.60–3.54 (m, 1H), 2.92–2.84 (m, 1H), 2.80 (s, 3H), 2.77–2.66 (m, 2H), 2.19–2.07 (m, 6H), 1.30–1.28 (m, 2H). ¹³C NMR (125 MHz, Methanol-*d*₄) δ : 174.6, 171.7, 169.2, 169.1, 163.3, 160.7, 156.4, 155.6, 143.3, 135.5, 134.3, 131.8, 126.9, 126.0, 124.5, 120.3, 117.4, 117.2, 116.3, 113.8, 106.4, 105.2, 105.0, 90.5, 76.1, 56.4, 55.3, 54.2, 54.1, 50.4, 34.0, 33.1, 32.2, 30.7, 25.8, 25.7, 23.8. HRMS (ESI-Q-TOF): *m/z* calcd for $C_{45}H_{44}F_2N_{10}O_5^+$ [M + H]⁺: 839.3224; found, 839.3205. UPLC-MS: *m/z* calcd for $C_{45}H_{44}F_2N_{10}O_5^+$ [M + H]⁺: 839.32; found, 839.32. UPLC-retention time: 3.44 min, purity >95%.

5-(4-((1-(4-((1R,5S)-3,8-diazabicyclo[3.2.1]octan-3-yl)-7-(8-ethynyl-7-fluoro-3-hydroxynaphthalen-1-yl)-8-fluoropyrido[4,3-d]-pyrimidin-2-yl)azetidin-3-yl)(methyl)amino)methyl)piperidin-1-yl)-2-(2,6-dioxopiperidin-3-yl)-6-fluoroisoindoline-1,3-dione (C01). ¹H NMR (400 MHz, Methanol-*d*₄) δ : 9.02 (s, 1H), 7.91 (dd, *J* = 9.2, 5.5 Hz, 1H), 7.51 (d, *J* = 11.0 Hz, 1H), 7.48–7.45 (m, 1H), 7.45–7.43 (m, 1H), 7.39 (d, *J* = 8.8 Hz, 1H), 7.35 (dd, *J* = 6.0 Hz, 1H), 5.09 (dd, 1H), 4.79–4.63 (m, 6H), 4.47–4.36 (m, 1H), 4.27 (d, *J* = 14.9 Hz, 2H), 4.09 (d, 1H), 3.95 (d, *J* = 13.4 Hz, 1H), 3.72–3.65 (m, 3H), 3.20–3.12 (m, 2H), 3.00 (s, 3H), 2.96–2.92 (m, 1H), 2.88–2.81 (m, 1H), 2.80–2.70 (m, 2H), 2.21–2.11 (m, 6H), 2.05–1.97 (m, 2H), 1.60–1.57 (m, 2H), 1.29–1.27 (m, 2H). ¹³C NMR (125 MHz, DMSO-*d*₆) δ : 172.8, 170.0, 166.7, 166.2, 166.2, 161.1, 159.7, 158.3, 156.3, 154.3, 149.2, 145.6, 145.5, 132.5, 128.8, 128.8, 125.1, 123.1, 123.0, 123.0, 116.1, 115.9, 113.9, 112.1, 111.9, 111.8, 109.5, 103.8, 103.7, 91.6, 58.4, 54.9, 54.1, 54.0, 49.3, 49.1, 40.4, 31.0, 30.4, 29.3, 24.5, 22.1. HRMS (ESI-Q-TOF): *m/z* calcd for $C_{48}H_{46}F_2N_{10}O_5^+$ [M + H]⁺: 899.3599; found, 899.3611. UPLC-MS: *m/z* calcd for $C_{48}H_{46}F_2N_{10}O_5^+$ [M + H]⁺: 899.36; found, 899.58. UPLC-retention time: 3.41 min, purity >95%.

5-(4-((1-(4-((1R,5S)-3,8-diazabicyclo[3.2.1]octan-3-yl)-7-(8-ethynyl-7-fluoro-3-hydroxynaphthalen-1-yl)-8-fluoropyrido[4,3-d]-pyrimidin-2-yl)azetidin-3-yl)(methyl)amino)piperidin-1-yl)-2-(2,6-dioxopiperidin-3-yl)-6-fluoroisoindoline-1,3-dione (C02). ¹H NMR (400 MHz, Methanol-*d*₄) δ : 8.95 (s, 1H), 7.89 (dd, *J* = 9.1, 5.6 Hz, 1H), 7.56 (d, *J* = 11.0 Hz, 1H), 7.50 (d, *J* = 7.2 Hz, 1H), 7.41 (d, *J* = 2.6 Hz, 1H), 7.36 (t, *J* = 8.9 Hz, 1H), 7.27 (d, *J* = 2.6 Hz, 1H), 5.10 (dd, *J* = 12.6, 5.4 Hz, 1H), 4.82–4.70 (m, 2H), 4.67–4.60 (m, 4H), 4.60–4.52 (m, 1H), 4.25 (d, *J* = 10.5 Hz, 2H), 3.98 (d, *J* = 13.7 Hz, 1H), 3.90 (d, *J* = 14.0 Hz, 1H), 3.82 (d, *J* = 12.0 Hz, 2H), 3.73–3.61 (m, 1H), 3.57–3.46 (m, 1H), 3.02 (t, *J* = 12.0 Hz, 2H), 2.92 (s, 3H), 2.89–2.81 (m, 1H), 2.79–2.65 (m, 2H), 2.20–2.12 (m, 6H), 2.07–2.01 (m, 2H), 1.36–1.18 (m, 2H). ¹³C NMR (125 MHz, Methanol-*d*₄) δ : 174.6, 171.5, 168.2, 167.8, 165.2, 163.4, 161.4, 158.6, 155.6, 155.6, 146.5, 146.4, 143.1, 134.3, 131.9, 131.8, 130.4, 126.8, 126.3, 126.2, 124.6, 117.5, 117.3, 115.3, 113.9, 112.9, 112.7, 105.1, 105.0, 76.0, 62.2, 53.9, 53.7, 50.7, 33.9, 32.1, 30.7, 25.7, 25.7, 23.7, 23.7. HRMS (ESI-Q-TOF): *m/z* calcd for $C_{47}H_{44}F_2N_{10}O_5^+$ [M + H]⁺: 885.3443; found, 885.3474. UPLC-MS: *m/z* calcd for $C_{47}H_{44}F_2N_{10}O_5^+$ [M + H]⁺: 885.34; found, 885.53. UPLC-retention time: 3.30 min, purity >95%.

5-(3-((1-(4-((1R,5S)-3,8-diazabicyclo[3.2.1]octan-3-yl)-7-(8-ethynyl-7-fluoro-3-hydroxynaphthalen-1-yl)-8-fluoropyrido[4,3-d]-pyrimidin-2-yl)azetidin-3-yl)(methyl)amino)azetidin-1-yl)-2-(2,6-dioxopiperidin-3-yl)-6-fluoroisoindoline-1,3-dione (C03). ¹H NMR (400 MHz, Methanol-*d*₄) δ : 8.95 (s, 1H), 7.90 (dd, *J* = 9.2, 5.6 Hz, 1H), 7.47 (d, *J* = 10.8 Hz, 1H), 7.42 (d, *J* = 2.5 Hz, 1H), 7.36 (*t*, *J* = 8.9

Hz, 1H), 7.28 (d, *J* = 2.6 Hz, 1H), 7.01 (d, *J* = 7.4 Hz, 1H), 5.06 (dd, 1H), 4.81–4.71 (m, 2H), 4.55–4.46 (m, 4H), 4.45–4.39 (m, 2H), 4.37–4.31 (m, 2H), 4.26 (d, 2H), 3.99 (d, *J* = 13.8 Hz, 1H), 3.91 (d, *J* = 14.0 Hz, 1H), 3.58–3.53 (m, 1H), 2.90–2.83 (m, 1H), 2.79 (s, 3H), 2.77–2.68 (m, 2H), 2.20–2.07 (m, 6H), 1.29–1.28 (m, 2H). ¹³C NMR (125 MHz, Methanol-*d*₄) δ : 174.6, 171.6, 168.4, 168.1, 165.1, 163.3, 160.7, 157.0, 155.6, 155.6, 155.1, 145.1, 145.0, 134.2, 126.9, 124.5, 117.4, 117.2, 113.6, 112.3, 112.1, 109.7, 105.2, 90.4, 90.3, 76.1, 57.3, 56.4, 54.9, 54.2, 54.0, 52.7, 52.3, 50.6, 34.1, 33.1, 32.2, 30.7, 25.8, 25.7, 23.7. HRMS (ESI-Q-TOF): *m/z* calcd for $C_{45}H_{46}F_3N_{10}O_5^+$ [M + H]⁺: 857.3130; found, 857.3158. UPLC-MS: *m/z* calcd for $C_{45}H_{46}F_3N_{10}O_5^+$ [M + H]⁺: 857.31; found, 857.50. UPLC-retention time: 3.72 min, purity >95%.

General Procedure for the Synthesis of Compounds B04~B05, A08~A09, and C04 ~ C05. A mixture of Compounds 26a (200 mg, 0.70 mmol, 1.0 equiv), 25a (260 mg, 1.05 mmol, 1.5 equiv) in DCM (5 mL) was stirred at rt for 30 min, NaBH(OAc)₄ (798 mg, 2.10 mmol, 3.0 equiv) was added and the mixture was stirred at rt for another 8 h. The mixture was diluted with water and extracted with DCM. The organic layer was separated, dried, and concentrated in vacuo. The residue obtained above was dissolved in MeOH (10 mL) and Pd/C (10% Pd/C (55% Water)) (74 mg, 0.2 eq, 20 wt %) was added. The mixture was stirred at 40 °C under H₂ (balloon) after degassing with H₂ for three times. After 12 h, the reaction mixture was filtered, the filtrate was collected and concentrated in vacuo to afford compound 28a, and was used directly for the next step without further purification.

To a stirred solution of compounds 28a (266 mg, 0.70 mmol, 1.0 equiv), 16a (240 mg, 0.70 mmol, 1.0 equiv) and DIPEA (0.48 mL, 2.80 mmol, 4.0 equiv) in dry DMF (4 mL) was stirred under argon at 110 °C for 2 h. After being cooled to rt, the mixture was diluted with water and extracted with DCM. The organic layers were separated, washed with brine, dried, and concentrated in vacuo. The intermediate (151 mg, 34% in total) was obtained by prep-TLC (DCM/MeOH) = 10/1. The intermediate was dissolved in MeOH (0.5 mL), HCl (4 M in 1,4-dioxane, 2.8 mL, 16 equiv) was added. The mixture was stirred at 0 °C. After 45 min, the volatiles were removed under reduced pressure to afford compound 29Aa. The crude compound 29Aa was used directly for the next step without further purification.

A mixture of compounds 29Aa (100 mg, 0.18 mmol, 1.0 equiv), 13 (148 mg, 0.18 mmol, 1.0 equiv) and DIPEA (0.12 mL, 0.72 mmol, 4.0 equiv) in dry DMF (2 mL) was stirred under argon at 45 °C for 5 h. After being cooled to rt, the mixture was diluted with water and extracted with DCM. The organic layers were separated, washed with brine, dried, and concentrated in vacuo. The residues were dissolved in MeOH (0.5 mL) and HCl (4 M in 1,4-dioxane, 0.8 mL, 16 equiv) was added. The mixture was stirred at 0 °C. After 45 min, the volatiles were removed under reduced pressure. The residues were dissolved in DMF (0.5 mL) and CsF (272 mg, 1.80 mmol, 10 equiv) was added. The mixture was stirred at rt for 12 h and then was filtered. The organic layers were concentrated in vacuo. Compound B04 (71 mg, 41% in total) was obtained by preparative HPLC. Following the procedures used to prepare compound B04, compounds B05, A08 ~ A09, and C04 ~ C05 were obtained by the same methods.

4-(4-((1-(4-((1R,5S)-3,8-diazabicyclo[3.2.1]octan-3-yl)-7-(8-ethynyl-7-fluoro-3-hydroxynaphthalen-1-yl)-8-fluoropyrido[4,3-d]-pyrimidin-2-yl)azetidin-3-yl)(methyl)amino)piperidin-1-yl)-2-(2,6-dioxopiperidin-3-yl)isoindoline-1,3-dione (B04). ¹H NMR (400 MHz, Methanol-*d*₄) δ : 8.98 (s, 1H), 7.91 (dd, *J* = 9.2, 5.7 Hz, 1H), 7.66 (dd, *J* = 8.4, 7.1 Hz, 1H), 7.43 (d, *J* = 2.5 Hz, 1H), 7.40 (d, 1H), 7.35 (d, *J* = 1.8 Hz, 1H), 7.33–7.31 (m, 1H), 7.30 (d, 1H), 5.11 (dd, 1H), 4.81–4.72 (m, 2H), 4.63–4.60 (m, 4H), 4.55–4.50 (m, 1H), 4.25 (d, *J* = 12.8 Hz, 2H), 4.07–3.96 (m, 2H), 3.95–3.88 (m, 1H), 3.87–3.85 (m, 1H), 3.81–3.78 (m, 2H), 3.58–3.52 (m, 1H), 3.19–3.13 (m, 4H), 2.97–2.92 (m, 2H), 2.87 (s, 3H), 2.85–2.82 (m, 1H), 2.77–2.72 (m, 2H), 2.36–2.29 (m, 4H), 2.16–2.11 (m, 6H), 1.96–1.92 (m, 2H), 1.64–1.59 (m, 2H), 1.38–1.24 (m, 2H). ¹³C NMR (125 MHz, Methanol-*d*₄) δ : 174.7, 171.8, 169.0, 168.0, 165.2, 164.9, 163.2, 161.2, 155.5, 153.0, 151.7, 151.0, 143.0, 136.8, 135.2, 134.1, 131.8, 131.2, 126.7, 125.0, 124.7, 118.5, 117.4, 117.2, 116.2, 114.0, 110.6, 104.9, 104.8, 75.9, 63.4, 58.5, 56.2, 53.9, 53.8, 52.6, 51.9, 50.4,

33.7, 32.2, 30.9, 25.7, 25.6, 23.6. HRMS (ESI-Q-TOF): m/z calcd for $C_{53}H_{56}F_2N_{11}O_5^+ [M + H]^+$: 964.4428 found: 964.4441. UPLC-MS: m/z calcd for $C_{53}H_{56}F_2N_{11}O_5^+ [M + H]^+$: 964.44; found, 964.54. UPLC-retention time: 2.91 min, purity >95%.

5-(4-((4-(((1-(4-((1R,5S)-3,8-diazabicyclo[3.2.1]octan-3-yl)-7-(8-ethynyl-7-fluoro-3-hydroxynaphthalen-1-yl)-8-fluoropyrido[4,3-d]-pyrimidin-2-yl)azetidin-3-yl)(methyl)amino)methyl)piperidin-1-yl)methyl)piperidin-1-yl)-2-(2,6-dioxopiperidin-3-yl)isoindoline-1,3-dione (B05). 1H NMR (400 MHz, Methanol- d_4) δ : 9.01 (s, 1H), 7.90 (dd, $J = 9.2, 5.7$ Hz, 1H), 7.62 (t, $J = 7.8$ Hz, 1H), 7.44 (d, 1H), 7.37–7.32 (m, 3H), 7.27 (d, $J = 8.4$ Hz, 1H), 5.09 (dd, $J = 6.9$ Hz, 1H), 4.82–4.71 (m, 2H), 4.67–4.59 (m, 4H), 4.40–4.33 (m, 1H), 4.26 (d, $J = 13.0$ Hz, 2H), 4.06 (d, $J = 16.8$ Hz, 1H), 3.91 (d, $J = 14.0$ Hz, 1H), 3.78–3.68 (m, 4H), 3.62–3.52 (m, 1H), 3.18–3.08 (m, 4H), 2.98 (s, 3H), 2.95–2.89 (m, 2H), 2.88–2.82 (m, 1H), 2.79–2.67 (m, 2H), 2.24–2.03 (m, 10H), 1.94–1.87 (m, 2H), 1.82–1.67 (m, 2H), 1.62–1.52 (m, 2H), 1.35–1.25 (m, 2H). ^{13}C NMR (125 MHz, Methanol- d_4) δ : 174.7, 171.7, 169.0, 168.0, 165.2, 163.2, 161.4, 155.5, 151.7, 136.8, 135.3, 134.2, 131.7, 131.6, 126.9, 124.9, 124.4, 118.6, 117.3, 117.1, 116.2, 113.5, 110.8, 105.2, 105.1, 90.3, 76.0, 63.8, 59.7, 57.3, 56.3, 53.7, 51.9, 50.4, 38.3, 32.2, 32.0, 31.0, 30.7, 28.2, 25.8, 25.7, 23.6. HRMS (ESI-Q-TOF): m/z calcd for $C_{54}H_{58}F_2N_{11}O_5^+ [M + H]^+$: 978.4585; found, 978.4626. UPLC-MS: m/z calcd for $C_{54}H_{58}F_2N_{11}O_5^+ [M + H]^+$: 978.46; found, 978.56. UPLC-retention time: 3.22 min, purity >95%.

5-(4-((4-((1-(4-((1R,5S)-3,8-diazabicyclo[3.2.1]octan-3-yl)-7-(8-ethynyl-7-fluoro-3-hydroxynaphthalen-1-yl)-8-fluoropyrido[4,3-d]-pyrimidin-2-yl)azetidin-3-yl)(methyl)amino)piperidin-1-yl)methyl)piperidin-1-yl)-2-(2,6-dioxopiperidin-3-yl)isoindoline-1,3-dione (A08). 1H NMR (400 MHz, Methanol- d_4) δ : 8.94 (s, 1H), 7.90 (dd, $J = 9.1, 5.7$ Hz, 1H), 7.67 (d, $J = 8.5$ Hz, 1H), 7.41 (d, $J = 2.5$ Hz, 1H), 7.37 (d, $J = 8.9$ Hz, 1H), 7.35–7.33 (m, 1H), 7.26 (d, $J = 2.5$ Hz, 1H), 7.22 (dd, $J = 8.6, 2.3$ Hz, 1H), 5.07 (dd, $J = 12.4, 5.4$ Hz, 1H), 4.81–4.68 (m, 2H), 4.62–4.53 (m, 4H), 4.51–4.44 (m, 1H), 4.25 (d, $J = 10.8$ Hz, 2H), 4.07 (d, $J = 13.0$ Hz, 2H), 3.97 (d, $J = 14.2$ Hz, 1H), 3.88 (d, $J = 13.5$ Hz, 1H), 3.82–3.68 (m, 2H), 3.57–3.44 (m, 1H), 3.23–3.08 (m, 4H), 3.07–2.99 (m, 2H), 2.89–2.85 (m, 1H), 2.84 (s, 3H), 2.79–2.65 (m, 2H), 2.34–2.24 (m, 4H), 2.19–2.07 (m, 6H), 1.98–1.90 (m, 2H), 1.46–1.36 (m, 2H), 1.30–1.28 (m, 2H). ^{13}C NMR (125 MHz, Methanol- d_4) δ : 174.7, 171.7, 169.4, 168.9, 165.3, 165.2, 163.3, 161.3, 156.8, 155.6, 143.3, 135.7, 134.3, 131.8, 131.7, 126.9, 126.1, 124.6, 120.2, 119.4, 117.4, 117.2, 113.8, 110.7, 109.5, 105.2, 105.0, 76.0, 58.5, 56.4, 56.3, 54.1, 53.8, 50.4, 49.5, 49.3, 48.3, 33.7, 32.5, 32.2, 30.7, 30.2, 25.7, 25.7, 23.8, 23.7. HRMS (ESI-Q-TOF): m/z calcd for $C_{53}H_{56}F_2N_{11}O_5^+ [M + H]^+$: 964.4428; found, 964.4418. UPLC-MS: m/z calcd for $C_{53}H_{56}F_2N_{11}O_5^+ [M + H]^+$: 964.44; found, 964.32. UPLC-retention time: 3.70 min, purity >95%.

5-(4-((4-((1-(4-((1R,5S)-3,8-diazabicyclo[3.2.1]octan-3-yl)-7-(8-ethynyl-7-fluoro-3-hydroxynaphthalen-1-yl)-8-fluoropyrido[4,3-d]-pyrimidin-2-yl)azetidin-3-yl)(methyl)amino)methyl)piperidin-1-yl)methyl)piperidin-1-yl)-2-(2,6-dioxopiperidin-3-yl)isoindoline-1,3-dione (A09). 1H NMR (400 MHz, Methanol- d_4) δ : 8.94 (s, 1H), 7.90 (dd, $J = 9.2, 5.7$ Hz, 1H), 7.66 (d, $J = 8.5$ Hz, 1H), 7.41 (d, $J = 2.5$ Hz, 1H), 7.37 (d, $J = 8.9$ Hz, 1H), 7.35–7.33 (m, 1H), 7.26 (d, $J = 2.6$ Hz, 1H), 7.22 (dd, $J = 8.6, 2.3$ Hz, 1H), 5.07 (dd, $J = 12.4, 5.5$ Hz, 1H), 4.81–4.67 (m, 2H), 4.63–4.53 (m, 4H), 4.33–4.29 (m, 1H), 4.25 (d, $J = 12.0$ Hz, 2H), 4.07 (d, $J = 13.1$ Hz, 2H), 3.97 (d, $J = 13.9$ Hz, 1H), 3.88 (t, $J = 14.1$ Hz, 1H), 3.76–3.67 (m, 2H), 3.52–3.41 (m, 1H), 3.13–3.05 (m, 4H), 3.03–2.99 (m, 2H), 2.95 (s, 3H), 2.89–2.81 (m, 1H), 2.78–2.65 (m, 2H), 2.25–2.06 (m, 10H), 1.94–1.88 (m, 2H), 1.80–1.64 (m, 2H), 1.48–1.37 (m, 2H), 1.32–1.27 (m, 2H). ^{13}C NMR (125 MHz, Methanol- d_4) δ : 174.7, 171.7, 169.4, 168.9, 165.3, 163.3, 161.5, 156.8, 155.6, 155.6, 143.7, 135.7, 134.2, 131.7, 131.7, 127.0, 126.1, 124.4, 120.2, 119.4, 117.3, 117.1, 113.5, 110.9, 109.4, 105.3, 105.2, 90.2, 63.5, 59.7, 57.3, 56.4, 50.4, 48.3, 38.3, 32.3, 32.2, 30.7, 30.3, 28.2, 25.8, 25.7, 23.8. HRMS (ESI-Q-TOF): m/z calcd for $C_{54}H_{58}F_2N_{11}O_5^+ [M + H]^+$: 978.4585; found, 978.4602. UPLC-MS: m/z calcd for $C_{54}H_{58}F_2N_{11}O_5^+ [M + H]^+$: 978.46; found, 978.52. UPLC-retention time: 3.66 min, purity >95%.

5-(4-((1-(4-((1R,5S)-3,8-diazabicyclo[3.2.1]octan-3-yl)-7-(8-ethynyl-7-fluoro-3-hydroxynaphthalen-1-yl)-8-fluoropyrido[4,3-d]-pyrimidin-2-yl)azetidin-3-yl)(methyl)amino)piperidin-1-yl)methyl)-

piperidin-1-yl)-2-(2,6-dioxopiperidin-3-yl)-6-fluoroisoindoline-1,3-dione (C04). 1H NMR (400 MHz, Methanol- d_4) δ : 8.95 (s, 1H), 7.90 (dd, $J = 9.2, 5.7$ Hz, 1H), 7.54 (d, $J = 11.1$ Hz, 1H), 7.48 (d, $J = 7.3$ Hz, 1H), 7.42 (d, $J = 2.6$ Hz, 1H), 7.37 (t, $J = 8.9$ Hz, 1H), 7.27 (d, $J = 2.6$ Hz, 1H), 5.09 (dd, $J = 12.5, 5.4$ Hz, 1H), 4.85–4.68 (m, 2H), 4.66–4.55 (m, 4H), 4.55–4.45 (m, 1H), 4.25 (d, $J = 11.5$ Hz, 2H), 3.98 (d, $J = 13.7$ Hz, 1H), 3.91 (d, 1H), 3.87–3.79 (m, 2H), 3.72–3.66 (m, 2H), 3.57–3.46 (m, 1H), 3.26–3.07 (m, 4H), 2.99–2.90 (m, 2H), 2.86 (s, 3H), 2.84–2.81 (m, 1H), 2.78–2.68 (m, 2H), 2.38–2.23 (m, 4H), 2.18–2.09 (m, 6H), 2.01–1.91 (m, 2H), 1.62–1.46 (m, 2H), 1.34–1.26 (m, 2H). ^{13}C NMR (125 MHz, Methanol- d_4) δ : 174.6, 171.5, 168.4, 167.9, 165.3, 165.2, 163.3, 161.3, 160.5, 158.5, 155.6, 147.4, 147.3, 143.5, 134.2, 131.8, 131.7, 130.4, 130.4, 126.9, 125.5, 125.4, 124.5, 117.4, 117.2, 114.9, 113.7, 112.8, 112.6, 110.8, 110.7, 105.2, 105.1, 90.3, 76.0, 58.5, 56.3, 54.1, 53.8, 50.8, 50.7, 33.7, 32.2, 32.2, 30.8, 25.7, 25.7, 23.7. HRMS (ESI-Q-TOF): m/z calcd for $C_{53}H_{55}F_3N_{11}O_5^+ [M + H]^+$: 982.4334; found, 982.4349. UPLC-MS: m/z calcd for $C_{53}H_{55}F_3N_{11}O_5^+ [M + H]^+$: 982.43; found, 982.50. UPLC-retention time: 3.31 min, purity >95%.

5-(4-((1-(4-((1R,5S)-3,8-diazabicyclo[3.2.1]octan-3-yl)-7-(8-ethynyl-7-fluoro-3-hydroxynaphthalen-1-yl)-8-fluoropyrido[4,3-d]-pyrimidin-2-yl)azetidin-3-yl)(methyl)amino)methyl)piperidin-1-yl)-2-(2,6-dioxopiperidin-3-yl)-6-fluoroisoindoline-1,3-dione (C05). 1H NMR (400 MHz, Methanol- d_4) δ : 8.95 (s, 1H), 7.90 (dd, $J = 9.2, 5.6$ Hz, 1H), 7.54 (d, $J = 11.1$ Hz, 1H), 7.48 (d, $J = 7.3$ Hz, 1H), 7.42 (d, $J = 2.6$ Hz, 1H), 7.37 (t, $J = 8.9$ Hz, 1H), 7.27 (d, $J = 2.5$ Hz, 1H), 5.09 (dd, $J = 12.6, 5.4$ Hz, 1H), 4.83–4.68 (m, 2H), 4.63–4.54 (m, 4H), 4.36–4.30 (m, 1H), 4.25 (d, $J = 12.5$ Hz, 2H), 3.99 (t, $J = 13.9$ Hz, 1H), 3.88 (d, $J = 14.1$ Hz, 1H), 3.77–3.64 (m, 4H), 3.56–3.46 (m, 1H), 3.15–3.08 (m, 4H), 3.07–3.00 (m, 2H), 2.96 (s, 3H), 2.88–2.81 (m, 1H), 2.79–2.67 (m, 2H), 2.29–2.06 (m, 10H), 1.98–1.90 (m, 2H), 1.81–1.66 (m, 2H), 1.61–1.43 (m, 2H), 1.35–1.25 (m, 2H). ^{13}C NMR (125 MHz, Methanol- d_4) δ : 174.6, 171.5, 168.3, 167.9, 165.1, 163.2, 161.3, 160.5, 158.4, 155.6, 155.6, 147.3, 147.3, 134.2, 131.8, 131.7, 130.4, 130.3, 126.8, 125.4, 125.3, 124.5, 117.4, 117.2, 114.9, 114.8, 113.7, 112.7, 112.5, 110.7, 90.4, 76.0, 63.5, 59.7, 57.3, 56.3, 53.7, 50.8, 50.6, 40.4, 38.3, 32.1, 32.0, 30.8, 28.2, 25.7, 25.7, 23.6. HRMS (ESI-Q-TOF): m/z calcd for $C_{54}H_{57}F_3N_{11}O_5^+ [M + H]^+$: 996.4491; found, 996.4510. UPLC-MS: m/z calcd for $C_{54}H_{57}F_3N_{11}O_5^+ [M + H]^+$: 996.45; found, 996.62. UPLC-retention time: 3.05 min, purity >95%.

General Procedure for the Synthesis of Compounds B06, A10, and C06. A mixture of Compounds 26a (200 mg, 0.70 mmol, 1.0 equiv), benzyl 3-oxoazetidine-1-carboxylate (215 mg, 1.05 mmol, 1.5 equiv) in DCM (5 mL) was stirred at rt for 30 min. NaBH(OAc) (780 mg, 2.10 mmol, 3.0 equiv) was added and the mixture was stirred at rt for another 8 h. The mixture was diluted with water and extracted with DCM. The organic layer was separated, dried, and concentrated in vacuo. The residue obtained above was dissolved in MeOH (10 mL) and Pd/C (10% Pd/C (55% Water)) (74 mg, 0.2 eq, 20 wt %) was added. The mixture was stirred at 40 °C under H₂ (balloon) after degassing with H₂ for three times. After 12 h, the reaction mixture was filtered, the filtrate was collected and concentrated in vacuo to afford compound 30, and was used directly for the next step without further purification.

To a stirred solution of compounds 30 (237 mg, 0.70 mmol, 1.0 equiv), 16a (240 mg, 0.70 mmol, 1.0 equiv) and DIPEA (0.48 mL, 2.80 mmol, 4.0 equiv) in dry DMF (4 mL) was stirred under argon at 110 °C for 2 h. After being cooled to rt, the mixture was diluted with water and extracted with DCM. The organic layers were separated, washed with brine, dried, and concentrated in vacuo. The intermediate (191 mg, 46% in total) was obtained by prep-TLC (DCM/MeOH) = 10/1. The intermediate was dissolved in MeOH (0.5 mL), HCl (4 M in 1,4-dioxane, 1.2 mL, 16 equiv) was added. The mixture was stirred at 0 °C. After 45 min, the volatiles were removed under reduced pressure to afford compound 31a. The crude compound 31a was used directly for the next step without further purification.

A mixture of compounds 31a (100 mg, 0.20 mmol, 1.0 equiv), 13 (164 mg, 0.20 mmol, 1.0 equiv) and DIPEA (0.14 mL, 0.80 mmol, 4.0 equiv) in dry DMF (2 mL) was stirred under argon at 45 °C for 5 h.

After being cooled to rt, the mixture was diluted with water and extracted with DCM. The organic layers were separated, washed with brine, dried, and concentrated in vacuo. The residues were dissolved in MeOH (0.5 mL) and HCl (4 M in 1,4-dioxane, 0.8 mL, 16 equiv) was added. The mixture was stirred at 0 °C After 45 min, the volatiles were removed under reduced pressure. The residues were dissolved in DMF (0.5 mL) and CsF (304 mg, 2.00 mmol, 10 equiv) was added. The mixture was stirred at rt for 12 h and then was filtered. The organic layers were concentrated in vacuo. Compound B06 (86 mg, 46% in total) was obtained by preparative HPLC. Following the procedures used to prepare compound B06, compounds A10, and C06 were obtained by the same methods.

4-(3-((1-(4-(3,8-diazabicyclo[3.2.1]octan-3-yl)-7-(8-ethynyl-7-fluoro-3-hydroxynaphthalen-1-yl)-8-fluoropyrido[4,3-d]pyrimidin-2-yl)azetidin-3-yl)(methyl)amino)methyl)piperidin-1-yl)azetidin-1-yl)-2-(2,6-dioxopiperidin-3-yl)isoindoline-1,3-dione (B06). ^1H NMR (400 MHz, Methanol- d_4) δ : 9.01 (s, 1H), 7.91 (dd, J = 9.2, 5.7 Hz, 1H), 7.58 (t, J = 7.8 Hz, 1H), 7.45 (d, J = 2.5 Hz, 1H), 7.41–7.32 (m, 2H), 7.23 (d, J = 7.1 Hz, 1H), 6.84 (d, J = 8.4 Hz, 1H), 5.08 (dd, 1H), 4.88–4.79 (m, 2H), 4.76–4.64 (m, 4H), 4.61–4.56 (m, 2H), 4.52–4.43 (m, 2H), 4.42–4.34 (m, 1H), 4.26 (d, J = 15.9 Hz, 2H), 4.08 (d, J = 13.9 Hz, 1H), 3.94 (d, J = 14.1 Hz, 1H), 3.76–3.58 (m, 3H), 3.23–3.14 (m, 2H), 3.12–3.02 (m, 2H), 2.97 (s, 3H), 2.92–2.79 (m, 1H), 2.79–2.64 (m, 2H), 2.31–2.21 (m, 2H), 2.19–2.05 (m, 6H), 1.86–1.67 (m, 2H), 1.33–1.24 (m, 2H). ^{13}C NMR (125 MHz, Methanol- d_4) δ : 174.7, 171.7, 169.0, 168.1, 165.1, 163.2, 155.6, 153.1, 151.1, 148.3, 143.5, 136.4, 134.9, 134.2, 131.8, 131.7, 126.8, 124.5, 121.0, 117.4, 117.2, 114.6, 113.7, 113.4, 110.8, 105.2, 105.0, 90.6, 57.4, 56.8, 56.4, 53.9, 52.7, 52.1, 50.3, 38.4, 33.0, 32.2, 30.7, 30.4, 25.8, 25.7, 23.7, 23.6. HRMS (ESI-Q-TOF): m/z calcd for $\text{C}_{21}\text{H}_{25}\text{F}_2\text{N}_4\text{O}_5^+ [M + \text{H}]^+$: 936.4115; found, 936.4152. UPLC-MS: m/z calcd for $\text{C}_{21}\text{H}_{25}\text{F}_2\text{N}_4\text{O}_5^+ [M + \text{H}]^+$: 936.41; found, 936.73. UPLC-retention time: 2.94 min, purity >95%.

5-(3-((1-(4-(3,8-diazabicyclo[3.2.1]octan-3-yl)-7-(8-ethynyl-7-fluoro-3-hydroxynaphthalen-1-yl)-8-fluoropyrido[4,3-d]pyrimidin-2-yl)azetidin-3-yl)(methyl)amino)methyl)piperidin-1-yl)azetidin-1-yl)-2-(2,6-dioxopiperidin-3-yl)isoindoline-1,3-dione (A10). ^1H NMR (400 MHz, Methanol- d_4) δ : 8.97 (s, 1H), 7.90 (dd, J = 9.2, 5.7 Hz, 1H), 7.69 (d, J = 8.2 Hz, 1H), 7.42 (d, J = 2.5 Hz, 1H), 7.37 (t, J = 8.9 Hz, 1H), 7.28 (d, J = 2.6 Hz, 1H), 6.93 (d, J = 2.2 Hz, 1H), 6.76 (dd, J = 8.2, 2.2 Hz, 1H), 5.07 (dd, J = 12.5, 5.4 Hz, 1H), 4.81–4.70 (m, 2H), 4.63–4.55 (m, 4H), 4.43–4.36 (m, 2H), 4.32–4.24 (m, 5H), 3.99 (d, J = 13.5 Hz, 1H), 3.89 (d, J = 14.1 Hz, 1H), 3.73–3.63 (m, 2H), 3.58–3.52 (m, 1H), 3.19–3.12 (m, 2H), 3.11–3.01 (m, 2H), 2.96 (s, 3H), 2.88–2.80 (m, 1H), 2.79–2.67 (m, 2H), 2.27–2.19 (m, 2H), 2.18–2.08 (m, 6H), 1.79–1.63 (m, 2H), 1.31–1.27 (m, 2H). ^{13}C NMR (125 MHz, Methanol- d_4) δ : 174.6, 171.7, 169.0, 169.0, 165.3, 165.2, 163.3, 161.4, 155.9, 155.6, 143.4, 135.6, 134.3, 131.8, 131.7, 126.9, 126.0, 124.5, 121.0, 117.4, 117.2, 116.4, 113.7, 110.8, 106.4, 105.2, 105.1, 90.3, 57.4, 56.4, 54.8, 53.9, 52.8, 52.1, 50.4, 38.3, 32.2, 31.7, 30.7, 28.1, 25.7, 23.8. HRMS (ESI-Q-TOF): m/z calcd for $\text{C}_{21}\text{H}_{25}\text{F}_2\text{N}_4\text{O}_5^+ [M + \text{H}]^+$: 936.4115; found, 936.4103. UPLC-MS: m/z calcd for $\text{C}_{21}\text{H}_{25}\text{F}_2\text{N}_4\text{O}_5^+ [M + \text{H}]^+$: 936.41; found, 936.41. UPLC-retention time: 3.22 min, purity >95%.

5-(3-((1-(4-((1R,5S)-3,8-diazabicyclo[3.2.1]octan-3-yl)-7-(8-ethynyl-7-fluoro-3-hydroxynaphthalen-1-yl)-8-fluoropyrido[4,3-d]pyrimidin-2-yl)azetidin-3-yl)(methyl)amino)methyl)piperidin-1-yl)azetidin-1-yl)-2-(2,6-dioxopiperidin-3-yl)-6-fluoroisoindoline-1,3-dione (C06). ^1H NMR (400 MHz, Methanol- d_4) δ : 8.95 (s, 1H), 7.90 (dd, J = 9.1, 5.6 Hz, 1H), 7.50 (d, J = 10.8 Hz, 1H), 7.41 (d, J = 2.5 Hz, 1H), 7.36 (t, J = 8.9 Hz, 1H), 7.27 (d, J = 2.5 Hz, 1H), 7.04 (d, J = 7.2 Hz, 1H), 5.07 (dd, J = 12.7, 5.4 Hz, 1H), 4.80–4.70 (m, 2H), 4.64–4.56 (m, 4H), 4.54–4.50 (m, 2H), 4.45–4.39 (m, 2H), 4.34–4.28 (m, 1H), 4.25 (d, J = 11.5 Hz, 2H), 3.98 (d, J = 13.6 Hz, 1H), 3.88 (d, J = 11.8 Hz, 1H), 3.72–3.64 (m, 2H), 3.54–3.45 (m, 1H), 3.17–3.12 (m, 2H), 3.11–3.01 (m, 2H), 2.95 (s, 3H), 2.88–2.81 (m, 1H), 2.79–2.67 (m, 2H), 2.27–2.19 (m, 2H), 2.18–2.07 (m, 6H), 1.79–1.65 (m, 2H), 1.32–1.27 (m, 2H). ^{13}C NMR (125 MHz, Methanol- d_4) δ : 174.6, 171.6, 168.2, 165.4, 165.2, 163.3, 161.5, 157.1, 155.6, 155.1, 144.4, 144.3, 143.9, 134.2, 131.7, 131.6, 130.9, 127.0, 124.3, 122.8, 117.3, 117.1, 113.4, 112.4, 112.2, 110.9, 109.6, 105.3, 105.2, 90.1, 76.1, 57.3,

56.4, 53.9, 52.7, 52.2, 50.6, 38.4, 33.1, 32.2, 30.7, 25.8, 25.7, 23.7. HRMS (ESI-Q-TOF): m/z calcd for $\text{C}_{21}\text{H}_{25}\text{F}_2\text{N}_4\text{O}_5^+ [M + \text{H}]^+$: 954.4021; found, 954.441. UPLC-MS: m/z calcd for $\text{C}_{21}\text{H}_{25}\text{F}_2\text{N}_4\text{O}_5^+ [M + \text{H}]^+$: 954.40; found, 954.36. UPLC-retention time: 2.90 min purity >95%.

General Procedure for the Synthesis of Compounds A11. A mixture of Compounds 16b (200 mg, 0.72 mmol, 1.0 equiv), 2-azaspiro[3.5]nonan-7-one (150 mg, 1.08 mmol, 1.5 equiv) and DIPEA (0.50 mL, 2.88 mmol, 4.0 equiv) in dry DMF (4 mL) was stirred under argon at 110 °C for 2 h. After being cooled to rt, the mixture was diluted with water and extracted with DCM. The organic layers were separated, washed with brine, dried, and concentrated in vacuo. The compound 32 (233 mg, 82%) was obtained by prep-TLC (DCM/MeOH) = 30/1.

A mixture of compounds 32 (233 mg, 0.59 mmol, 1.0 equiv), 17 (109 mg, 0.59 mmol, 1.0 equiv) in DCM (5 mL) was stirred at rt for 30 min, $\text{NaBH}(\text{OAc})_3$ (673 mg, 1.77 mmol, 3.0 equiv) was added and the mixture was stirred at rt for another 8 h. The mixture was diluted with water and extracted with DCM. The organic layer was separated, dried, and concentrated in vacuo. The intermediate (143 mg, 43%) was obtained by prep-TLC (DCM/MeOH) = 20/1. The intermediate was dissolved in MeOH (0.5 mL), HCl (4 M in 1,4-dioxane, 1.0 mL, 16 equiv) was added. The mixture was stirred at 0 °C After 45 min, the volatiles were removed under reduced pressure to afford compound 33. The crude compound 33 was used directly for the next step without further purification.

A mixture of compounds 33 (100 mg, 0.21 mmol, 1.0 equiv), 13 (173 mg, 0.21 mmol, 1.0 equiv) and DIPEA (0.15 mL, 0.84 mmol, 4.0 equiv) in dry DMF (2 mL) was stirred under argon at 45 °C for 5 h. After being cooled to rt, the mixture was diluted with water and extracted with DCM. The organic layers were separated, washed with brine, dried, and concentrated in vacuo. The residues were dissolved in MeOH (0.5 mL) and HCl (4 M in 1,4-dioxane, 0.8 mL, 16 equiv) was added. The mixture was stirred at 0 °C After 45 min, the volatiles were removed under reduced pressure. The residues were dissolved in DMF (0.5 mL) and CsF (319 mg, 2.10 mmol, 10 equiv) was added. The mixture was stirred at rt for 12 h and then was filtered. The organic layers were concentrated in vacuo. Compound A11 (68 mg, 36% in total) was obtained by preparative HPLC.

5-(3-((1-(4-(3,8-diazabicyclo[3.2.1]octan-3-yl)-7-(8-ethynyl-7-fluoro-3-hydroxynaphthalen-1-yl)-8-fluoropyrido[4,3-d]pyrimidin-2-yl)azetidin-3-yl)(methyl)amino)-2-azaspiro[3.5]-nonan-2-yl)-2-(2,6-dioxopiperidin-3-yl)isoindoline-1,3-dione (A11). ^1H NMR (400 MHz, Methanol- d_4) δ : 8.96 (s, 1H), 7.89 (dd, J = 9.2, 5.7 Hz, 1H), 7.60 (d, J = 8.3 Hz, 1H), 7.42 (d, J = 2.6 Hz, 1H), 7.36 (t, J = 8.9 Hz, 1H), 7.29 (d, J = 2.6 Hz, 1H), 6.78 (d, J = 2.1 Hz, 1H), 6.60 (dd, J = 8.5, 2.2 Hz, 1H), 5.05 (dd, 1H), 4.81–4.71 (m, 2H), 4.67–4.59 (m, 4H), 4.56–4.48 (m, 1H), 4.25 (d, J = 10.5 Hz, 2H), 3.98 (d, J = 13.6 Hz, 1H), 3.91 (d, J = 14.1 Hz, 1H), 3.84–3.77 (m, 2H), 3.75–3.68 (m, 2H), 3.48–3.37 (m, 1H), 2.86 (s, 3H), 2.78–2.74 (m, 1H), 2.73–2.67 (m, 1H), 2.19–2.07 (m, 8H), 2.05–1.98 (m, 2H), 1.79–1.64 (m, 4H), 1.30–1.26 (m, 2H). ^{13}C NMR (125 MHz, DMSO- d_6) δ : 173.0, 170.3, 167.6, 167.3, 163.6, 163.2, 161.2, 159.8, 159.3, 159.0, 158.8, 158.5, 155.2, 154.4, 151.4, 149.3, 148.6, 143.0, 134.0, 132.6, 130.8, 125.1, 125.0, 123.3, 117.6, 116.8, 116.3, 116.1, 115.2, 114.2, 112.9, 112.1, 109.5, 104.4, 103.8, 103.7, 91.8, 91.3, 74.9, 61.2, 60.5, 54.3, 52.6, 51.6, 51.0, 48.8, 35.1, 33.5, 32.7, 31.1, 24.6, 24.1, 22.4, 21.1. HRMS (ESI-Q-TOF): m/z calcd for $\text{C}_{29}\text{H}_{34}\text{F}_2\text{N}_4\text{O}_5^+ [M + \text{H}]^+$: 907.3850; found, 907.3856. UPLC-MS: m/z calcd for $\text{C}_{29}\text{H}_{34}\text{F}_2\text{N}_4\text{O}_5^+ [M + \text{H}]^+$: 907.38; found, 907.60. UPLC-retention time: 3.58 min, purity >95%.

Molecular Docking. Download the crystal structure of KRAS^{G12D} with MRTX1133 (PDB: 7RPZ)¹⁵ from the RCSB Protein Data Bank. Protein was prepared using AutodockTools-1.5.7, which involved the removal of water molecules and heteroatoms, the addition of polar hydrogens and Kollman charges. Ligand was prepared by adding polar hydrogens and charges, and detecting root and choosing torsions. Then a receptor grid was generated using Grid Box panel. Finally, docking was performed using the Lamarckian G4 (4.2) algorithm with default parameters.

Cell Culture. The MDA-MB-231 cell line was obtained from the Cell Bank/Stem Cell Bank of the Chinese Academy of Sciences, while

AGS, GP2D, and CFPAC-1 were acquired from Procell Life Science and Technology Co., Ltd. (Wuhan, China). AsPC-1 cells were maintained in RPMI-1640 medium (Procell, cat.# PM150110), GP2D and HEK-293T cells in DMEM (Procell, cat.# PM150210), AGS cells in Ham's F-12 (Procell, cat.# PM150810), A549 cells in Ham's F-12K (Procell, cat.# PM150910), MDA-MB-231 cells in DMEM/F12 (Procell, cat.# PM150312), and CFPAC-1 and K562 cells in IMDM (Procell, cat.# PM150510). All media were supplemented with 10% FBS (Procell, cat.# 164210) and 1% penicillin–streptomycin (Procell, cat.# PM180120). Additionally, 2.5% horse serum (Procell, cat.# 164215) was added to the medium for MIA PaCa-2 cells. All cells were maintained at 37 °C in a 5% CO₂ atmosphere.

Western Blot. Cells were seeded at 4 × 10³ cells/well in 12-well plates and cultured overnight. After treating the cells with compounds under different conditions according to different experimental purposes, cells were washed with PBS and lysed on ice for 20 min using RIPA buffer supplemented with 1% protease inhibitor cocktail (Roche, cat.# 11697498001) and 10% PhosSTOP (Roche, cat.# 04906837001). Lysates were centrifuged at 14,000 rpm for 15 min at 4 °C, and supernatants were collected for protein quantification via BCA assay. Equal protein amounts were resolved on 12% SDS-PAGE gels, transferred to PVDF membranes, and blocked with 5% nonfat milk in TBST for 1 h at room temperature. Membranes were incubated with primary antibodies overnight at 4 °C followed by HRP-conjugated secondary antibodies (goat antirabbit IgG-HRP, P03S02 or goat antimouse IgG-HRP, P03S01) for 1 h at room temperature. Protein bands were detected using ECL reagents.

The following antibodies were used: KRAS^{G12D} antibody (Abcam, cat.# ab221163) was used for homozygous cell line AsPC-1. KRAS^{G12D} antibody (Cell Signaling Technology, cat.# D8H7) was used for heterozygous cell line GP2D and AGS. anti-pERK (Cell Signaling Technology, cat.# 4370S), anti-ERK1/2 (Santa Cruz Biotechnology, cat.# sc-514302), anti-Vinculin (Cell Signaling Technology, cat.# 13901S), anti- α Tubulin (Beijing Ray Antibody Biotech, cat.# RM2007). Anti-KRAS (ABclonal Technology, cat.# A23382), anti-CK1 α (Cell Signaling Technology, cat.# 4265SS), anti-GSPT1 (Abcam, cat.# ab234433).

Immunoprecipitation Assay. AsPC-1 cells were seeded at 7 × 10⁶ cells in 10 cm dish and cultured overnight. Cells were pretreated with 3 μ M MG132 for 4 h and add ZJK-807 1 μ M for 12 h. For polyubiquitination analysis, AsPC-1 cells are lysed with IP buffer containing protease inhibitors and the supernatant is collected by centrifugation at 12,000 rpm for 15 min. Protein A/G agarose beads were pretreated and incubated with beads using 1 μ g anti-KRAS (Santa Cruz Biotechnology, cat.# sc-30) for 4 h. The collected supernatants were incubated with the anti-KRAS and beads complex for 8 h at 4 °C. Polyubiquitinated KRAS was detected by immunoblotting using anti-Ubiquitin (Zenbio, cat.# 381080) antibody. For ternary complex analysis, HA-KRAS^{G12D} plasmids were obtained from Qingke Biotechnology Co., Ltd. (Beijing, China). After 48 h of HA-KRAS^{G12D} transfection, AsPC-1 cells were lysed in IP buffer containing protease inhibitors, and the supernatant was collected by centrifugation. The collected supernatants were incubated with DMSO or ZJK-807 (1 μ M) for 8 h at 4 °C, followed by overnight incubation with Anti-HA Magnetic Beads (HY-K0201). CRBN recruitment to KRAS^{G12D} was assessed by immunoblotting with anti-CRBN (Cell Signaling Technology, cat.# 71810S) and anti-HA (Proteintech, cat.# HRP-81290) antibodies.

Plasmid Transfection. KRAS^{G12D/95mut} and KRAS^{G12D/96mut} plasmids were obtained from Qingke Biotechnology Co., Ltd. (Beijing, China). AGS cells were seeded in 60 mm culture dishes and cultured overnight under standard conditions. Cells were transfected with 4 μ g/well of KRAS^{G12D/95mut} or KRAS^{G12D/96mut} plasmid using Lipofectamine 3000 (Thermo Fisher, cat.# L300001S) according to the manufacturer's instructions. After 48 h, transfected cells were reseeded into 24-well plates and treated with varying concentrations of ZJK-807 for 24 h to assess its degradation effects on KRAS^{G12D/95mut} and KRAS^{G12D/96mut} resistant mutants.

Cell Viability Assay. To assess the inhibitory effects on cancer cell viability, cells were seeded in 96-well plates at densities of 2 × 10³ cells/

well (AsPC-1, GP2D, AGS, A549, MDA-MB-231, MIA PaCa-2) or 3 × 10³ cells/well (CFPAC-1, K562, HEK-293T, SV-HUC-1) in 100 μ L medium. After adherence, cells were treated with specified concentrations of test compounds or 0.1% DMSO (control) for the desired duration. For the CCK-8 assay, 10 μ L of CCK-8 reagent (Biosharp, cat.# BS350A) was added to each well, followed by 4 h of incubation. Absorbance was measured at 450 nm using a Tecan Spark microplate reader. For secondary mutant cell lines (Ba/F3), cells were seeded at 3 × 10³ cells/well, treated with ZJK-807 for 72 h, and analyzed using the CellTiter-Glo assay. Luminescence was measured after 20 min of incubation. Data were analyzed and visualized using Prism 9.4.0.

RNA Sequencing and Data Processing. AsPC-1 cells were treated with 10 μ M ZJK-807 or 300 nM MRTX1133 for 48 h and total RNA was extracted using Trizol reagent (Bioteck, cat.# R0016). RNA libraries were sequenced by OE Biotech (Shanghai, China) on the DNASEq-T7 platform, generating 150 bp paired-end reads with effective data volumes of 6.24–7.01 G per sample. Reads were aligned to the reference genome, and protein-coding gene expression analysis identified 17,529–19,243 genes per sample. Differential expression analysis was performed using DESeq2, identifying DEGs with \log_2 fold change > 2 and q-value < 0.05. Heatmap visualization expression trends of DEGs associated with RAS and MAPK pathways. KEGG pathway enrichment analysis was conducted using R (v3.2.0) based on the hypergeometric distribution, and the top 20 significantly enriched pathways were ranked by ascending $-\log_{10}(P)$ value.

PK Study. For the PK study, six-week-old male ICR mice were administered 30 mg/kg A04 or ZJK-807 via IP administration, 10 mg/kg 80 or 10 and 30 mg/kg ZJK-807 via SC administration, with a vehicle control group (10% Captisol in 50 mM citrate buffer, pH 5.0). Blood samples were collected at specified time points (0.25, 0.5, 1, 2, 4, 6, 8, 12, 24 h) postdosing, placed in heparinized tubes, and centrifuged to obtain plasma. Plasma concentrations were quantified using LC–MS/MS, and PK parameters were calculated to evaluate drug exposure and bioavailability. All procedures were approved by the Animal Care and Ethics Committee of Ocean University of China.

Xenograft Tumor Assay. All experimental protocols involving animals were reviewed and approved by the Animal Care and Ethics Committee of Ocean University of China, No. E-MBDX-20255-1-3. For the *in vivo* efficacy study, 5.0 × 10⁶ AsPC-1 cells suspended in 100 μ L of PBS and Matrigel (Corning, cat. # 354234) were subcutaneously implanted into the right flank of male BALB/c nude mice. Tumor growth was monitored daily, and caliper measurements began once palpable tumors were detected. When the average tumor volume reached 100–200 mm³, mice were randomized into three groups ($n = 6$ per group): vehicle control, ZJK-807 (30 mg/kg in vehicle), or MRTX1133 (30 mg/kg in vehicle). ZJK-807 was administered by SC administration once daily, while MRTX1133 was treated by IP administration twice daily. The vehicle control group alternated between the two administration modes daily. Tumor dimensions were recorded every 3 days to evaluate therapeutic efficacy, and body weight was measured every 2 days to monitor safety. After 28 days, the mice were humanely euthanized, and tumor tissues were harvested for subsequent analysis of KRAS^{G12D} protein expression level.

Statistical Analysis. All experiments were repeated independently two or three times and all data are expressed as mean ± standard deviation (SD). Differences in means between groups were analyzed by Ordinary one-way ANOVA or two-tailed unpaired t test using GraphPad Prism 9.4.1 software. Significance level was set as * $P < 0.05$, ** $P < 0.01$, *** $P < 0.001$, **** $P < 0.0001$.

ASSOCIATED CONTENT

Supporting Information

The Supporting Information is available free of charge at <https://pubs.acs.org/doi/10.1021/acs.jmedchem.Sc01034>.

Supporting Figures, Table, experimental methods and materials, as well as copies [¹H, ¹³C] NMR spectra, and HPLC purity (PDF)

Molecular formula strings (CSV)

AUTHOR INFORMATION

Corresponding Authors

Shumin Ma — Key Laboratory of Marine Drugs, Chinese Ministry of Education, School of Medicine and Pharmacy, Ocean University of China, Qingdao, Shandong 266003, China; Center for Targeted Protein Degradation and Drug Discovery, Ocean University of China, Qingdao, Shandong 266003, China; Marine Biomedical Research Institute of Qingdao, Qingdao, Shandong 266071, China;
Email: mashumin@ouc.edu.cn

Xiao Wang — Key Laboratory of Marine Drugs, Chinese Ministry of Education, School of Medicine and Pharmacy, Ocean University of China, Qingdao, Shandong 266003, China; Center for Targeted Protein Degradation and Drug Discovery, Ocean University of China, Qingdao, Shandong 266003, China; Marine Biomedical Research Institute of Qingdao, Qingdao, Shandong 266071, China;  orcid.org/0000-0001-7364-2459; Email: wx1024@ouc.edu.cn

Chong Qin — Key Laboratory of Marine Drugs, Chinese Ministry of Education, School of Medicine and Pharmacy, Ocean University of China, Qingdao, Shandong 266003, China; Laboratory for Marine Drugs and Bioproducts, Qingdao Marine Science and Technology Center, Qingdao, Shandong 266137, China; Center for Targeted Protein Degradation and Drug Discovery, Ocean University of China, Qingdao, Shandong 266003, China; Marine Biomedical Research Institute of Qingdao, Qingdao, Shandong 266071, China;  orcid.org/0000-0001-8108-1698; Email: qc@ouc.edu.cn

Authors

Zhaojuan Liu — Key Laboratory of Marine Drugs, Chinese Ministry of Education, School of Medicine and Pharmacy, Ocean University of China, Qingdao, Shandong 266003, China

Heping Zheng — Key Laboratory of Marine Drugs, Chinese Ministry of Education, School of Medicine and Pharmacy, Ocean University of China, Qingdao, Shandong 266003, China

Yanqing Tian — Key Laboratory of Marine Drugs, Chinese Ministry of Education, School of Medicine and Pharmacy, Ocean University of China, Qingdao, Shandong 266003, China

Zhuoyue Li — Key Laboratory of Marine Drugs, Chinese Ministry of Education, School of Medicine and Pharmacy, Ocean University of China, Qingdao, Shandong 266003, China; Center for Targeted Protein Degradation and Drug Discovery, Ocean University of China, Qingdao, Shandong 266003, China; Marine Biomedical Research Institute of Qingdao, Qingdao, Shandong 266071, China

Sai Zhang — Key Laboratory of Marine Drugs, Chinese Ministry of Education, School of Medicine and Pharmacy, Ocean University of China, Qingdao, Shandong 266003, China; Center for Targeted Protein Degradation and Drug Discovery, Ocean University of China, Qingdao, Shandong 266003, China; Marine Biomedical Research Institute of Qingdao, Qingdao, Shandong 266071, China

Siqi Zhang — Key Laboratory of Marine Drugs, Chinese Ministry of Education, School of Medicine and Pharmacy, Ocean University of China, Qingdao, Shandong 266003, China; Center for Targeted Protein Degradation and Drug Discovery, Ocean University of China, Qingdao, Shandong 266003, China;  orcid.org/0000-0001-8682-1683

Complete contact information is available at:

<https://pubs.acs.org/10.1021/acs.jmedchem.Sc01034>

Author Contributions

¹Z.L. and H.Z. authors contributed equally. The manuscript was written through contributions of all authors. All authors have given approval to the final version of the manuscript.

Funding

We gratefully acknowledge the financial support from the Key Research and Development Program of Shandong Province (2022CXPT038), and Qingdao Key Technology Research and Industrialization Demonstration Projects (24—1—4-xxgg-15nsh).

Notes

The authors declare no competing financial interest.

ACKNOWLEDGMENTS

The authors thank the Ocean University of China and the Pilot National Laboratory for Marine Science and Technology for the supports. The authors wish to express sincere gratitude to the Prof. Tianfeng Xu's research group (Shanghai Institute of Materia Medica, Chinese Academy of Sciences) for their generous provision of compound 8o.

ABBREVIATIONS

AUC_{last}, area under the curve from the time of dosing to the time of the last observation; C_{max}, maximum drug concentration; CBN, cereblon; CRC, colorectal cancers; DEGs, differentially expressed genes; GSEA, gene set enrichment analysis; HBDS, hydrogen bond donors; IMIDs, immunomodulatory drugs; KRAS, Kirsten rat sarcoma viral oncogene homologue; MAPK, mitogen-activated protein kinase; MW, molecular weight; ORR, objective response rate; PDAC, pancreatic ductal adenocarcinoma; PI3K, phosphatidylinositol-3 kinase; PK, pharmacokinetics; POI, protein of interest; PROTAC, proteolysis targeting chimera; RTK, receptor tyrosine kinase; t_{max}, the time take to reach C_{max}; t_{1/2}, terminal half-life; UPS, ubiquitin-proteasome system; VHL, von Hippel-Lindau.

REFERENCES

- (1) Huang, L.; Guo, Z.; Wang, F.; Fu, L. KRAS Mutation: From Undruggable to Druggable in Cancer. *Signal Transduct. Target. Ther.* **2021**, *6* (1), 386.
- (2) Prior, I. A.; Lewis, P. D.; Mattos, C. A Comprehensive Survey of Ras Mutations in Cancer. *Cancer Res.* **2012**, *72* (10), 2457–2467.
- (3) Tang, Y.; Pu, X.; Yuan, X.; Pang, Z.; Li, F.; Wang, X. Targeting KRASG12D Mutation in Non-Small Cell Lung Cancer: Molecular Mechanisms and Therapeutic Potential. *Cancer Gene Ther.* **2024**, *31* (7), 961–969.
- (4) Herdeis, L.; Gerlach, D.; McConnell, D. B.; Kessler, D. Stopping the Beating Heart of Cancer: KRAS Reviewed. *Curr. Opin. Struct. Biol.* **2021**, *71*, 136–147.
- (5) Cox, A. D.; Fesik, S. W.; Kimmelman, A. C.; Luo, J.; Der, C. J. Drugging the Undruggable RAS: Mission Possible? *Nat. Rev. Drug Discovery* **2014**, *13* (11), 828–851.
- (6) Xu, K.; Park, D.; Magis, A. T.; Zhang, J.; Zhou, W.; Sica, G. L.; Ramalingam, S. S.; Curran, W. J.; Deng, X. Small Molecule KRAS Agonist for Mutant KRAS Cancer Therapy. *Mol. Cancer* **2019**, *18* (1), 85.
- (7) Waters, A. M.; Der, C. J. KRAS: The Critical Driver and Therapeutic Target for Pancreatic Cancer. *Cold Spring Harb. Perspect. Med.* **2018**, *8* (9), a031435.
- (8) Simanshu, D. K.; Nissley, D. V.; McCormick, F. RAS Proteins and Their Regulators in Human Disease. *Cell* **2017**, *170* (1), 17–33.

- (9) Wood, K.; Hensing, T.; Malik, R.; Salgia, R. Prognostic and Predictive Value in KRAS in Non-Small-Cell Lung Cancer: A Review. *JAMA Oncol.* 2016, 2 (6), 805.
- (10) Ostrem, J. M. L.; Shokat, K. M. Direct Small-Molecule Inhibitors of KRAS: From Structural Insights to Mechanism-Based Design. *Nat. Rev. Drug Discovery.* 2016, 15 (11), 771–785.
- (11) Canon, J.; Rex, K.; Saiki, A. Y.; Mohr, C.; Cooke, K.; Bagal, D.; Gaida, K.; Holt, T.; Knutson, C. G.; Koppada, N.; Lanman, B. A.; Werner, J.; Rapaport, A. S.; San Miguel, T.; Ortiz, R.; Osgood, T.; Sun, J.-R.; Zhu, X.; McCarter, J. D.; Volak, L. P.; Houk, B. E.; Fakih, M. G.; O’Neil, B. H.; Price, T. J.; Falchook, G. S.; Desai, J.; Kuo, J.; Govindan, R.; Hong, D. S.; Ouyang, W.; Henary, H.; Arvedson, T.; Cee, V. J.; Lipford, J. R. The Clinical KRAS(G12C) Inhibitor AMG 510 Drives Anti-Tumour Immunity. *Nature.* 2019, 575 (7781), 217–223.
- (12) Hallin, J.; Engstrom, L. D.; Hargis, L.; Calinisan, A.; Aranda, R.; Briere, D. M.; Sudhakar, N.; Bowcut, V.; Baer, B. R.; Ballard, J. A.; Burkard, M. R.; Fell, J. B.; Fischer, J. P.; Vigors, G. P.; Xue, Y.; Gatto, S.; Fernandez-Banet, J.; Pavlicek, A.; Velastegui, K.; Chao, R. C.; Barton, J.; Pierobon, M.; Baldelli, E.; Patricoin, E. F.; Cassidy, D. P.; Marx, M. A.; Rybkin, I. I.; Johnson, M. L.; Ou, S.-H. I.; Lito, P.; Papadopoulos, K. P.; Jänne, P. A.; Olson, P.; Christensen, J. G. The KRASG12C Inhibitor MRTX849 Provides Insight toward Therapeutic Susceptibility of KRAS-Mutant Cancers in Mouse Models and Patients. *Cancer Discovery.* 2020, 10 (1), 54–71.
- (13) Ou, S.-H. I.; Jänne, P. A.; Leal, T. A.; Rybkin, I. I.; Sabari, J. K.; Barve, M. A.; Bazhenova, L.; Johnson, M. L.; Velastegui, K. I.; Cilliers, C.; Christensen, J. G.; Yan, X.; Chao, R. C.; Papadopoulos, K. P. First-in-Human Phase I/IB Dose-Finding Study of Adagrasib (MRTX849) in Patients With Advanced KRAS G12C Solid Tumors (KRYSKAL-1). *J. Clin. Oncol.* 2022, 40 (23), 2530–2538.
- (14) Hallin, J.; Bowcut, V.; Calinisan, A.; Briere, D. M.; Hargis, L.; Engstrom, L. D.; Laguer, J.; Medwid, J.; Vanderpool, D.; Lifset, E.; Trinh, D.; Hoffman, N.; Wang, X.; David Lawson, J.; Gunn, R. J.; Smith, C. R.; Thomas, N. C.; Martinson, M.; Bergstrom, A.; Sullivan, F.; Bouhana, K.; Winski, S.; He, L.; Fernandez-Banet, J.; Pavlicek, A.; Haling, J. R.; Rahbaek, L.; Marx, M. A.; Olson, P.; Christensen, J. G. Anti-Tumor Efficacy of a Potent and Selective Non-Covalent KRASG12D Inhibitor. *Nat. Med.* 2022, 28 (10), 2171–2182.
- (15) Wang, X.; Allen, S.; Blake, J. F.; Bowcut, V.; Briere, D. M.; Calinisan, A.; Dahlke, J. R.; Fell, J. B.; Fischer, J. P.; Gunn, R. J.; Hallin, J.; Laguer, J.; Lawson, J. D.; Medwid, J.; Newhouse, B.; Nguyen, P.; O’Leary, J. M.; Olson, P.; Pajk, S.; Rahbaek, L.; Rodriguez, M.; Smith, C. R.; Tang, T. P.; Thomas, N. C.; Vanderpool, D.; Vigors, G. P.; Christensen, J. G.; Marx, M. A. Identification of MRTX1133, a Noncovalent, Potent, and Selective KRAS G12D Inhibitor. *J. Med. Chem.* 2022, 65 (4), 3123–3133.
- (16) Zhou, C.; Li, C.; Luo, L.; Li, X.; Jia, K.; He, N.; Mao, S.; Wang, W.; Shao, C.; Liu, X.; Huang, K.; Yu, Y.; Cai, X.; Chen, Y.; Dai, Z.; Li, W.; Yu, J.; Li, J.; Shen, F.; Wang, Z.; He, F.; Sun, X.; Mao, R.; Shi, W.; Zhang, J.; Jiang, T.; Zhang, Z.; Li, F.; Ren, S. Anti-Tumor Efficacy of HRS-4642 and Its Potential Combination with Proteasome Inhibition in KRAS G12D-Mutant Cancer. *Cancer Cell.* 2024, 42 (7), 1286–1300.
- (17) Knox, J. F.; Burnett, G. L.; Weller, C.; Jiang, J.; Zhang, D.; Vita, N.; Marquez, A.; Seamon, K. J.; Gould, A.; Menard, M.; Quintana, E.; Chen, Z.; Wang, Z.; Koltun, E. S.; Singh, M.; Jiang, J.; Wildes, D.; Smith, J. A. M.; Gill, A. L. Abstract ND03: Discovery of RMC-9805, an Oral, Covalent Tri-Complex KRASG12D(ON) Inhibitor. *Cancer Res.* 2024, 84 (Suppl. 7), ND03.
- (18) Mao, Z.; Xiao, H.; Shen, P.; Yang, Y.; Xue, J.; Yang, Y.; Shang, Y.; Zhang, L.; Li, X.; Zhang, Y.; Du, Y.; Chen, C. C.; Guo, R. T.; Zhang, Y. KRAS(G12D) Can Be Targeted by Potent Inhibitors via Formation of Salt Bridge. *Cell Discovery.* 2022, 8 (1), 5.
- (19) Kim, D.; Herdeis, L.; Rudolph, D.; Zhao, Y.; Böttcher, J.; Vides, A.; Ayala-Santos, C. I.; Pourfarjam, Y.; Cuevas-Navarro, A.; Xue, J. Y.; Mantouidis, A.; Broker, J.; Winberg, T.; Schaaf, O.; Popow, J.; Wolkerstorfer, B.; Kropatsch, K. G.; Qu, R.; De Stanchina, E.; Sang, B.; Li, C.; McConnell, D. B.; Kraut, N.; Lito, P. Pan-KRAS Inhibitor Disables Oncogenic Signalling and Tumour Growth. *Nature.* 2023, 619 (7968), 160–166.
- (20) Mirati Therapeutics Inc. A Phase 1/2 Multiple Expansion Cohort Trial of MRTX1133 in Patients with Advanced Solid Tumors Harboring a KRAS G12D Mutation; Clinical Trial Registration NCT05737706; clinicaltrials.gov, 2025.
- (21) Zhou, C.; Li, W.; Song, Z.; Zhang, Y.; Zhang, Y.; Huang, D.; Yang, Z.; Zhou, M.; Mao, R.; Huang, C.; Li, X.; Wang, J. LBA33 A First-in-Human Phase I Study of a Novel KRAS G12D Inhibitor HRS-4642 in Patients with Advanced Solid Tumors Harboring KRAS G12D Mutation. *Ann. Oncol.* 2023, 34, S1273.
- (22) Spira, A. I.; Papadopoulos, K. P.; Kim, D. W.; Parikh, A. R.; Barve, M. A.; Powderly, J. D.; Starodub, A.; Strickler, J. H.; Li, B. T.; Oberstein, P. E.; Hassan, F.; Yang, M.; McCleland, M.; Lally, S.; Lin, W.; Sohoni, S.; Hong, D. S. Preliminary Safety, Antitumor Activity, and Circulating Tumor DNA (ctDNA) Changes with RMC-9805, an Oral, RAS(ON) G12D-Selective Tri-Complex Inhibitor in Patients with KRAS G12D Pancreatic Ductal Adenocarcinoma (PDAC) from a Phase 1 Study in Advanced Solid Tumors. *J. Clin. Oncol.* 2025, 43 (Suppl. 4), 724.
- (23) Choi, J.; Shin, J.; Kim, T. K.; Kim, K.; Kim, J.; Jeon, E.; Park, J.; Han, Y. D.; Kim, K.-A.; Sim, T.; Kim, H. K.; Kim, H. S. Site-Specific Mutagenesis Screening in KRAS Mutant Library to Uncover Resistance Mechanisms to KRASG12D Inhibitors. *Cancer Lett.* 2024, 591, 216904.
- (24) Keats, M. A.; Han, J. J. W.; Lee, Y.-H.; Lee, C.-S.; Luo, J. A. Nonconserved Histidine Residue on KRAS Drives Paralog Selectivity of the KRASG12D Inhibitor MRTX1133. *Cancer Res.* 2023, 83 (17), 2816–2823.
- (25) Awad, M. M.; Liu, S.; Rybkin, I. I.; Arbour, K. C.; Dilly, J.; Zhu, V. W.; Johnson, M. L.; Heist, R. S.; Patil, T.; Riely, G. J.; Jacobson, J. O.; Yang, X.; Persky, N. S.; Root, D. E.; Lowder, K. E.; Feng, H.; Zhang, S. S.; Haigis, K. M.; Hung, Y. P.; Sholl, L. M.; Wolpin, B. M.; Wiese, J.; Christiansen, J.; Lee, J.; Schrock, A. B.; Lim, L. P.; Garg, K.; Li, M.; Engstrom, L. D.; Waters, L.; Lawson, J. D.; Olson, P.; Lito, P.; Ou, S.-H. I.; Christensen, J. G.; Jänne, P. A.; Aguirre, A. J. Acquired Resistance to KRASG12C Inhibition in Cancer. *N. Engl. J. Med.* 2021, 384 (25), 2382–2393.
- (26) Lai, A. C.; Crews, C. M. Induced Protein Degradation: An Emerging Drug Discovery Paradigm. *Nat. Rev. Drug Discovery.* 2017, 16 (2), 101–114.
- (27) Békés, M.; Langley, D. R.; Crews, C. M. PROTAC Targeted Protein Degraders: The Past Is Prologue. *Nat. Rev. Drug Discovery.* 2022, 21 (3), 181–200.
- (28) Isermann, T.; Sers, C.; Der, C. J.; Papke, B. KRAS Inhibitors: Resistance Drivers and Combinatorial Strategies. *Trends Cancer.* 2025, 11 (2), 91–116.
- (29) Petrylak, D. P.; McKean, M.; Lang, J. M.; Gao, X.; Dreicer, R.; Geynman, D. M.; Stewart, T. F.; Gandhi, M.; Appleman, L. J.; Dorff, T. B.; Chatta, G. S.; Tutron, R.; De La Cerdá, J.; Berghorn, E.; Gong, J.; Yu, T.; Dominy, E.; Chan, E.; Shore, N. D. ARV-766, a Proteolysis Targeting Chimera (PROTAC) Androgen Receptor (AR) Degrader, in Metastatic Castration-Resistant Prostate Cancer (mCRPC): Initial Results of a Phase 1/2 Study. *J. Clin. Oncol.* 2024, 42 (Suppl. 16), 5011.
- (30) Zhu, Y.; Ye, X.; Wu, Y.; Shen, H.; Cai, Z.; Xia, F.; Min, W.; Hou, Y.; Wang, L.; Wang, X.; Xiao, Y.; Yang, P. Design, Synthesis, and Biological Evaluation of Novel EGFR PROTACs Targeting C797S Mutation. *J. Med. Chem.* 2024, 67 (9), 7283–7300.
- (31) Park, E. S.; Ahn, J. Y.; Baddour, J.; Chaturvedi, P.; Chiu, M. I.; Cole, K. S.; Crystal, A. S.; Duplessis, M.; Fisher, S. L.; Good, A. C.; Hird, A. W.; Huang, H.; Hulton, C. H.; Ladd, B.; Michael, R. E.; Nasveschuk, C. G.; Phillips, A. J.; Pollock, R. M.; Sarkissian, G.; Rahman, F.; Simard, J. R. Preclinical Evaluation of CFT8919 as a Mutant Selective Degrader of EGFR with L858R Activating Mutations for the Treatment of Non-Small Cell Lung Cancer. Presented at the Keystone - Targeted Protein Degradation, Virtual Meeting, June 2021.
- (32) Robbins, D. W.; Noviski, M. A.; Tan, Y. S.; Konst, Z. A.; Kelly, A.; Auger, P.; Brathaban, N.; Cass, R.; Chan, M. I.; Cherala, G.; Clifton, M. C.; Gajewski, S.; Ingallinera, T. G.; Karr, D.; Kato, D.; Ma, J.; McKinney, J.; McIntosh, J.; Mihalic, J.; Murphy, B.; Pang, J. R.; Peng, C.; Powers, J.; Perez, L.; Rountree, R.; Lenn-McClellan, A.; Sands, A. T.; Weiss, D. R.; Wu, J.; Ye, J.; Guiducci, C.; Hansen, G.; Cohen, F. Discovery and Preclinical Pharmacology of NX-2127, an Orally

- Bioavailable Degrader of Bruton's Tyrosine Kinase with Immunomodulatory Activity for the Treatment of Patients with B Cell Malignancies. *J. Med. Chem.* 2024, 67 (4), 2321–2336.
- (33) Bond, M. J.; Chu, L.; Nalawansha, D. A.; Li, K.; Crews, C. M. Targeted Degradation of Oncogenic KRASG12C by VHL-Recruiting PROTACs. *ACS Central Sci.* 2020, 6 (8), 1367–1375.
- (34) Zhou, C.; Fan, Z.; Gu, Y.; Ge, Z.; Tao, Z.; Cui, R.; Li, Y.; Zhou, G.; Huo, R.; Cao, M.; Wang, D.; He, W.; Zheng, M.; Zhang, S.; Xu, T. Design, Synthesis, and Biological Evaluation of Potent and Selective PROTAC Degraders of Oncogenic KRASG12D. *J. Med. Chem.* 2024, 67 (2), 1147–1167.
- (35) Popow, J.; Farnaby, W.; Gollner, A.; Kofink, C.; Fischer, G.; Wurm, M.; Zollman, D.; Wijaya, A.; Mischerikow, N.; Hasenoehrl, C.; Prokofeva, P.; Arnhoff, H.; Arce-Solano, S.; Bell, S.; Boeck, G.; Diers, E.; Frost, A. B.; Goodwin-Tindall, J.; Karolyi-Oezguer, J.; Khan, S.; Klawatsch, T.; Koegl, M.; Kousek, R.; Kratochvil, B.; Kropatsch, K.; Lauber, A. A.; McLennan, R.; Olt, S.; Peter, D.; Petermann, O.; Roessler, V.; Stolt-Bergner, P.; Strack, P.; Strauss, E.; Trainor, N.; Vetma, V.; Whitworth, C.; Zhong, S.; Quant, J.; Weinstabl, H.; Kuster, B.; Ettmayer, P.; Cuulli, A. Targeting Cancer with Small-Molecule Pan-KRAS Degraders. *Science* 2024, 385 (6715), 1338–1347.
- (36) Tolcher, A. W.; Park, W.; Wang, J. S.; Spira, A. I.; Janne, P. A.; Lee, H.-J.; Gill, S.; LoRusso, P.; Herzberg, B.; Goldman, J. W.; Morgensztern, D.; Berlin, J.; Kasi, A.; Fujii, H.; Pelster, M. Trial in Progress: A Phase 1, First-in-Human, Open-Label, Multicenter, Dose-Escalation and Dose-Expansion Study of ASP3082 in Patients with Previously Treated Advanced Solid Tumors and KRAS G12D Mutations. *J. Clin. Oncol.* 2023, 41 (Suppl 4), TPS764.
- (37) Sun, W.; Ye, J.; Deng, T.; Wang, L.; Guo, L.; Zhao, S.; Zhai, W.; Liu, D. KRAS-PROTAC Chimeric Compound and Use Thereof. WO 2025061079 A1, 2025.
- (38) Zhang, C.; He, P.; Huang, Q.; Qin, L.; Liao, P.; Li, Y.; Yan, P. Compound Capable of Degrading KRAS and Application of Compound in Medicine. CN119219669A, 2024.
- (39) Sun, Y.; Fu, J.; Zeng, H. Bifunctional Compounds for Degrading KRAS G12D via Ubiquitin Proteasome Pathway. WO 2024050742 A1, 2024.
- (40) Ji, X.; Li, H.; Wu, G.; Zhang, Q.; He, X.; Wu, Y.; Zong, B.; Xu, X.; Liang, C.; Wang, B.; Zhang, Y.; Hu, Q.; Deng, C.; Shen, L.; Chen, Z.; Bai, B.; Wang, L.; Ai, J.; Zhang, L.; Zhou, H.; Sun, S.; Wang, Y.; Wang, Y.; Fan, Q.; Chen, D.; Zhou, T.; Kong, X.; Lu, J. Discovery and Characterization of RP03707: A Highly Potent and Selective KRASG12D PROTAC. *J. Med. Chem.* 2025, 68 (10), 10238–10254.
- (41) Edmondson, S. D.; Yang, B.; Fallon, C. Proteolysis Targeting Chimeras (PROTACs) in beyond Rule-of-Five Chemical Space: Recent Progress and Future Challenges. *Bioorg. Med. Chem. Lett.* 2019, 29 (13), 1555–1564.
- (42) Zhou, C.; Fan, Z.; Zhou, Z.; Li, Y.; Cui, R.; Liu, C.; Zhou, G.; Diao, X.; Jiang, H.; Zheng, M.; Zhang, S.; Xu, T. Discovery of the First-in-Class Agonist-Based SOS1 PROTACs Effective in Human Cancer Cells Harboring Various KRAS Mutations. *J. Med. Chem.* 2022, 65 (5), 3923–3942.
- (43) Nguyen, T. M.; Sreekanth, V.; Deb, A.; Kokkonda, P.; Tiwari, P. K.; Donovan, K. A.; Shoba, V.; Chaudhary, S. K.; Mercer, J. A. M.; Lai, S.; Sadagopan, A.; Jan, M.; Fischer, F. S.; Liu, D. R.; Ebert, B. L.; Choudhary, A. Proteolysis-Targeting Chimeras with Reduced off-Targets. *Nat. Chem.* 2024, 16 (2), 218–228.



CAS BIOFINDER DISCOVERY PLATFORM™

**STOP DIGGING
THROUGH DATA
— START MAKING
DISCOVERIES**

CAS BioFinder helps you find the right biological insights in seconds

Start your search

